Spin-Adapted Coupled Cluster Theory for Open-shell Molecules using the Normal-Ordered Exponential *Ansatz*

Alexander D. Gunasekera

Balliol College

University of Oxford

A thesis submitted for the degree of

Doctor of Philosophy

Michaelmas 2025/26

Acknowledgements

First and foremost, credit for this thesis and the work it represents must go to my supervisor, David, whose patient and careful guidance made all of this possible. His attention to detail and insight in seeing through to the heart of a problem made all of our conversations productive and highly motivating, and his confidence in my ideas inspired me to push them through to their implementation.

Thanks also to the other members of the Tew group, several of whose material contribution to this work should be recognised individually. Nick's work on CSFs and normal ordering, as well as his encyclopaedic knowledge of the literature, made him a vital asset in discussions on various approaches to spin-adapted coupled cluster. His efforts also were invaluable in preparing the manuscript for the Faraday Discussions paper, which was instrumental in the organisation both of preceding and of subsequent work that ended up this thesis. Early discussions with Daniel about CSFs and the nature and formalism of spin-coupling were illuminating, and helped solidify our views on strong correlation more generally.

Across the Tew group, there have been many discussions which have had an indirect but profound impact on this work. Chris has so many insights and ideas about many-body methods that whenever one gets the chance to talk to him, the spirit of learning seems to spark anew — his work relating coupled cluster and Green's function methods surely represents one of best examples of cross-fertilisation of ideas between theoretical Chemistry and Physics, and provided valuable insight into the physical processes represented in a spin-adapted coupled cluster ansatz. Speaking with Andrew has been both useful and enjoyable, from discussing theoretical ideas about orbital invariances and practical implementation ideas, to distractions of coffee or working on some linear algebra problem on the whiteboard. The entire Tew group, and indeed many other residents of the theory annexe, have my thanks for many such helpful, encouraging, and entertaining interactions over the years.

I am indebted to the EPSRC CDT in Theory and Modelling in the Chemical Sciences for funding, the CDT and PTCL departmental staff for their organisational assistance, and I thank Prof. Mark Wilson, Prof. Barford, and colleagues for giving me this chance. I am grateful to Balliol College for having me and for making my time such a vibrant one, both intellectually and in wider college life.

The number of people who have made my life in Oxford so enjoyable is far too many to name; between the orchestras, quiz society, squash club, college choir, and the general community, this city and university has given me so many incredible friends and colleagues, all of whom I owe a great deal for the many small and large acts of kindness that have sustained me. I have been blessed to have shared houses with some amazing people, from Holywell Manor to Walton Well Road, Temple Street, and the Tawney Street family, whose contribution to this thesis was not merely in support, but often in surprise theoretical discussions, for example about numerical analysis or Sobolev spaces, whose effect on my understanding may be visible to the reader in the presentation of this work.

The last and most significant thanks must go to my family, for their unfailing belief in me, and for their limitless support and encouragement. Words will never be enough to thank you for all you have done for me.

Abstract

A new unlinked formulation of Lindgren's normal-ordered exponential coupled cluster (NOECC) *ansatz* is devised, with a careful truncation procedure that includes terms in the exponential only up to linear or quadratic order in the amplitudes while minimising size inconsistency errors. This is implemented in a new python package which we have named Open-shell Coupled Cluster using Spin Free Diagrammatic construction (OCCSFrD), which automatically generates, and then solves, spin-adapted coupled cluster equations with an arbitrary configuration state function (CSF) as reference. After verifying that the quadratic-truncated unlinked NOECC faithfully replicates the traditional (quartic-terminating) coupled cluster for single-reference closed shells, the open-shell NOECC energies are found for several high-spin doublets, without the spin contamination introduced in traditional methods. The NOECC framework is then tested in several single-reference multi-determinant cases: the splitting of the 2-electron open-shell singlet from its corresponding high-spin triplet in the beryllium atom, the size consistency of two open shell doublet lithium atoms, the low-lying multi-determinant singlet state in the Oxygen molecule. Some potential energy surfaces are also calculated using NOECCSD for the methylene diradical and for H_4 in a range of rectangular geometries, and the 3-electron doublet and quartet energies of the nitrogen atom are calculated with the linear-truncated NOECC. As a contribution towards a general theoretical model for quantum chemistry, this framework achieves a systematically improvable spin-adapted treatment of dynamic correlation for the general statically correlated single-reference wavefunction, clarifying the 'genuine' multireference problem that remains to be solved.

Declaration

Except where otherwise indicated, the work presented in this thesis consists wholly of my own work, completed under the supervision of Prof. David Tew. Work completed in collaboration is solely that which is published in the Faraday Discussions paper, "Multi-reference coupled cluster theory using the normal ordered exponential ansatz."[1] That manuscript consisted primarily of my own work, with a significant contribution to the writing and editing from my co-author, Nicholas Lee. The relevant sections will all be indicated in place.

Alexander Gunasekera, January 2026

[1] Gunasekera, A. D. *et al.* Multi-reference coupled cluster theory using the normal ordered exponential ansatz. *Faraday Discuss.* **254,** 170–190. doi:10.1039/D4FD00044G (6th Nov. 2024).

Contents

List of Figures

1 Introduction

1.1 Motivation

Electronic structure theory, as part of the broader field of theoretical chemistry, aims to develop methods to simulate chemical systems and calculate properties in order to explain, and ultimately predict, the results of experiments. The utility of electronic structure methods in research and development of new materials and molecules, as well as in probing environments both near and remote, has already been realised for several decades, showing the benefit of vast increases in available computing power in that time. Although the equations governing the physics of electrons have long been known, the quest for fast, scaleable, and accurate methods to solve these equations remains an ongoing task.

Over the years, the criteria by which a method for quantum chemistry should be judged have been discussed, and are often encapsulated in the concept of a 'model chemistry,' an idea which guided much theoretical development in the second half of the 20th century, and which John Pople brought to popular attention in his 1998 Nobel acceptance speech.[2] A desirable theoretical model for chemistry would be a well-defined method that models a sufficiently general range of chemical systems (without unphysical discontinuities) to a defined target accuracy, so as to be able first to replicate experimental data, and then to

explain and later predict the results of new experiments. The requirement for general applicability leads to a set of conditions that are widely agreed upon, although their relative importance is still subject to discussion, given that no single method yet fulfils them all.

Some sensible criteria that a model chemistry should satisfy in order to align with Pople's vision were laid out in a 1981 review by Rodney Bartlett.[3] Foremost among these were: accuracy, size-consistency and size-extensivity, as well as a reasonably-scaling computational cost, such that practical calculations can actually be carried out. The traditional measure of 'chemical accuracy' imitates the precision of a standard laboratory experiment, generally declaring two electronic energies to match to 'chemical accuracy' if they differ by no more than 1 kcal/mol,[2] or about $1.6\,\mathrm{mE_H}$. It was considered an important feature of a method that it provide a strict upper bound to the ground state energy by the variational principle, and so the progress of systematic improvement of a method be observable in the monotonic decrease of the energy towards the exact answer. Nowadays, this is not so important, and only the systematic improvability is considered the critical feature of a family of methods, allowing increased computational resources to be spent in order to approach the exact answer, but without necessarily guaranteeing monotonicity. Many non-variational methods, including coupled cluster, may be considered 'quasi-variational,' being variational in the leading orders of perturbation theory, and in any case the variational principle will not apply to the difference between two energies, even if they were separately calculated by a variational method.

The idea of a model, not just *for* chemistry, but *of* chemistry, may lead one to consider that the details of a computational algorithm may reflect the details of the physics it is trying to simulate. This rather more philosophical point does not have to be assumed: it may be that the most efficient solver of the equations for a chemical system has no regard for the behaviour of individual electrons, electron pairs, or other components of the system. However, a consideration of the more detailed processes can often lead to more efficient description of the overall, for

instance by identifying which contributions should be neglected to achieve the greatest computational speedup for the smallest loss of accuracy. As a byproduct, this may also yield a method that is more readily interpretable in physical terms, and hence offers improved explanatory power. With recent advances in machine learning and other algorithms for which numerical performance takes precedence over interpretability, such questions may remain relevant in aiding the design of new molecules and materials.

With a useful combination of these attributes, Coupled Cluster (CC) theory based on a single Slater-determinant reference wavefunction has become firmly established and is widely used in high-accuracy electronic structure calculations[4]. It is accurate compared to methods of comparable cost, it is size-consistent and size-extensive, and its lack of variationality is not a serious flaw in practice; CCSD(T) is often considered the 'gold standard' in single-reference cases for achieving agreement to chemical accuracy with the 'exact' energy obtained by Full Configuration Interaction (FCI). However, its domain of applicability is not sufficiently general for a number of important applications: many chemical systems, including diradicals, transition metals, and molecules at non-equilibrium geometries, display open-shell configurations for which multi-determinant reference states are required. Transition metal complexes are classic systems with near-degeneracies and spin-dependent properties, for which increasingly accurate simulations are an invaluable tool in the development of new catalysts, dyes, nanomaterials and many other new technologies. Atmospheric chemistry often involves radicals and diradicals, open shell systems for which accurate correlated methods would be influential in the simulation of dynamics and spectroscopic interactions. The central ambition of Multi-Reference Coupled Cluster (MRCC) theory is to extend CC theory to tackle these types of problems, obtaining continuous and smooth potential energy surfaces and treating general open-shell spin systems, while preserving the benefits of the single-reference theory. This has been an area of active research for several decades, with no clear

consensus yet on how to deal with the complexities that arise in defining wave operators and working equations for multi-determinant reference spaces[5–7].

A wish-list for a multireference coupled cluster method was set out by Köhn et al, in particular how the generalisation from single-reference CC (SRCC) should be done in a way to reliably obtain accurate and smooth potential energy surfaces.[5] Desirable properties that a MRCC should retain from SRCC would be that it is size extensive and consistent, invariant to rotations separately among core and virtual orbitals, and numerically stable achieving accurate results in a reasonable computation time. A so-called 'genuine' multireference treatment should not be biased towards any one model space configuration, while reducing to SRCC in the limit of one reference configuration. It should solve a proper residual condition, and ideally would be spin-adapted without introducing too much additional theoretical complexity.

For molecules with un-paired electrons, the requirement that different spin states be resolved may also be added to the model chemistry criteria, when considering a non-relativistic approximation. Truly spin-adapted methods allow a particular spin eigenspace to be specified beforehand, and return correlated states afterwards while rigorously preserving the correct spin eigenvalues throughout. As yet, coupled cluster methods are well-equipped for certain types of open-shell calculations, but cannot in general tackle all open shell configurations. If these could be tackled, spectroscopic properties, intersystem crossings, and other experimental observables would be accessible, to add to the highly accurate energies for closed shell molecules that coupled cluster can already deliver.

Owing to the limitations of the single Slater determinant picture, open-shell systems are often misidentified as multi-reference. Multi-reference treatments are necessary when competing configurations are involved in bonding or when targeting excited state spectra, but are not necessary[8] for states that are correctly represented by a single open-shell configuration state function (CSF), which are eigenfunctions of the spin operators. Many open-shell systems, such as

organic radicals and transition metal spin states may be treated using single-reference open-shell coupled-cluster theory. In these cases, it is not necessary to perform a full CAS calculation, whose cost formally scales exponentially with the number of open-shell electrons.

This thesis serves to demonstrate a new implementation of the normal-ordered coupled cluster technique that has been proposed previously,[9] widening the scope of its application to low-spin and general multi-determinant single-reference wavefunctions. Previous implementations of normal-ordered coupled cluster theory have been limited to only high-spin cases, so this represents a significant generalisation of the approach. It also offers a perspective on the intuition of strong vs. weak correlation, and the domain of applicability of single- and multi-reference methods.

In this work, we explore fully spin-adapted coupled-cluster theory for correlating single open-shell CSF reference states. Our *ansatz* takes the form of the internally contracted theories, but where the coefficients of the multi-determinant reference state are pre-determined by spin and spatial symmetry constraints. Our work concerns the generalisation of closed-shell coupled-cluster theory to arbitrary open-shell states while retaining full spin-adaption, through a state-specific formulation. Full spin-adaptation of is achieved through the use of spin-free excitation operators in our cluster operator, in a manner similar to unitary group approaches[10–14].

1.2 Literature Review

The exponential *ansatz* of coupled cluster was originally proposed by Coester and Kümmel to describe atomic nuclei as systems of fermions interacting at short range.[15, 16] It was only a few years later that Čížek and Paldus, with developments by Sinanoğlu, realised the applicability of this *ansatz* to the electronic structure problem.[17–19] The early coupled cluster programs were being developed over the 1970s, with implementations of CCD,[20–22] CCSD,[23] and later CCSDT[24, 25] (coupled cluster with, respectively, Double, Single

and Double, and Single and Double and Triple excitations) being applied to small molecules and showing accurate results in single-reference systems. The single-reference coupled cluster method has gone on to become one of the most widely-used methods for highly accurate electronic structure calculations, with the CCSD(T) method, which treats the effect of triple excitations as a perturbative correction to CCSD,[26, 27] being widely considered as offering the 'gold standard' of accuracy versus computational cost.[4]

While coupled cluster was recognised as an accurate method for the treatment of dynamic correlation, the need for a multireference treatment of systems showing strong correlation was also known. At a mean-field level, the MCSCF methods were developed, with the active space-based methods such as CAS and RAS SCF[28] giving the ability to obtain continuous potential energy curves, even through intermediate bonding regimes that present the hardest cases for single-reference methods. Multireference wavefunctions are considered in depth in the CASSCF methods developed by Björn Roos,[29, 30] which brought the concept of active space selection to the fore when describing chemical processes such as bond breaking and formation. Correlated methods based on these wavefunctions in widespread application have been limited to perturbation theory at second order, such as the CASPT2[31] or NEVPT2[32] methods.

Attempts at a multireference coupled cluster theory began almost immediately after the original application of coupled cluster to electronic structure.[33] After Mukherjee's initial formulation for a single reference of multiple determinants, Jeziorski and Monkhorst proposed an *ansatz* to treat spaces of multiple reference functions in a so-called 'genuinely multireference' way, *i.e.* without prioritising any reference function over another. This Jeziorski–Monkhorst (J–M) *ansatz* applies an exponential operator, each with its own set of amplitudes, to each of a set of reference functions spanning a model space.[34] While originally intended for a State-Universal MRCC (SU-MRCC) approach in which all of the reference functions are correlated simultaneously, the J–M *ansatz* can also be applied to find one specific (*e.g.* ground) state, but this leads to a severe overparametrisation, as

there are more amplitudes to be determined than equations to solve for them. By either providing additional constraints or eliminating redundant amplitudes, a system of working equations with a unique solution may be obtained. These different choices define different State-Specific MRCC (SS-MRCC) theories, which may be distinguished by which of the MRCC criteria (size-extensivity, orbital invariance, *etc.*) they fulfil.[6, 35]

In addition to State-Specific and State-Universal MRCC theories, which are formulated in a Hilbert Space of constant particle number, there are Valence-Universal (VU-MRCC), or Fock Space (FSCC) approaches, in which the wave operator does not necessarily conserve particle number. Work by Kutzelnigg demonstrated the hierarchical solution of many-body equations in sectors of Fock space of different particle and hole numbers relative to the reference,[36] similarly to the subspace embedding conditions formulated by Haque and Mukherjee in the original FSCC approaches.[37, 38] FSCC was applied by those authors and later Uzi Kaldor to find smooth potential energy surfaces,[39] and work by Bartlett and coworkers later applied it in an intermediate Hamiltonian formalism to obtain excitation energies, electron affinities, and ionisation potentials.[40, 41] Related to those intermediate Hamiltonian methods are the many-body similarity transforms developed by Nooijen *et al.* for equation-of-motion coupled cluster methods for excited and ionised states.[42–45]

The analysis of coupled cluster as a partial infinite sum of a perturbation series led to Lindgren's proposal of a normal ordered exponential wave operator, which has been maintained as an idea to this day, but not implemented in full generality.[9] Mukherjee and Kutzelnigg generalised the concept of normal ordering to multi-determinant reference functions, to attempt to generalise the use of Wick's theorem in deriving single-reference CC equations.[46, 47]

For specific problems of bond-breaking that would require active spaces of only two orbitals, a single-reference approach was developed by Piecuch et al that augmented a CCSD ansatz with the specific triple and quadruple

excitations needed to generate the single and double excited states out of the other multireference configurations.[48]

Unitary group approaches to the problem of spin adaptation were first employed in the context of configuration interaction. The Unitary Group Approach to Configuration Interaction (UGA-CI), and then its 'Graphical' variant GUGA-CI represented a significant step forward in efficiency in the calculation of spin-adapted matrix elements.[49–52] Attempts to bring the same benefits to coupled cluster has been made ever since, but some formal difficulties have prevented there from being one universal approach that solves every issue in spin-adapted CC. The most comprehensive account of a Unitary Group Approach to Coupled Cluster (UGA-CC) was the series of papers by Paldus and Li that aimed to develop an orthogonally spin-adapted CC theory.[10–14, 53, 54] In their approach, the basis states between which the cluster operator transforms are fully spin-adapted according to irreducible representations of the unitary group. Other approaches since have abandoned the idea of an orthogonally spin-adapted basis for CC, but have constructed the cluster operator from unitary group generators, and are still referred to as unitary group approaches.

Although the first automated code generators for coupled cluster were developed in the 1990s,[11, 55] it was only in the 2010s that automated equation generators began to be seen as a more widespread approach to the derivation of the complicated equations that arise in spin-adapted coupled cluster theories.[56–59]

One attempt to bypass the challenge of full spin adaptation was the spin-restricted OS-CC, which projected out contaminating contributions to the total spin expectation value. Although this gave some reasonable energies with only very minimal spin-contamination, it was only applied to high-spin doublets, leaving the general problem for multiple open shells unsolved.[60]

Around 2000, Mukherjee's MRCC was devised, which has become the most widely implemented Hilbert-space MRCC.[61, 62] Mukherjee *et al.* later developed the Combinatoric Open-Shell CC method.[63, 64]. This reintroduced some of the contractions that are neglected in the normal-ordered exponential, to

account for orbital relaxation before the treatment of dynamic correlation. The use of so-called 'automorphic factors' was required to recover the property that each diagram appears exactly once in the equations. Although this has been implemented in high-spin cases, it has not yet reached widespread use.[65]

The internally contracted MRCC methods are another approach to treating the dynamic correlation on top of an orbitally-optimised single reference wavefunction, and work is ongoing to put this on an equal footing to SRCC.[5, 66] Following initial work by Banerjee and Simons,[67], Evangelista, Gauss, Köhn and coworkers developed the complicated working equations needed to icMRCC, first in a state-specific formalism,[57, 68, 69] and later in a multi-state approach using the similarity transformed Hamiltonian.[70] In icMRCC, the fact that the multireference coefficients are allowed to be relaxed means that active-active excitations may be excluded, greatly simplifying the theory.[5, 57] In addition, the requirement for a unique set of amplitudes to solve the CC equations is met by restricting the amplitudes to those that generate independent excited stated from the reference, which may be found by a singular value decomposition.[5, 71, 72]

Herrmann and Hanrath's use of a spin-complete projection manifold was a further development towards an accurate spin-adapted method.[73–75] They also applied a method of spin paths to evaluate the number of different spin components surviving in each term in the equations.

Even with the prospect of well-defined and accurate methods for spin-adapted and multireference coupled cluster, perhaps the most important hurdle to overcome is making these methods fast and scalable enough to be practically applied for chemical systems that are actually interesting in the real world. Whether in single- or multi-reference problems, the standard coupled cluster algorithms fundamentally always scale very poorly to obtain any reasonable accuracy (see for example, the 7^{th} power scaling of CPU time for single-reference CCSD(T)).[76] One approach to enable treatment of larger molecules is the use of local correlation methods, generally based on natural orbitals (NOs) or pair natural orbitals (PNOs), which correlate the electrons with a compressed space of virtual orbitals

that is defined individually for each electron or electron pair, but is independent of the system size.[77, 78] These have been successful in achieving coupled cluster results in near-linear scaling CPU time in molecules, and work is ongoing to apply the same techniques in (insulating) periodic materials.

The fact that correlated methods aim to account for the first-derivative discontinuity ("cusp") that occurs when electrons coincide[79], which is very difficult to capture in terms of products of one-electron functions, means that they require large basis sets to converge towards the complete basis set limit. By augmenting the basis of one-electron functions ("orbitals") with two-electron functions ("geminals") that show the correct cusp condition, a much better approximation to the basis set limit can be achieved for a given number of basis functions.[80] These 'explicitly correlated' methods such as the r_{12} and latterly f_{12} approaches have been very promising, particularly when combined with the local correlation methods that mitigate the increase in cost they incur.[81–83]

Even after a long history of varied approaches, the problem of a general, efficient, multireference coupled cluster still remains to be solved. The contribution of this work is the practical demonstration that Lindgren's normal-ordered coupled cluster can be applied to general single-CSF references, giving a useful treatment of dynamic correlation in cases where the multireference character can be simplified by spin or other symmetries. It is not a 'genuine' MRCC for obtaining smooth potential energy curves, but it does address the problem of high- and low-spin open shell states of molecules, as generally as possible and with comparable accuracy to single reference cases.

2
Background Theory

This chapter describes the preliminary theory on which our formulation of a spin-adapted normal-ordered exponential coupled cluster theory for open-shell molecules is built. Pedagogical treatments of the background theory are available in the standard textbooks by Szabo and Ostlund [84], and in more depth in that of Helgaker et al. [76]. The diagrammatic approaches to many-body perturbation theory and coupled cluster are detailed in the textbook by Shavitt and Bartlett [85].

After a brief description of the electronic structure problem in section 2.1, section 2.2 outlines the mathematical apparatus used to describe wavefunctions and operators. Section 2.3 describes the implications of spin on many-electron wavefunctions, and how to formulate correctly spin-adapted wavefunctions as appropriate for a non-relativistic theory. Section 2.4 introduces the standard methods used to solve electronic structure, leading up to the traditional single-reference coupled cluster, and a brief overview of existing multireference coupled cluster methods. This lays the foundation for chapter 3, in which we formulate our normal-ordered exponential coupled cluster theory to treat dynamic correlation starting from reference wavefunctions already incorporating static correlation due to spin coupling.

2.1 The Electronic Structure Problem

The central equation of electronic structure is the time independent molecular electronic Schrödinger equation

$$\hat{H} \left|\Psi\right\rangle = E \left|\Psi\right\rangle \tag{2.1.0.1}$$

where $\left|\Psi\right\rangle$ describes the state of the system of multiple electrons, and the Hamiltonian operator $\hat{H}$ their total energy under the Born–Oppenheimer approximation (described in section 2.1.1), which has allowed the separation in equation 2.1.0.1 of quantum mechanical electronic degrees of freedom from the classical motion of the nuclei. In the basis of coordinates $\mathbf{x}_i$ of the electrons $i = 1, 2, \ldots, N$, the state $\left|\Psi\right\rangle$ of N electrons is represented by the wavefunction $\left\langle \mathbf{x}_1, \mathbf{x}_2, \ldots, \mathbf{x}_N \,\middle|\, \Psi \right\rangle = \Psi\left(\mathbf{x}_1, \mathbf{x}_2, \ldots, \mathbf{x}_N\right)$, where $\mathbf{x}_i$ is the combined coordinate of the real-space position $\mathbf{r}_i$ and a spin coordinate, for the i-th electron. These eigenfunctions $\left|\Psi\right\rangle$ of the Hamiltonian $\hat{H}$ are separable solutions to the time-dependent Schrödinger equation, and may be considered stationary states with the energy eigenvalue E modulating a time-dependent complex phase factor, which shall be considered implicit and hereafter ignored. While the Schrödinger equation generally admits many solutions, the most important in chemistry are generally the electronic states with the lowest energy eigenvalues. As with most of the longest-established electronic-structure techniques, the work in this thesis primarily targets the ground state and a few particular low-lying excited states.

In a wavefunction-based electronic structure method such as coupled cluster theory, (an approximation to) the wavefunction itself is sought, in contrast to density-based methods, which seek only to describe the electron density, and may or may not return some wavefunction that reproduces it.[86] While the lower cost of density-based methods such as Density Functional Theory (DFT) has led to their predominance in applied calculations for molecules and materials, there is as yet no general and systematically improvable approximation to the exchange-correlation functional, and so DFT cannot universally be guaranteed to approach the exact electronic energy without prior knowledge of the specific

system under consideration.[87] Wavefunction methods therefore offer a better prospect of a black-box method to simulate the electron correlation and exchange effects *ab initio*, *i.e.* without introducing empirical or semi-empirical parameters. The challenge of electronic structure theory is that the Schrödinger equation is not analytically solvable even for two electrons except in special cases, let alone for more complicated systems of chemical interest. Approximations must be made in order to solve it numerically, capturing enough of the important physical effects required to be useful while ignoring enough of the irrelevant details to be practical.

2.1.1 The Born–Oppenheimer Approximation

The Born–Oppenheimer (B–O) approximation uses the fact that the nuclei are much heavier than the electrons to decouple the electronic part of the wavefunction from the motion of the nuclei.[88] The combined state of the electrons and nuclei is represented as a product of a nuclear part and an electronic part

$$|\Psi\rangle = |\Psi_{nuc}\rangle \otimes |\Psi_{el}\rangle \tag{2.1.1.1}$$

obeying the Schrödinger equation under the full non-relativistic Hamiltonian (written in atomic units)

$$\hat{H} = \sum_{I<J} \frac{Z_I Z_J}{R_{IJ}} - \sum_{I=1}^{N} \frac{1}{2m_I} \nabla_I^2 - \frac{1}{2} \sum_{i=1}^{n} \nabla_i^2 - \sum_{i=1}^{n} \sum_{I=1}^{N} \frac{Z_I}{r_{iI}} + \sum_{i<j} \frac{1}{r_{ij}} \tag{2.1.1.2}$$

where the nuclear wavefunction $\Psi_{nuc}(\{\mathbf{R}_I\})$ is independent of the electrons and the electronic wavefunction $\Psi_{el}(\{\mathbf{r}_i\};\{\mathbf{R}_I\})$ depends parametrically on the coordinates of the nuclei.[88] The B–O approximation neglects the derivatives of $|\Psi\rangle_{el}$ with respect to the nuclear positions ($\nabla_I |\Psi\rangle_{el} \approx 0$), as the electronic wavefunction is assumed to rearrange instantaneously in response to the nuclei. This leaves a Schrödinger equation that itself is separable into an electronic part

$$E_{el} |\Psi\rangle_{el} = \hat{H}_{el} |\Psi\rangle_{el} = \left(-\frac{1}{2} \sum_{i=1}^{n} \nabla_i^2 - \sum_{i=1}^{n} \sum_{I=1}^{N_{nuc}} \frac{Z_I}{r_{iI}} + \sum_{i<j} \frac{1}{r_{ij}} \right) |\Psi\rangle_{el} + E_{NN} \tag{2.1.1.3}$$

and a nuclear part

$$E\left|\Psi\right\rangle_{nuc} = \hat{H}_{nuc}\left|\Psi\right\rangle_{nuc} = -\sum_{I=1}^{N}\frac{1}{2m_I}\nabla_I^2\left|\Psi\right\rangle_{nuc} + E_{el} \tag{2.1.1.4}$$

The notion of "electronic structure" is predicated on this separation of electronic and nuclear degrees of freedom.

The electronic part of the B–O Hamiltonian, can be written

$$\hat{H} = \sum_{I<J}\frac{Z_I Z_J}{R_{IJ}} - \frac{1}{2}\sum_{i=1}^{n}\nabla_i^2 - \sum_{i=1}^{n}\sum_{I=1}^{N_{nuc}}\frac{Z_I}{r_{iI}} + \sum_{i<j}\frac{1}{r_{ij}} \tag{2.1.1.5}$$

$$= E_{NN} + \sum_i \hat{h}_i + \sum_{i<j}\hat{g}_{ij} \tag{2.1.1.6}$$

where the one- and two-electron parts have been denoted $\hat{h}$ and $\hat{g}$ respectively, and E_{NN} is the nuclear-nuclear repulsion energy.

Over varying spatial arrangements ("geometries") of the nuclei, the eigenvalues of the B–O Hamiltonian form potential energy surfaces (PESs),[88] which may provide binding curves or surfaces on which geometry optimisations or nuclear dynamical simulations may be performed. The B–O approximation is very accurate for the majority of ground state chemical systems, and will always be assumed in this thesis.

Simulation of excited state dynamics and other time-dependent processes may involve situations in which the B–O approximation can no longer be assumed, and nuclear quantum effects must also be included. Methods for those 'non-adiabatic' dynamics (including surface-hopping and Ehrenfest dynamics, among others[89]) often begin from a calculation of multiple B–O potential energy surfaces, using a Born–Huang representation for the combined quantum nuclear-electronic wavefunction.[90] Therefore, solving the electronic structure problem (for ground and excited states) will be of foundational importance to molecular simulations, whether the nuclei are treated classically, as in the B–O approximation, or quantum-mechanically.

2.1.2 On the nature of electron-electron correlation

Most approximations to an N-electron wavefunction that is an eigenstate of a two-body (*e.g.* electronic B–O) Hamiltonian begin from an effective one-body ('mean-field,' or 'independent electron') approximation, such as a Hartree–Fock determinant (see subsection 2.4.1). The difference between a mean-field approximation and the exact solution is known as the electron-electron correlation, and the calculation of its contribution to the energy is the principal theoretical and computational difficulty in the electronic structure problem. While the time for a Hartree–Fock iteration (without additional improvements) scales with a measure N of the system size as N^4, correlated wavefunction methods in regular use can scale as the 5^{th}, 6^{th}, 7^{th}, or even 8^{th} power of N. The time for an exact calculation of the electron correlation energy in general scales with $N!$, so these represent huge computational savings that are necessary for any practical method, but there is great scope to improve the trade-off between computational scaling and accuracy.

The correlation energy is often separated into contributions that might be better treated by different methods, and given names such 'strong' and 'weak' correlation, or the more evocative 'static' and 'dynamic' correlation,[91] although many choices are possible.[92] The former distinction is generally considered between 'weak' correlation effects that can be captured by perturbative and coupled cluster methods from a single reference, and 'strong' correlation that requires non-perturbative or multi-reference treatments. On the other hand, 'static' correlation generally refers to a state for which a single determinant cannot provide a good mean-field reference,[93, 94] with 'dynamic' correlation often considered to be the effect of direct electron-electron repulsions on top of some multi-configurational reference function.

These distinctions are identical in the traditional picture of a single Hartree–Fock reference, but in light of the fact that Hartree–Fock already incorporates the two-body exchange effect, there is no reason in principle not to consider other zero-order states such as Configuration State Functions (CSFs, see section 2.3.2), that may account for other symmetries or static correlation effects in an

effective one-body framework. If the appropriate multi-determinant reference can be defined, then a large part of what might otherwise be called strong or static correlation might be viewed not as any type of correlation at all, leaving only the 'dynamical' or 'weak' correlation to be treated by *e.g.* perturbative or CC methods, to which it will likely be well suited. In cases where symmetry or near-degeneracy do not offer a suitable single CSF reference, then the problem is one that can strictly be called 'strong' correlation, and a 'genuinely'[5, 6] multireference method will be required.

2.2 Theoretical Apparatus

To describe the theoretical methods used to treat electronic correlation, it is first useful to explain some foundational concepts and notational frameworks. In particular, the description of wavefunctions as elements of a Hilbert space will be outlined, beginning with the Hilbert space of one-electron functions in subsection 2.2.1. The projection of this space into a discrete (and finite) computational basis set is described in subsection 2.2.2, followed by the construction of many-electron wavefunctions and the spaces they inhabit, in subsection 2.2.3. Operators on these spaces are themselves elements of a vector space, which will form the algebra of second quantization, described in subsection 2.2.4 The second quantized operators lead to a concise formulation of Wick's theorem, which is instrumental in the derivation of the theoretical techniques described in later sections.

2.2.1 One-particle functions

The wavefunction describing a system of multiple electrons will be built up from single-particle functions, known as spin-orbitals. A spin-orbital is a (generally complex) function of position $\mathbf{r}$ in real space and a spin coordinate m_s, usually combined into the single coordinate $\mathbf{x}$. In a nonrelativistic theory, a spin-orbital can be written as a product of a function of space (an orbital) $\psi_i(\mathbf{r})$ and a spin

function $\sigma(m_s)$

$$\psi_i(\mathbf{x}) = \psi_i(\mathbf{r})\,\sigma_i(m_s) \tag{2.2.1.1}$$

As a fermion of total spin $\frac{1}{2}$, an electron has two possible values of the projected spin along a principal axis, $m_s = \pm 1/2$ (described as "up" or "down,"). The two possible spin functions for an electron are usually labelled $\sigma(m_s) = \alpha(m_s), \beta(m_s)$, for which

$$\alpha\left(\frac{1}{2}\right), \alpha\left(-\frac{1}{2}\right) = 1, 0$$
$$\beta\left(\frac{1}{2}\right), \beta\left(-\frac{1}{2}\right) = 0, 1$$

The orbitals are square-integrable functions of real space, elements of the Hilbert space $L^2(\mathbb{R}^3)$ under the Hermitian inner product defined by

$$\langle\psi_i|\psi_j\rangle = \int \psi_i^*(\mathbf{r})\,\psi_j(\mathbf{r})\; d\mathbf{r} \tag{2.2.1.2}$$

The Dirac bra-ket notation may also be employed in the shorthand $\langle i|j\rangle \equiv \langle\psi_i|\psi_j\rangle$ The squared norm $\langle i|i\rangle$ is interpreted as the total (squared) probability of an electron in orbital i being found somewhere over all space; unless otherwise specified, orbitals will always be considered to be scaled such that $\langle i|i\rangle = 1$

One-electron operators such as the position, momentum, and kinetic energy operators

$$\hat{x} = \mathbf{x}\cdot \tag{2.2.1.3}$$
$$\hat{p} = -\mathrm{i}\nabla \tag{2.2.1.4}$$
$$\hat{t} = \hat{p}^2 = -\nabla^2 \tag{2.2.1.5}$$

are linear operators on the one-particle Hilbert space, transforming one-particle functions into other one-particle functions (or $\mathbb{R}^3$-vectors thereof). The expectation value of an observable corresponding to an operator $\hat{o}$ for a particle in a state i is given by

$$\langle o\rangle = \langle i|\hat{o}|i\rangle = \int \psi_i^*(\mathbf{r})\,\hat{o}\psi_i(\mathbf{r})\; d\mathbf{r} \tag{2.2.1.6}$$

The adjoint $\hat{O}^\dagger$ of an operator $\hat{O}$ is given by the relation $\langle \hat{O}^\dagger \psi_i | \psi_j \rangle = \langle \psi_i | \hat{O} \psi_j \rangle$. If $\hat{O}$ is self-adjoint, satisfying $\hat{O} = \hat{O}^\dagger$, then its matrix representation $O^i_j = \left\langle i \middle| \hat{O} \middle| j \right\rangle$ will be Hermitian: $O^i_j = \left(O^j_i\right)^*$. For an observable to be real, its corresponding operator should have real eigenvalues, for which it is sufficient (but not necessary) that it be Hermitian.

2.2.2 Basis sets

Wavefunctions and operators must be discretised in order to be represented on a classical computer. This amounts to expressing the orbitals as linear combinations of some set of basis functions $\chi(\mathbf{r})$.

$$\psi_i(\mathbf{r}) = C^\mu_i \chi_\mu(\mathbf{r}) \tag{2.2.2.1}$$

The basis $\{\chi_\mu\}$ is said to be complete if it spans the entire Hilbert space, satisfying the completeness relation

$$\hat{1} = \sum_\mu |\chi_\mu\rangle \langle \chi_\mu| \tag{2.2.2.2}$$

A finite one-particle basis set does not span the complete Hilbert space of one-electron functions, but instead spans a finite-dimensional one-particle Hilbert space which will be denoted $\mathcal{H}$. Integrals of operators and functions over a continuous variable become multiplications of matrices and vectors over a discrete index, where an operator $\hat{O}$ is represented by the matrix $\mathbf{O}$ with elements O^μ_ν defined by

$$O^\nu_\mu = \langle \mu | \hat{O} | \nu \rangle \tag{2.2.2.3}$$

The inner product becomes the standard (Hermitian) dot product,

$$\begin{aligned} |\psi\rangle &= |\mu\rangle C_\mu \\ |\phi\rangle &= |\mu\rangle B_\mu \\ \langle \phi | \psi \rangle &= \langle \mu | \nu \rangle B^*_\mu C_\nu \\ &= S^\nu_\mu B^*_\mu C_\nu \\ &= \mathbf{B}^\dagger \mathbf{S} \mathbf{C} \end{aligned} \tag{2.2.2.4}$$

where the overlap (metric) matrix $S_\mu^\nu = \langle\mu|\nu\rangle = \delta_\mu^\nu$ if the basis is orthonormal. Applying an operator to a state becomes a matrix multiplication of the coefficients

$$\begin{aligned}\hat{O}\,|\psi\rangle &= |\mu\rangle\,\langle\mu|\hat{O}|\nu\rangle\,C_\nu \\ &= |\mu\rangle\,O_\mu^\nu C_\nu \\ &= |\mu\rangle\,(\mathbf{OC})_\mu\end{aligned} \tag{2.2.2.5}$$

One way to discretise wavefunctions and operators is to represent real space as a grid of points at which a wavefunction may take some value, but this is extremely inefficient for the purposes of most molecular electronic structure problems. Much more efficient is to use known features of the electron density to develop basis sets that capture the important physics in a minimal number of functions. In molecular electronic structure theory, the fact that electron density in a molecule is primarily localised in the neighbourhood of the atomic nuclei leads many basis sets to be chosen to approximate the hydrogen-like (or 'Slater-type') atomic orbitals, with $\mathrm{e}^{-\alpha r}$ dependence on the radial distance from a nucleus and angular dependence given by a spherical harmonic.

Gaussian type functions, with e^{-r^2} radial dependency, are computationally efficient, as the product of two Gaussians is another Gaussian, speeding up integral evaluation.

$$\mathrm{e}^{-a(r-r_1)^2}\mathrm{e}^{-b(r-r_2)^2} = A\mathrm{e}^{-(a+b)(r-r_0)^2} \tag{2.2.2.6}$$

$$A = \mathrm{e}^{-\frac{2ar_1br_2-(2a^2+ab)r_1^2-(ab+2b^2)r_2^2}{a+b}} \tag{2.2.2.7}$$

$$r_0 = \frac{ar_1 + br_2}{a+b} \tag{2.2.2.8}$$

As a result, these are the most common basis functions for molecular electronic structure theory. In order to better approximate the Slater-type orbitals, a basis function may be constructed from multiple Gaussians $\mathrm{e}^{-\zeta r^2}$ with a different scaling factor ζ in the exponent, contracted together with coefficients c:

$$\chi\,(\mathbf{r}) = \sum_i c_i \mathrm{e}^{-\zeta_i r^2} \tag{2.2.2.9}$$

Choosing larger and larger basis sets to approach the complete basis set limit is one half of the procedure to approach the exact solution to the Schrödinger equation (the other being the level of theoretical approximation made to the model wavefunction). Basis sets have been developed to capture as much of the electron density as efficiently as possible for wide varieties of systems. They have also been developed in families of concomitantly increasing size, accuracy, and computational cost. Table 2.1 shows the number of basis functions per atom for a range of basis sets commonly used for wavefunction-based molecular electronic structure methods. The "STO-3G" basis set is a minimal basis set, *i.e.* each atomic orbital is represented by exactly one basis function, and the only virtual orbitals are those left unoccupied in the valence shell. Each Slater type orbital is approximated by an optimised linear combination of 3 Gaussians with different widths and different weights.[95, 96] The "6-31G" basis set is a split-valence basis set of the type developed by John Pople, where the core orbitals are contracted from 6 Gaussians and the valence orbitals are represented by two basis functions, one contracted from 3 Gaussians and the other a single Gaussian.[96, 97] The "cc-PVnZ" basis sets are from the "correlation-consistent" family of basis sets developed by Thom Dunning, with polarisation functions and a split valence with n basis functions for each valence orbital.[96, 98]

Elements	STO-3G	6-31G	cc-PVDZ	cc-PVTZ	cc-PVQZ	cc-PV5Z	cc-PV6Z
H-He	1	2	5	14	30	59	91
Li-Be	5	9	14	30	55	91	140**
B-Ne	5	9	14	30	55	91	140
Na-Mg	9	13	18	34	59	95	
Al-Ar	9	13	18	34	59	95	144
K-Ca	13	27	27*	43*	68*	104*	
Sc-Zn	18	27	43	68	104	153	
Ga-Kr	18	27	27	43	68	104	

Table 2.1: Number of basis functions for different atoms in basis sets of increasing size. * the Dunning-type cc-PVnZ basis sets are not available for potassium. ** the Dunning-type cc-PV6Z basis set is not available for lithium.

The fact that a basis set can be chosen to systematically improve the quality of a calculation at the expense of increased computational cost is an important part

of the general applicability of electronic structure methods. Using a consistent family of basis sets, not only can the systematic improvement in the correlation energy be seen with increasing basis set size, but extrapolation schemes can be implemented to approximate the complete basis set limit, using two or more basis sets in the same family.[99–101] The inclusion of diffuse[102, 103] and polarisation functions[104] allows an accurate treatment of anions and atoms in asymmetric chemical environments, where the electron density may not be close enough to the nuclei to be well represented by the basis sets for neutral isolated atoms. The non-orthogonality of atomic-centred basis sets can lead to basis set superposition errors, particularly in large basis sets, and techniques such as counterpoise correction may be required.[105] For correlated wavefunction-based methods, the Dunning-type family of correlation consistent basis sets best exemplifies a family of basis sets that offers a balanced progression towards the complete basis set limit, and will be used for the majority of calculations in this work. On occasion, the smaller Pople-type 6-31G basis set will be used for small calculations, where reduced computation time is of more importance than numerical accuracy.

2.2.3 Many-body wavefunctions

A wavefunction for N electrons is an element of the space constructed from the direct product of the one particle Hilbert space N times.

$$|\Psi\rangle = \sum_{i_1 i_2 \ldots i_N} c_{i_1 i_2 \ldots i_N} |\psi_{i_1}\rangle \otimes |\psi_{i_2}\rangle \otimes \cdots \otimes |\psi_{i_N}\rangle \in \mathcal{H}^{\otimes N} \tag{2.2.3.1}$$

This space of $N-$electron functions is itself a Hilbert space, with inner product defined by applying the inner product in each copy of the one particle Hilbert space. For two functions Ψ, defined as above, and Φ, defined as follows:

$$|\Phi\rangle = \sum_{j_1 j_2 \ldots j_N} b_{j_1 j_2 \ldots j_N} |\phi_{j_1}\rangle \otimes |\phi_{j_2}\rangle \otimes \cdots \otimes |\phi_{j_N}\rangle \,, \tag{2.2.3.2}$$

the inner product is given by

$$\langle \Phi \,|\, \Psi \rangle = \sum_{i_1 i_2 \ldots i_N} \sum_{j_1 j_2 \ldots j_N} b^{i_1 i_2 \ldots i_N *} c^{j_1 j_2 \ldots j_N} \langle \phi_{i_1} | \psi_{j_1} \rangle \langle \phi_{i_2} | \psi_{j_2} \rangle \ldots \langle \phi_{i_N} | \psi_{j_N} \rangle \tag{2.2.3.3}$$

The simplest wavefunction for multiple electrons in some specified orbitals is the Hartree product, written as a product of one-electron functions for each of the N electrons.

$$\Psi\left(\mathbf{x}_1, \mathbf{x}_2, \ldots, \mathbf{x}_N\right) = \psi_{i_1}\left(\mathbf{x}_1\right) \psi_{i_2}\left(\mathbf{x}_2\right) \ldots \psi_{i_N}\left(\mathbf{x}_N\right) \tag{2.2.3.4}$$

Electrons being fermions, it must be ensured that the wavefunction is antisymmetric with respect to exchange of any two electrons. The simplest such wavefunction is a determinant, known as a Slater determinant (SD).[106]

$$\Psi\left(\mathbf{x}_1, \mathbf{x}_2, \ldots, \mathbf{x}_N\right) = \mathcal{A}\left(\psi_{i_1}\left(\mathbf{x}_1\right), \psi_{i_2}\left(\mathbf{x}_2\right), \ldots, \psi_{i_N}\left(\mathbf{x}_N\right)\right) \tag{2.2.3.5}$$

$$= \frac{1}{\sqrt{N!}} \begin{vmatrix} \psi_{i_1}\left(\mathbf{x}_1\right) & \psi_{i_2}\left(\mathbf{x}_1\right) & \cdots & \psi_{i_N}\left(\mathbf{x}_1\right) \\ \psi_{i_1}\left(\mathbf{x}_2\right) & \psi_{i_2}\left(\mathbf{x}_2\right) & \cdots & \psi_{i_N}\left(\mathbf{x}_2\right) \\ \vdots & \vdots & \ddots & \vdots \\ \psi_{i_1}\left(\mathbf{x}_N\right) & \psi_{i_2}\left(\mathbf{x}_N\right) & \cdots & \psi_{i_N}\left(\mathbf{x}_N\right) \end{vmatrix} \tag{2.2.3.6}$$

The Slater determinants form a basis for the space of antisymmetric states of N electrons in n orbitals *i.e.* any multiple-electron wavefunction that guarantees this antisymmetry can be expressed as a linear combination of SDs. The "exact" lowest energy state within this antisymmetrised Hilbert space will be that obtained by Full Configuration Interaction (FCI). This space is sometimes known as the FCI Hilbert space, or the N-electron sector of Fock space (see subsection 2.2.4).

Given a set of orthonormal orbitals, the Slater determinants are just one possible basis for the FCI Hilbert space. Alternative N-electron basis functions can be constructed as linear combinations of SDs, such as the Configuration State Functions (see section 2.3.2). For many systems, which can be said to show weak correlation, a single Slater determinant also constitutes a good approximation to the physical ground state, but in cases of static correlation a single CSF can provide a better reference.

The N-electron FCI Hilbert space can be considered mathematically as the N-fold alternating product on the one-particle Hilbert space.

$$\mathcal{F}_N = \mathcal{A}\left(\mathcal{H}^{\otimes N}\right) \tag{2.2.3.7}$$

Operators on this space of functions can be categorised by the number of factors of the one-particle Hilbert space they act on. Many operators only act on one electron (*e.g.* position, momentum, or kinetic energy) or two electrons (*e.g.* Coulombic repulsion) at a time, within an antisymmetrised N-electron state $|\Psi\rangle$:

$$\hat{O}_1 |\Psi\rangle = \mathcal{A}\left(\hat{o}_1 \psi_{i_1}\left(\mathbf{x}_1\right), \psi_{i_2}\left(\mathbf{x}_2\right), \ldots, \psi_{i_N}\left(\mathbf{x}_N\right)\right) \tag{2.2.3.8}$$

$$\hat{O}_2 |\Psi\rangle = \mathcal{A}\left(\hat{o}_2\left(\psi_{i_1}\left(\mathbf{x}_1\right), \psi_{i_2}\left(\mathbf{x}_2\right)\right), \ldots, \psi_{i_N}\left(\mathbf{x}_N\right)\right) \tag{2.2.3.9}$$

Such operators can be considered to act on one or two copies of $\mathcal{H}$, with the other copies of $\mathcal{H}$ left unchanged (*i.e.* acted only on by the identity $\hat{1}$):

$$\hat{O}_1 = \left(\hat{o}_1\right)_1 \otimes \hat{1}_2 \otimes \hat{1}_3 \otimes \cdots \otimes \hat{1}_N \tag{2.2.3.10}$$

$$\hat{O}_2 = \left(\hat{o}_2\right)_{1,2} \otimes \hat{1}_3 \otimes \cdots \otimes \hat{1}_N \tag{2.2.3.11}$$

2.2.4 Second Quantization

Given a set of spin-orbitals $\{\phi_i\}$, a SD can be uniquely identified, up to multiplication by a scalar, by the occupation numbers k_i (0 or 1) for each spin-orbital.

$$|k_1, k_2, \ldots, k_n\rangle \tag{2.2.4.1}$$

where $k_i = 0$ represents ϕ_i being vacant in the corresponding SD, and $k_i = 1$ it being occupied.

A Fock space for a system of fermions can be defined as the direct sum of antisymmetrized Hilbert spaces constructed from the products of all orders of the one particle Hilbert space.[107]

$$\mathcal{F} = \sum_{N=0}^{\infty} \mathcal{F}_N \tag{2.2.4.2}$$

The occupation number representation of Slater determinants reveals their significance as basis vectors for this Fock space. The operators that transform between antisymmetric many-electron wavefunctions can now be mapped to a set of operators that transform between Fock space vectors.[107] This formalism, known as second quantization, is useful for many-body methods such as coupled

cluster theory, as it expresses operators independently of the total number of particles in the system.

For some set of one-particle states $\{\phi_i\}$ forming a basis for the one-particle Hilbert space, the annihilation operators $\hat{a}_i$ and the creation operators $\hat{a}^i$ are defined

$$\hat{a}^i \left|k_1, k_2, \ldots, k_i, \ldots, k_n\right\rangle = \delta_{0,k_i} (-1)^{\sum_{p=1}^{i-1} k_p} \left|k_1, k_2, \ldots, 1_i, \ldots, k_n\right\rangle \tag{2.2.4.3}$$

$$\hat{a}_i \left|k_1, k_2, \ldots, k_i, \ldots, k_n\right\rangle = \delta_{1,k_i} (-1)^{\sum_{p=1}^{i-1} k_p} \left|k_1, k_2, \ldots, 0_i, \ldots, k_n\right\rangle \tag{2.2.4.4}$$

and are adjoint to each other: $\hat{a}^i = \hat{a}_i^\dagger$. The Kronecker deltas δ_{0,k_i} and δ_{1,k_i} indicate that the creation and annihilation operators $\hat{a}^i$ and $\hat{a}_i$ act only on states in which $\{\phi_i\}$ is respectively unoccupied or occupied, otherwise the entire state goes to 0. The phase factor $(-1)^{\sum_{p=1}^{i-1} k_p}$ appears due to the fermionic antisymmetry.

Our notation for the elementary operators in second quantization borrows a convention from tensor algebra, in which the quantities have components that are covariant or contravariant with the basis, and are expressed respectively with indices in subscript or superscript. An elementary annihilation operator referring to an orbital ϕ_i is written as $\hat{a}_i$, with the index as subscript. These operators are themselves elements of a vector space, spanned by the $\hat{a}_\mu$ corresponding to annihilation from the basis functions ϕ_μ spanning $\mathcal{H}$.

The creation operators map from the annihilation operators to scalars (which are basis-invariant) and so form a basis for the dual space for this vector space. Accordingly, they are expressed with superscript indices. When an operator is expressed as a coefficient tensor multiplied by some creation and annihilation operators, the tensor will have lower (contravariant) indices that match those of the creation operators, and upper (covariant) indices that match those of the annihilation operators. Applying the Einstein summation convention, each index appearing once as superscript and once as subscript is summed over, to leave an operator-valued quantity that is invariant to rescaling of the basis.

The creation and annihilation operators satisfy anticommutation relations

$$\left[\hat{a}^i, \hat{a}^j\right]_+ = \left[\hat{a}_i, \hat{a}_j\right]_+ = 0 \tag{2.2.4.5}$$

$$\left[\hat{a}^i, \hat{a}_j\right]_+ = \delta_j^i \tag{2.2.4.6}$$

which preserve the antisymmetry of the states on which they act. $[,]_+$ here represents the anticommutator $[x,y]_+ = xy + yx$, to distinguish it both from the standard commutator $[x,y] = xy - yx$ and from the curly braces $\{\}$ that will later be used to denote normal ordering (see section 2.2.5).

The second-quantized operators are basis set dependent, since they only act within the finite-dimensional Fock space induced by the finite one-particle basis set. Any operator acting within this Fock space can be written in terms of these creation and annihilation operators. If an operator conserves particle number, it must only contain terms that are composed of an equal number of creation operators and annihilation operators. For example, the one-body (spin-)orbital substitution operators can be written as $\hat{X}^i_j = \hat{a}^i\hat{a}_j$, and any one-body operator acting in the Fock space can be written as a linear combination of these

$$\hat{O}_1 = O^j_i \hat{a}^i \hat{a}_j \tag{2.2.4.7}$$

for some coefficients O^j_i.

2.2.5 Normal Ordering

A normal ordering of operators is one in which all creation operators appear to the left of all annihilation operators. Since an annihilation operator acting to the right on the vacuum, or a creation operator acting to the left on the vacuum, will result in zero, the vacuum expectation value of any normal-ordered product is also zero, unless the operator is a scalar.

Any product of operators has a normal-ordered form, denoted between curly braces $\{\}$, in which the operators have been arranged in normal order, with the appropriate change of sign for any pairs of fermionic operators that have been commuted. For example:

$$\left\{\hat{a}_k\hat{a}^i\hat{a}_l\hat{a}^j\right\} = -\hat{a}^i\hat{a}^j\hat{a}_k\hat{a}_l \tag{2.2.5.1}$$

The power of normal ordering appears after a new, "Fermi" vacuum is defined, in which a certain set of orbitals are already occupied. The orbitals that are vacant

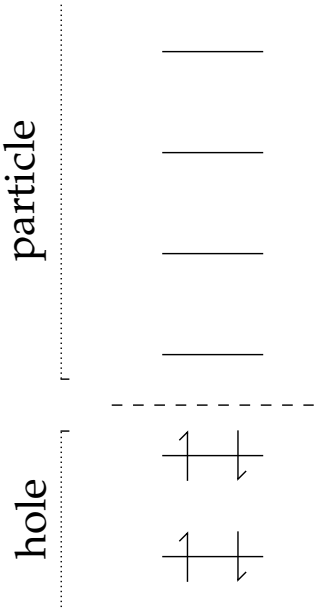

Figure 2.1: Particle and hole orbitals are defined in the Fermi vacuum

in the Fermi vacuum are labelled "particle" orbitals, and those that are occupied in the vacuum are labelled "hole" orbitals, as shown in figure 2.1. Creation and annihilation operators for an electron in the hole orbitals are considered respectively as annihilation and creation of a hole, *i.e.* the positively charged quasiparticle arising from the absence of an electron in an orbital that is occupied in the vacuum. Operators representing excitations of electrons from occupied to virtual orbitals in the vacuum now constitute creation of particle and hole pairs, simplifying the evaluation of matrix elements in the construction of many-body equations. Formally redefining the creation and annihilation operators

$$\hat{b}_i = \hat{a}_i, \qquad \hat{b}^i = \hat{a}^i \qquad i \in \{\text{particle}\} \tag{2.2.5.2}$$

$$\hat{b}_i = \hat{a}^i, \qquad \hat{b}^i = \hat{a}_i \qquad i \in \{\text{hole}\} \tag{2.2.5.3}$$

leaves the anticommutation relations unchanged (it is a canonical transformation). The quasiparticle (*i.e.* with respect to the Fermi vacuum) electrons and holes both still behave as fermions.

2.2.6 Contractions

The Fermionic antisymmetry is encoded in the anticommutation relations of the second-quantized operators. The Kronecker deltas that appear in these relations lead to a rank reduction in the operators, and constitute a contraction in the corresponding coefficient tensors. For some general one-electron creation operators $\hat{A}$ and $\hat{B}$

$$\begin{aligned} \hat{A} &= A^i \hat{a}_i \\ \hat{B} &= B^i \hat{a}_i \\ \left[\hat{A}, \hat{B}^\dagger\right]_+ &= A^i B_j \left[\hat{a}_i, \hat{a}^j\right]_+ = A^i B_j \delta_i^j = A^i B_i \end{aligned} \tag{2.2.6.1}$$

Number-conserving operators will always have an even number of creation and annihilation operators, so there will be no sign flip when commuting two of these operators. If two operators conserve particle number and there are no possible contractions between them, then they will commute.

The term 'normal ordered product,' is also used to describe a product of two operators where terms involving contractions between the two operators are neglected. The notation $\left\{\hat{A}\hat{B}\right\}$ is used to denote this product for two operators $\hat{A}$ and $\hat{B}$. If $\hat{A}$ and $\hat{B}$ are themselves in normal order, then this product will be fully normal-ordered, but if $\hat{A}$ or $\hat{B}$ is not in normal order, then there is an ambiguity that should be made clear from context. It is useful at this stage to note that, within a normal ordered product, operators each consisting of an even number of creation/annihilation operators (so that there is no overall sign flip) will commute under a normal-ordered product.

Writing out the anticommutator $\left[\hat{A}, \hat{B}^\dagger\right]_+ = \hat{A}\hat{B}^\dagger + \hat{B}^\dagger\hat{A}$,

$$\begin{aligned} \hat{A}\hat{B}^\dagger &= -\hat{B}^\dagger\hat{A} + A^i B_i \\ &= \left\{\hat{A}\hat{B}^\dagger\right\} + \overbrace{AB^\dagger} \end{aligned} \tag{2.2.6.2}$$

where the normal-ordered term $\left\{\hat{A}\hat{B}^\dagger\right\} = -\hat{B}^\dagger\hat{A}$ has picked up a change of sign from the anticommutator, and $\hat{A}$ and $\hat{B}^\dagger$ are contracted together in the term $A^i B_i$, as symbolised by the notation $\overbrace{AB^\dagger}$.

2.2.7 Wick's Theorem

Repeated application of this form of the anticommutation relation leads to Wick's theorem, which states that any product of operators can be written as the sum of its normal ordered form and the normal ordered form of every possible contracted product.[85, 108] For example,

$$\begin{aligned}\hat{a}_i\hat{a}^j\hat{a}_k\hat{a}_l\hat{a}^m\hat{a}^n = \Big(&\left\{\hat{a}_i\hat{a}^j\hat{a}_k\hat{a}_l\hat{a}^m\hat{a}^n\right\} \\ &+ \delta_i^j\left\{\hat{a}_k\hat{a}_l\hat{a}^m\hat{a}^n\right\} + \text{other single contractions} \\ &+ \delta_i^j\delta_k^m\left\{\hat{a}_l\hat{a}^n\right\} + \text{other double contractions} \\ &+ \delta_i^j\delta_l^m\delta_k^n - \delta_i^j\delta_k^m\delta_l^n\Big)\end{aligned}$$

An important consequence of Wick's theorem is that a vacuum expectation value has non-zero contributions only from those terms that are fully contracted to a scalar.

$$\left\langle (o_1)^i_j\,\hat{a}_i\hat{a}^j\,(o_2)^{kl}_{mn}\,\hat{a}_k\hat{a}_l\hat{a}^m\hat{a}^n\right\rangle = (o_1)^i_j\,(o_2)^{kl}_{mn}\left(\delta_i^j\delta_l^m\delta_k^n - \delta_i^j\delta_k^m\delta_l^n\right) \tag{2.2.7.1}$$

Contributions to tensors of non-zero rank can be found as those with indices left to be contracted. Finding such tensor contributions is central to the construction of equations in many-body methods such as perturbation theory and coupled cluster. Approaches to this task generally fall in to one of two categories. So-called "many-body" approaches build up the tensor in the correct form by progressively multiplying the constituent tensors and applying contractions. The alternative is a projective approach, in which the tensor is projected onto a tensor of the conjugate shape (*i.e.* with the upper and lower indices exchanged) and the non-zero contributions to the vacuum expectation value are calculated as the fully contracted terms. For simplicity and robustness of implementation, the projective approach will be the one taken in this work (see section 4.2).

2.3 Spin adaptation

The B–O Hamiltonian in the absence of an external field is independent of spin; that is, it commutes with the total (squared) and projected spin operators.

$$\left[\hat{H}, \hat{S}^2\right] = \left[\hat{H}, \hat{S}_z\right] = 0$$

There exists a set of eigenfunctions of the Hamiltonian that are also eigenfunctions of the projected spin $\hat{S}_z$ (with eigenvalues denoted M_S) and the total spin squared $\hat{S}^2 = \hat{\mathbf{S}} \cdot \hat{\mathbf{S}}$ (with eigenvalues $S\,(S+1)$, where S is the total spin quantum number). There is no eigenbasis of the vector operator for total spin $\hat{\mathbf{S}}$, due to a Heisenberg uncertainty principle between the components $\hat{S}_x, \hat{S}_y, \hat{S}_z$, but total spin S is a 'good' quantum number, of which the wavefunction can be constructed as an eigenfunction. By limiting the problem to states of one total spin eigenvalue, there is a potential benefit to computational efficiency, as the space in which the solution is being found is smaller. The separation of states of the desired spin from the rest of the N-particle Hilbert space can facilitate the identification of the approximate states obtained with the corresponding exact Hamiltonian eigenstates, and allow the calculation of spin-dependent properties.

The number of SDs for N electrons in $2n$ spin-orbitals is $\binom{2n}{N} = \frac{(2n)!}{N!(2n-N)!}$. Restricting to SDs with a given projected spin $M_S = N_\alpha - N_\beta$, the dimension of the FCI space is $\binom{n}{N+\frac{1}{2}M_S}\binom{n}{N-\frac{1}{2}M_S}$. The dimension of the spin-adapted subspace with the correct spin quantum number S and projected spin M_S is further reduced, given by Weyl's dimension formula,[109]

$$d = \frac{2S+1}{n+1}\binom{n+1}{n-\frac{1}{2}N-S}\binom{n+1}{\frac{1}{2}N-S} \tag{2.3.0.1}$$

2.3.1 Spin Contamination

The set of spin-orbitals used to construct a SD may be divided into those occupied by α electrons and those occupied by β. Methods which use the same spatial parts for those two sets of spin-orbitals are usually termed "restricted," in contrast

to "unrestricted" methods, in which the α orbitals differ from the β. A spin-unrestricted method will usually not produce a spin eigenfunction; often the wavefunction is contaminated with contributions from states of higher spin eigenvalues.[110]

2.3.1.1 Spin-contaminated reference states

Single SDs are not in general eigenfunctions of total spin, whether or not they are constructed with the same set of spatial orbitals for α and β electrons.

$$\left\langle \mathrm{SD} \left| \hat{S}^2 \right| \mathrm{SD} \right\rangle = \left\langle \mathrm{SD} \left| \hat{S}_z + \hat{S}_z^2 + \hat{S}_- \hat{S}_+ \right| \mathrm{SD} \right\rangle = M_S + M_S^2 + N_\beta - \sum_i^{\alpha,occ} \sum_j^{\beta,occ} \left| \langle \phi_i^\alpha | \phi_j^\beta \rangle \right|^2$$

A single SD will only be a spin eigenfunction if the electrons in open-shell orbitals (if there are any) are all aligned with the same m_S, i.e. they are all α or all β. These states maximise S for a given occupation of the (spatial) orbitals and so are termed "high-spin" configurations, but moreover they maximise the magnitude of M_S as well, with $M_S = \pm S$ (usually the positive choice is the one being considered). In those two cases, it can also be easily verified (e.g. by taking $M_S = S$, $N_\beta = 0$ or $M_S = -S$, $N_\beta = 2S$), that the $M_S = \pm S$ high-spin determinants are eigenfunctions of $\hat{S}^2$ with eigenvalue $S(S+1)$.

For a low spin configuration, or for an $|M_S| < S$ component of a high spin multiplet, instead of a single SD, the reference state should be a linear combination of SDs, known as a Configuration State Function (CSF), that correctly satisfies the total spin-squared eigenvalue equation.

$$\hat{S}^2 |\Phi_0\rangle = S(S+1) |\Phi_0\rangle \tag{2.3.1.1}$$

An example of such a configuration is the 2-electron open shell singlet, which requires 2 determinants to be represented.

$$|N=2, S=0\rangle \quad = \quad \begin{array}{|c|c|} \hline \uparrow & \downarrow \\ \hline \end{array} \quad - \quad \begin{array}{|c|c|} \hline \downarrow & \uparrow \\ \hline \end{array}$$

Figure 2.2: The 2-electron open-shell singlet, represented for two arbitrary orbitals

2.3.1.2 Spin-preserving wave operators

Avoiding spin contamination, even starting from a spin-pure reference, also requires use of a cluster operator that preserves total spin. The preservation of projected spin is trivially achieved by the fact that, in every term of the cluster operator, for each α annihilation operator there is an α creation operator, and for each β annihilation there is a β creation.

In order to preserve total spin, the excitations should be defined in spin-restricted orbitals, and summed up over all possible spin variations. This gives a cluster operator that is overall a spin singlet and hence that commutes with the total spin operator.[76]

For open shell systems, these spin free excitations may involve the singly-occupied orbitals in both the creation and annihilation spaces, and so no longer commute with each other.[111] This will mean that several aspects of the coupled cluster ansatz need to be modified, as discussed later.

2.3.2 Configuration State Functions

A CSF can be constructed by applying a genealogical spin-coupling scheme. This involves successively adding smaller angular momentum eigenfunctions using the Clebsch–Gordan coefficients.[109]

The open-shell part of the reference is a CSF of N electrons in N orbitals with total spin S and projected spin M, expressed through a linear combination of creation operator strings acting upon a closed shell vacuum, $|\Phi_0\rangle = |N, S, M; \mathbf{t}\rangle = \hat{O}_N^{S,M}(\mathbf{t})\,|0\rangle$[76]. When there are more than two open-shell electrons there can be cases of spin degeneracy, with more than one independent multiplet of the same N, S, M_S. Each specific CSF is then identified by its unique genealogical coupling vector $\mathbf{t}$. The creation operator $\hat{O}_N^{S,M}(\mathbf{t})$ is built up by recursively applying the definition

$$\hat{O}_N^{S,M}(\mathbf{t}) = C^{S,M}_{t_N,\frac{1}{2}}\hat{O}_{N-1}^{S-t_N,M-\frac{1}{2}}(\mathbf{t})\hat{a}^{N\alpha} + C^{S,M}_{t_N,-\frac{1}{2}}\hat{O}_{N-1}^{S-t_N,M+\frac{1}{2}}(\mathbf{t})\hat{a}^{N\beta} \qquad (2.3.2.1)$$

This recursive construction is known as a genealogical coupling scheme, as it depends on the history, specified by $\mathbf{t}$, of the configurations as the angular momentum of each electron is added in turn.[109] Each component t_N denotes whether each electron increases the total spin ($t_N = +\frac{1}{2}$) or decreases it ($t_N = -\frac{1}{2}$) when added ($\hat{a}^{N\alpha/\beta}$) in the N-th orbital to the previous $(N-1)$-electron CSF. The Clebsch-Gordan coefficients $C^{S,M}_{t_N,\pm\frac{1}{2}}$ for addition of a single electron simplify to $C^{S,M}_{+\frac{1}{2},\pm\frac{1}{2}} = \sqrt{\frac{S\pm M}{2S}}$ and $C^{S,M}_{-\frac{1}{2},\pm\frac{1}{2}} = \mp\sqrt{\frac{S\mp M+1}{2S+2}}$. For example, an open-shell singlet in orbitals p and q is formed from the closed shell vacuum $|0\rangle$ by the operator

$$\hat{O}^{0,0}_2 = \frac{1}{\sqrt{2}}\left(\hat{a}^{p\alpha}\hat{a}^{q\beta} - \hat{a}^{p\beta}\hat{a}^{q\alpha}\right) \tag{2.3.2.2}$$

and the $M = 0$ component of a triplet by

$$\hat{O}^{1,0}_2 = \frac{1}{\sqrt{2}}\left(\hat{a}^{p\alpha}\hat{a}^{q\beta} + \hat{a}^{p\beta}\hat{a}^{q\alpha}\right) \tag{2.3.2.3}$$

There are several different schemes by which a many-electron spin eigenfunction may be built up from smaller subunits. The numbers of possible CSFs of each total spin S for each number of electrons N can be seen on a branching diagram, figure 2.3.[109]

These Young–Yamanouchi coupling schemes can be shown to generate CSFs that form an orthogonal basis for the selected spin sector of the FCI Hilbert space. The coupling scheme defines a group subduction chain, under which each CSF transforms as a different irreducible representation. The CSFs adapted to a group subduction chain are therefore guaranteed to form an orthogonal basis.[112–115]

When constructing CSFs one electron at a time, the intermediate configurations of $1, 2, \ldots, N-1$ electrons transform as irreducible representations of the permutation (symmetric) group of order $1, 2, \ldots, N-1$, denoted S_1, S_2, etc. The resulting CSFs are said to be adapted to the group subduction chain

$$S_N \supset S_{N-1} \supset \ldots \supset S_1 \tag{2.3.2.4}$$

Methods using CSFs formed by this (electron-by-electron) scheme are consequently known as symmetric group approaches.[116, 117]

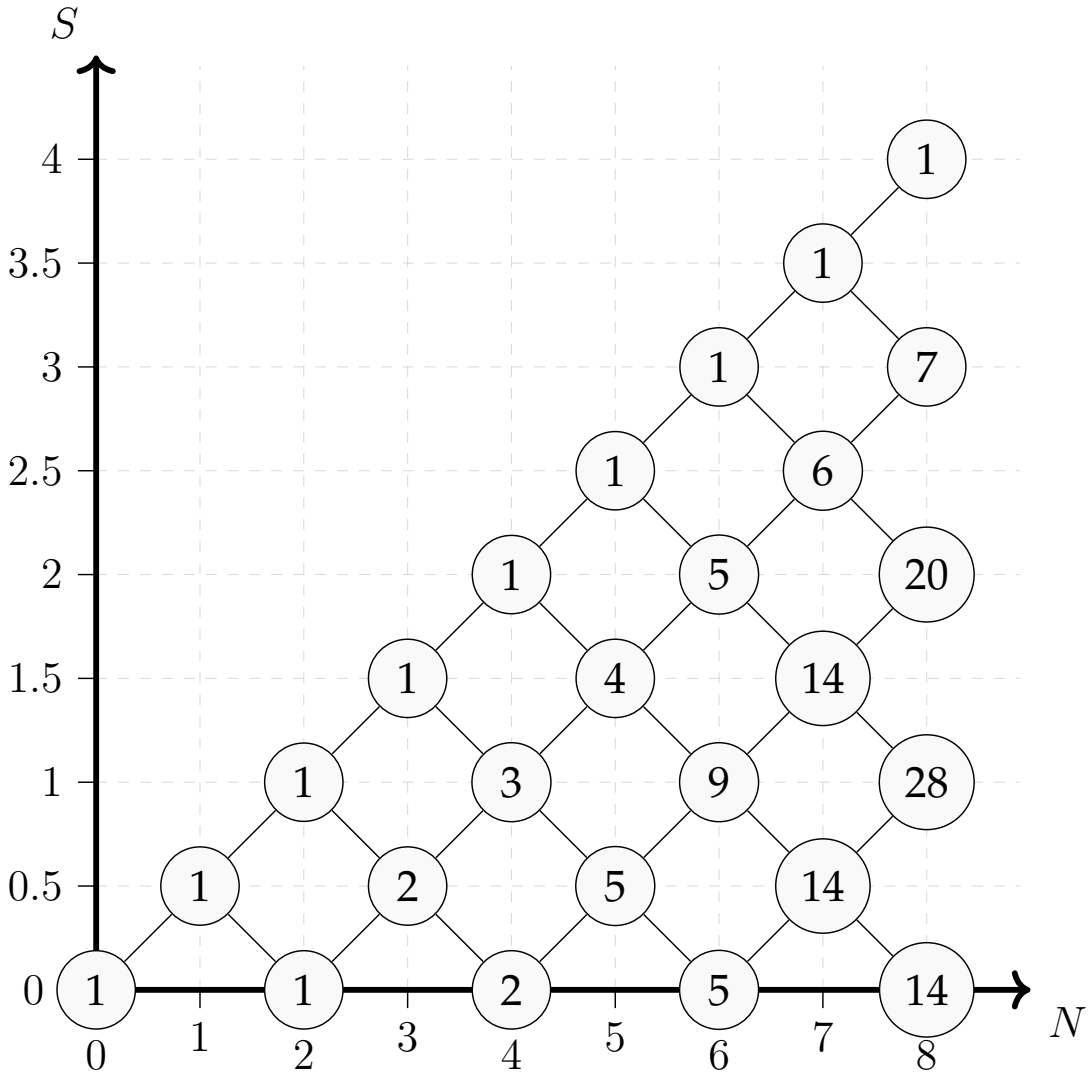

Figure 2.3: Branching diagram to show the number of independent CSFs for each number N of open-shell electrons and total spin S.

When constructing CSFs one (spatial) orbital at a time, the intermediate configurations, with $1, 2, \ldots, n$ orbitals, transform as irreps of the unitary group of order $1, 2, \ldots, n$, giving CSFs that are adapted to the group subduction chain

$$U(n) \supset U(n-1) \supset \ldots \supset U(1) \tag{2.3.2.5}$$

Methods using CSFs formed by this (orbital-by-orbital) scheme are consequently known as unitary group approaches.[109, 116] A basis of CSFs constructed by such a group subduction chain is known as a Gel'fand–Tsetlin basis.[115, 118, 119]

While the two approaches generate the same number of orthogonal basis

states for the overall spin-adapted Hilbert space, the SGA, which only considers the open-shell orbitals, splits the Hilbert space into sectors of different numbers of open-shell orbitals, or 'seniority'. Seniority is not generally preserved by the Hamiltonian, so multiple symmetric groups S_N will be required in order to represent the interacting subspaces in coupled cluster, compared to just a single unitary group $U(n)$, where n is the (constant) number of basis functions in the one-particle Hilbert space.[116] A single CSF reference state may be considered as having been constructed in either coupling scheme, but in forming operators for spin-adapted coupled cluster, the unitary group will be the more appropriate.[120]

2.3.3 The Unitary Group

The unitary group of order n is the group of $n \times n$ matrices U with the property $UU^\dagger = U^\dagger U = 1$. This is the group of automorphisms on the space of normalised functions spanned by n basis functions, or in other words the group of "rotations" of n orbitals that preserve the 1-particle Hilbert space they span. The excitation operators $\hat{X}^p_q = \hat{a}^p \hat{a}_q$ obey the commutation relations

$$\left[\hat{X}^p_q, \hat{X}^r_s\right] = \hat{X}^p_q \hat{X}^r_s - \hat{X}^r_s \hat{X}^p_q = \hat{X}^p_s \delta^r_q - \hat{a}^p \hat{a}^r \hat{a}_q \hat{a}_s - \hat{X}^r_q \delta^p_s + \hat{a}^r \hat{a}^p \hat{a}_s \hat{a}_q = \hat{X}^p_s \delta^r_q - \hat{X}^r_q \delta^p_s \tag{2.3.3.1}$$

If p, q, r, s run from 1 to $2n$, this is an expression of the structure constants for $\mathfrak{u}(2n)$, the Lie algebra whose elements u generate the unitary group $U(2n)$ when the exponential map $U = \mathrm{e}^{\mathrm{i}u}$ is applied. The excitation operators $\hat{X}^p_q$ form a basis for $\mathfrak{u}(2n)$, and are known as (infinitesimal) generators of the Lie group $U(2n)$.[109, 120, 121]

When restricting $2n$ spin-orbitals to have the same spatial parts for α and β spins, the subgroup $U(2n) \supset U(n) \times U(2)$ is considered. The spin part of the wavefunction transforms as an irreducible representation of $U(2)$, and the spatial part as one of $U(n)$.[121, 122]

The spin free excitation operators $\hat{E}_q^p$ are (infinitesimal) generators of the unitary group $U(n)$.[121]

$$\hat{E}_q^p = \hat{a}^{p\alpha}\hat{a}_{q\alpha} + \hat{a}^{p\beta}\hat{a}_{q\beta} \tag{2.3.3.2}$$

$$\left[\hat{E}_q^p, \hat{E}_s^r\right] = \hat{E}_s^p\delta_q^r - \hat{E}_q^r\delta_s^p \tag{2.3.3.3}$$

Two- and higher-body unitary group generators can be defined by similarly tracing out the spins of each electron:

$$\hat{E}_{rs}^{pq} = \sum_{\sigma_1\sigma_2} \hat{a}^{p\sigma_1}\hat{a}^{q\sigma_2}\hat{a}_{s\sigma_2}\hat{a}_{r\sigma_1}$$

The N-electron sector of Fock space is the antisymmetric part of the N-fold tensor product of the 1-particle Hilbert space.

$$\mathcal{F}_N = \mathcal{A}\left(\mathcal{H}^{\otimes N}\right) \tag{2.3.3.4}$$

Considering the action of the symmetric group S_N to permute the N factors of the one-electron Hilbert space, then the Pauli principle requires that all N-fermion wavefunctions must transform as the totally antisymmetric representation of S_N.

The unitary group $U(2n)$ is the group of automorphisms of the one-electron Hilbert space. When considering $U(2n)$ to act on all N factors of $\mathcal{H}$ in $\mathcal{F}_N$, the wavefunction must also transform as an irreducible representation of $U(2n)$. By a Schur-Weyl duality between the permutation group S_N and the unitary group $U(2n)$,[123, 124] the irreducible representations of $U(2n)$ are in one-to-one correspondence with the irreducible representations of S_N.

The irreducible representations of the permutation group S_N, and therefore also the irreps of $U(2n)$, can be labelled by Young diagrams.[122, 125] A standard Young diagram displays a partition of N boxes into rows of non-increasing length, *e.g.*:

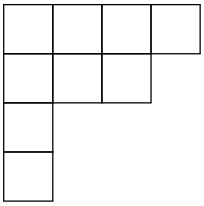

A conjugacy class in S_N consists of those permutations that may be decomposed into a set of cyclic permutations of the same orders. The orders of those cyclic permutations are the lengths of the rows in the corresponding Young diagram. For example, the Young diagram above represents the class of all permutations of 9 objects that can be decomposed into a 4-cycle, a 3-cycle, and two 1-cycles.

The elements of a conjugacy class may be specified by filling the boxes with number ("tokens"). A Young diagram that has been filled in with tokens is known as a Young tableau. For example, some permutations of 9 objects that belong to the class labelled by the Young diagram above are:

$$\begin{pmatrix}1&2&3&4&5&6&7&8&9\\2&3&4&1&6&7&5&8&9\end{pmatrix} = \begin{pmatrix}1&2&3&4\\2&3&4&1\end{pmatrix}\begin{pmatrix}5&6&7\\6&7&5\end{pmatrix}\begin{pmatrix}8\\8\end{pmatrix}\begin{pmatrix}9\\9\end{pmatrix}$$
$$\begin{pmatrix}1&2&3&4&5&6&7&8&9\\7&5&3&1&6&9&4&8&2\end{pmatrix} = \begin{pmatrix}2&5&6&9\\5&6&9&2\end{pmatrix}\begin{pmatrix}1&4&7\\7&1&4\end{pmatrix}\begin{pmatrix}3\\3\end{pmatrix}\begin{pmatrix}8\\8\end{pmatrix}$$

Since conjugacy classes correspond one-to-one with irreducible representations, the Young diagrams may also label irreps of S_N. These generalise the notion of symmetric and antisymmetric tensors to other symmetrisations (the technical details of the use of Schur functors to do this are not important here).[126] In this context, each row represents a symmetrisation, while each column represents an antisymmetrisation. Basis vectors for an irreducible representation can be specified by filling a Young diagram with tokens to form a Young tableau. For irreps of the unitary group, these Young tableaux are 'semistandard,' meaning that the tokens strictly increase down each column, and are non-decreasing across each row.[122]

With a spin-free Hamiltonian, the energy depends only on the spatial part of the wavefunction, which may be separated from the spin part by considering the subgroup

$$U(n) \times U(2) \subset U(2n) \tag{2.3.3.5}$$

(the distinction between $U(2)$ and $SU(2)$ for the spin group is not important here). The Young tableaux labelling irreps of $U(2)$ and $U(n)$ can have at most 2 and

n rows respectively, since it is not possible to antisymmetrise over a column longer than this.

Those irreducible representations of $U(n) \times U(2)$ that are also totally antisymmetric representations of S_N are direct products of conjugate representations of $U(n)$ and $U(2)$.[122] Conjugate tableaux are those that differ by a reflection across the diagonal, i.e. interchanging rows for columns and vice versa. This generalises the notion of symmetric spin functions being matched with antisymmetric spatial functions, and vice versa.

For example, a triplet of 4 electrons in 3 orbitals transforms as the $U(n) \times U(2)$ labelled

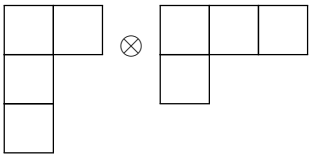

where the three components of the triplet could be specified by filling tokens to give the Young tableaux

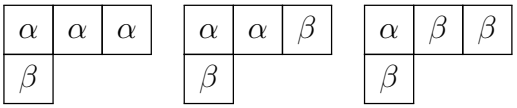

With 4 electrons in only 3 orbitals, there is only one triplet possible, and the spatial part of the wavefunction transforms as a 1-dimensional irrep, corresponding to the Young tableau

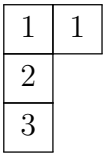

When writing these out as Slater determinants, the familiar triplet wavefunctions are obtained, with $M_S = +1, 0, -1$.

For a 4-electron singlet, the spin part transforms as the 1-dimensional $U(2)$ irrep

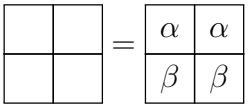

The spatial part transforms as the 6-dimensional $U(3)$ irrep

$$\begin{array}{|c|c|}\hline \ & \ \\ \hline \ & \ \\ \hline \end{array} = \left\{ \begin{array}{|c|c|}\hline 1 & 1 \\ \hline 2 & 2 \\ \hline \end{array} \quad \begin{array}{|c|c|}\hline 1 & 1 \\ \hline 3 & 3 \\ \hline \end{array} \quad \begin{array}{|c|c|}\hline 2 & 2 \\ \hline 3 & 3 \\ \hline \end{array} \quad \begin{array}{|c|c|}\hline 1 & 1 \\ \hline 2 & 3 \\ \hline \end{array} \quad \begin{array}{|c|c|}\hline 1 & 2 \\ \hline 2 & 3 \\ \hline \end{array} \quad \begin{array}{|c|c|}\hline 1 & 2 \\ \hline 3 & 3 \\ \hline \end{array} \right\}$$

Of these 6 basis vectors, the first 3 correspond to the closed shell singlet configurations

$$|\phi_{1\alpha}\phi_{1\beta}\phi_{2\alpha}\phi_{2\beta}\rangle\,, \qquad |\phi_{1\alpha}\phi_{1\beta}\phi_{3\alpha}\phi_{3\beta}\rangle\,, \qquad |\phi_{2\alpha}\phi_{2\beta}\phi_{3\alpha}\phi_{3\beta}\rangle\,,$$

while the last 3 correspond to the open shell singlets

$$\begin{aligned} &\frac{1}{\sqrt{2}}\left(|\phi_{1\alpha}\phi_{1\beta}\phi_{2\alpha}\phi_{3\beta}\rangle - |\phi_{1\alpha}\phi_{1\beta}\phi_{3\alpha}\phi_{2\beta}\rangle\right) \\ &\frac{1}{\sqrt{2}}\left(|\phi_{1\alpha}\phi_{2\beta}\phi_{2\alpha}\phi_{3\beta}\rangle - |\phi_{2\alpha}\phi_{1\beta}\phi_{3\alpha}\phi_{2\beta}\rangle\right) \\ &\frac{1}{\sqrt{2}}\left(|\phi_{1\alpha}\phi_{2\beta}\phi_{3\alpha}\phi_{3\beta}\rangle - |\phi_{2\alpha}\phi_{1\beta}\phi_{3\alpha}\phi_{3\beta}\rangle\right) \end{aligned}$$

2.3.4 GUGA construction of CSFs

In the genealogical coupling scheme used to construct CSFs in a unitary group approach, the subsystem angular momenta are taken to be those corresponding to each spatial orbital in turn. There are four options for each orbital: it may be vacant ($d = 0$), singly occupied and coupled so as to increase total spin S by $\frac{1}{2}$ ($d = 1$), singly occupied and coupled so as to decrease total spin S by $\frac{1}{2}$ ($d = 2$), or doubly occupied ($d = 3$).[127] Where single SDs are invariant to unitary transformations within the occupied and virtual spaces, CSFs in the GUGA basis are invariant to unitary transformations within the double occupied and virtual spaces, as well as subspaces defined by each series of consecutive open-shell orbitals having the same value of d.

The "Graphical" aspect of GUGA comes from the construction of Shavitt graphs, which reveal this invariance.[49] Figure 2.4 shows lines at four different inclinations to depict the four possibilities for coupling an additional orbital to a partial CSF.

Beginning from the origin at the bottom of the diagram, a directed walk represents one CSF of a particular N, S. The set of all possible directed walks

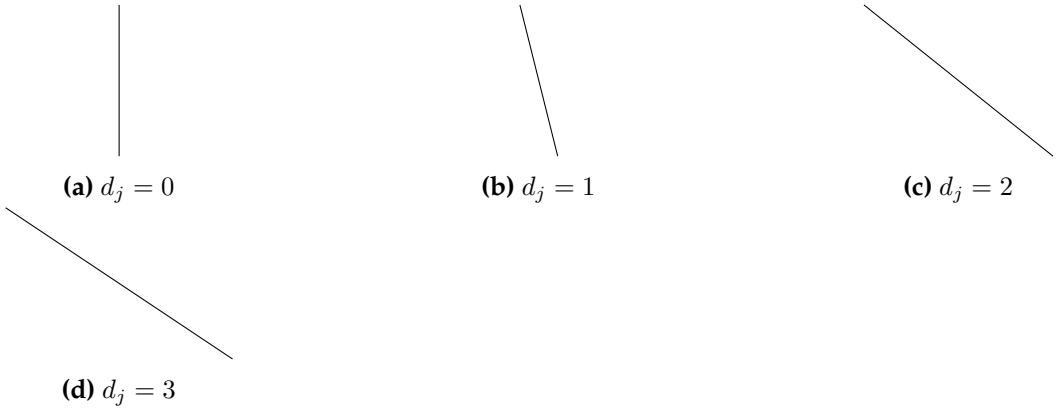

Figure 2.4: The 4 types of lines making up Shavitt diagrams in the Graphical Unitary Group Approach

ending at the same point represents the complete spin-adapted basis of Gel'fand–Tsetlin CSFs. For example, the GUGA CSF basis for the 4-electron triplet in 4 orbitals is shown in figure 2.5 The original application of the GUGA approach was for the construction of matrix elements between CSFs, required for spin-adapted Configuration Interaction methods, such as the MRCI implementations in the COLUMBUS package.[51, 52, 128–130]

2.3.4.1 GUGA-constructed cluster operators

The work of Paldus et al in the 1990s aimed to parametrise the cluster operator in a way that would produce G–T states from G–T references.[131] This leads to a complicated theory in which the cluster operators themselves are adapted to irreducible representations of the unitary group. For cases of two open-shell electrons, there were five independent sets of singles operators, and eight sets of doubles, before even including the extra triple excitations with spectators that generate an overall double excitation.[120]

While formally spin-adapted, this theory still suffered from the fundamental limitations imposed by non-commuting cluster operators.[10–14, 53, 54]

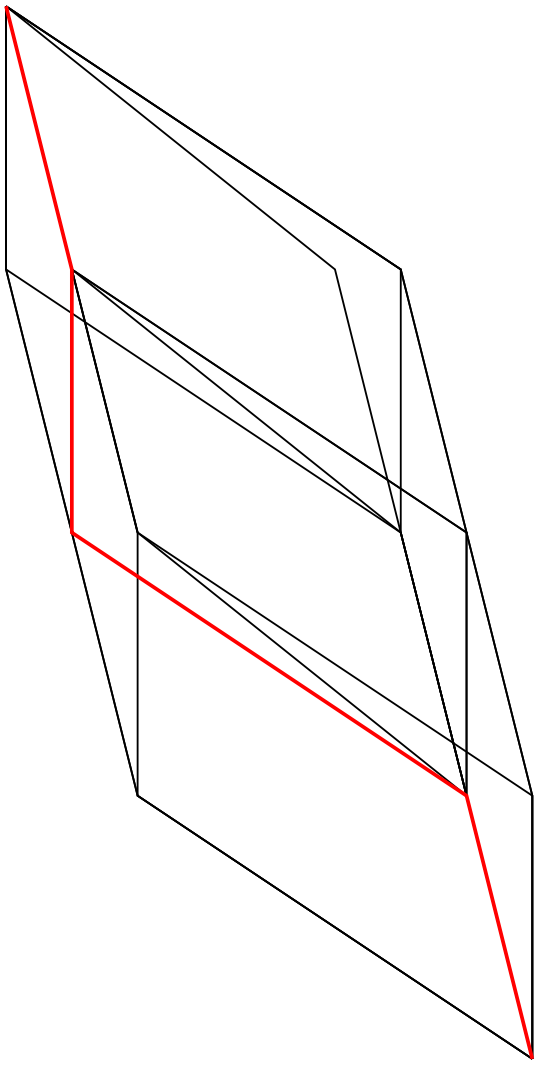

Figure 2.5: A Shavitt diagram showing the Gel'fand–Tsetlin basis of CSFs for triplets of 4 electrons in 4 orbitals, with the $\mathbf{d} = (1301)$ basis vector highlighted in red.

2.4 Electronic Structure Methods

Having developed some of the mathematical tools used to describe wavefunctions of electrons in molecules and operators thereon, the task of approximating the physical wavefunction, and the methods used to accomplish this, can now be expounded in detail. Much of the material in this section can be found in greater depth in the standard textbook of Helgaker et al.[76]

2.4.1 Hartree–Fock

The first approximation to most ground state electronic structure problems is the Hartree–Fock method, which optimises a single configurational wavefunction (usually a single Slater determinant) with respect to variations in the orbitals.[84, 132]

This is equivalent (by the Rayleigh–Ritz method) to finding the lowest-energy eigenfunction of the mean-field Hamiltonian

$$\hat{H}_{HF} = E_{nuc} + \hat{F} \tag{2.4.1.1}$$

where the Fock operator $\hat{F} = \sum_i \hat{f}_i$ is an effective one-body operator defined by

$$\hat{f}_i = \hat{h}_i + \sum_j \hat{g}_{ij} \left(\hat{1} - \hat{P}_{12} \right) \tag{2.4.1.2}$$

The permutation operator $\hat{P}_{12}$ accounts for the exchange interaction introduced by fermionic antisymmetry by swapping electrons 1 and 2 when they appear to the right. The sum over spin-orbitals j does not need to be restricted to $j \neq i$, as the exchange term will cancel with the direct Coulomb term in the case when $i = j$.[84]

The orbitals comprising the HF wavefunction are found as the eigenvectors of the Fock matrix. Since the Fock matrix itself depends on the orbitals, its diagonalisation must be done by an iterative procedure, updating the orbitals and constructing a new Fock matrix until they no longer change: the Self-Consistent Field (SCF) method.[84, 133]

In a basis of orthonormal molecular orbitals ϕ_p, the Fock matrix is written as

$$f_p^q = \left\langle \hat{a}^q \hat{H} \hat{a}_p \right\rangle = h_p^q + 2g_{pi}^{qi} - g_{pi}^{iq} \tag{2.4.1.3}$$

where i runs over the occupied MOs and p, q run over all MOs. This Fock matrix can be diagonalised

$$\mathbf{U}^T \mathbf{f} \mathbf{U} = \epsilon \tag{2.4.1.4}$$

where ϵ is the diagonal matrix of MO energies. The MOs are updated to be the corresponding eigenfunctions: $\phi \to \phi\mathbf{U}$, and the new Fock matrix constructed out of these orbitals. This is iterated until the orbitals no longer change.[76, 84]

In a (non-orthogonal) computational basis set of atomic orbitals, the HF equations become the Roothaan–Hall equations:[133, 134]

$$\tilde{\mathbf{f}}\mathbf{C} = \mathbf{S}\mathbf{C}\epsilon \tag{2.4.1.5}$$

where $\mathbf{C}$ is the matrix of orbital coefficients in the definition of molecular orbitals $\phi_p = \sum_\mu \chi_\mu C_p^\mu$ from atomic orbitals χ_μ, and $\mathbf{S}$ is the overlap matrix $S_\mu^\nu = \langle\nu|\mu\rangle$. The Latin letters $p, q, \ldots$ are used here to index molecular orbitals, while Greek letters $\mu, \nu, \ldots$ index atomic orbitals. The Fock matrix in the atomic orbital basis is obtained

$$\tilde{f}_\mu^\nu = h_\mu^\nu + \tilde{D}_\rho^\sigma \left(g_{\mu\sigma}^{\nu\rho} - \frac{1}{2} g_{\mu\sigma}^{\rho\nu} \right)$$

where $\tilde{\mathbf{D}}$ is the one particle density matrix transformed into the atomic orbital basis as

$$\tilde{\mathbf{D}} = \mathbf{C}\mathbf{D}\mathbf{C}^\dagger$$

The HF wavefunction is invariant to rotations between orbitals in the same space (i.e. within the occupied orbitals or within the virtuals), so the only requirement is that Fock matrix be block-diagonal. The canonical HF orbitals are those which fully diagonalise both blocks of the Fock matrix.[84]

The energy of the Hartree–Fock wavefunction is not merely the expectation value of the Fock operator itself, but the expectation of the true Hamiltonian in this single SD wavefunction. In the Møller–Plesset form of perturbation theory, it will be seen (see section 2.4.4) that this energy is correct to first order in the fluctuation potential (the zero-order energy being simply the lowest eigenvalue Fock operator), and the leading-order correction to the Hartree–Fock energy is at second order.[84, 135]

When the spatial parts of alpha and beta spin-orbitals are constrained to be the same, the procedure is Restricted HF (RHF). The alternative, when orbitals

for alpha and beta electrons can vary, is known as Unrestricted HF (UHF), and is the most common procedure for open shell systems. Using unrestricted orbitals means that the occupied and virtual (spin-)orbitals are distinct, but it introduces a factor of 2 in the number of orbitals. Since the time for an iteration scales as N^4 without other approximations, a closed-shell calculation is significantly more efficient (in principle approximately by a factor of 16) in restricted orbitals. A further drawback of unrestricted orbitals, when treating open shells, is the issue of spin contamination, described previously.[110]

Restricted Open-shell HF (ROHF) theory can also be performed, usually for high-spin states, which only consist of a single SD. The Fock matrix is replaced by Roothaan's effective Fock matrix

$$\mathbf{F} = \begin{pmatrix} \mathbf{R}_{cc} & \mathbf{F}_{ca} & \mathbf{F}_{cv} \\ \mathbf{F}_{ac} & \mathbf{R}_{aa} & \mathbf{F}_{av} \\ \mathbf{F}_{vc} & \mathbf{F}_{va} & \mathbf{R}_{vv} \end{pmatrix}$$

where the $\mathbf{R}$ can be any arbitrary combination of the $\mathbf{F}^{\alpha}$ and $\mathbf{F}^{\beta}$ In the high spin case, the energy is given by

$$E = 2h_p^p + 2g_{pq}^{pq} - g_{pq}^{qp}$$

Roothaan's original formulation of ROHF was developed more generally to allow for single configurations of multiple determinants such as low spin CSFs,[136, 137] but widespread applications have been limited to the high-spin cases. Recently, low spin implementations have been developed, obtaining orbitally-optimised CSFs of multiple determinants.[138–140] Implementing such a procedure in the future will be an important addition to the work presented in thesis, to put orbital-optimised low-spin CSF references on an equal footing to the closed-shell and high-spin cases.

2.4.2 Configuration interaction

Going beyond the mean-field approximation considered in Hartree–Fock theory, the simplest way to incorporate electron correlation is to take a linear combination

of SDs. Finding the coefficients that variationally optimise the energy constitutes the method known as Configuration Interaction (CI).

$$|\Psi\rangle = \sum_I C_I |\Phi_I\rangle \tag{2.4.2.1}$$

The appropriate coefficients C_I with respect to which the energy $E = \frac{\langle \Psi | \hat{H} | \Psi \rangle}{\langle \Psi | \Psi \rangle}$ is stationary are determined by the matrix diagonalisation

$$\mathbf{HC} = E\mathbf{C} \tag{2.4.2.2}$$

If the linear combination includes every possible SD that can be formed from the one particle basis, then this is Full CI (FCI), which gives the exact eigenvalues and eigenfunctions of the Hamiltonian, within the space spanned by a given basis set. The number of coefficients to be determined (and the size of the matrix to be diagonalised) scales exponentially with the number of electrons and basis functions, so this procedure is clearly infeasible for all but the very smallest systems.[76]

The traditional compromise to this has been to start from a single reference SD (usually a Hartree–Fock solution) and to include only SDs generated by excitations up to some pre-determined level. Configuration Interaction with Single and Double excitations (CISD) can give good estimates of the correlation energy in cases where the reference determinant is close to the true ground state.[84]

$$|\Psi_{CISD}\rangle = \left(1 + \sum_{\substack{a \\ i}} C_a^i \hat{E}_i^a + \sum_{\substack{ab \\ ij}} C_{ab}^{ij} \hat{E}_{ij}^{ab}\right) |\Phi_0\rangle \tag{2.4.2.3}$$

However, because CI does not include products of excitations in its ansatz, it fails to achieve size consistency and size extensivity, two of the desired characteristics for a model for chemistry. As the size of the system increases, truncated CI becomes less and less accurate, recovering none of the correlation energy in the limit as the number of electrons $N \to \infty$. The Davidson correction is often applied to approximate the effect on the correlation energy of quadruple

excitations that are products of double excitations.[141] While this improves the energy obtained by CISD, it does not fully achieve size extensivity.[76]

While the linear nature of CI leads to limitations in its treatment of dynamical correlation, static correlation can be well represented by the inclusion of appropriate additional determinants. Defining a configuration space to include exactly the determinants that are required for a good description of the static correlation is a matter of chemical insight. A common procedure is to choose, by consideration of the chemical system being modelled, a set of active (spatial) orbitals, and generate a complete active space (CAS) containing all the possible determinants with a given number of electrons in these orbitals. FCI within this space gives the CASCI method,[30, 142] or the active space may be restricted to determinants with some pre-defined partial occupations of active orbitals in Restricted Active Space CI (RASCI)[28].

Selected CI (SCI) procedures choose additional configurations to be included based on the significance of their contribution to the ground state. An early SCI method was the Configuration Interaction by Perturbation with Selection of zero-order wavefunction by an Iterative procedure (CIPSI), which finds the configurations that contribute the most to the first-order perturbative correction to the wavefunction, and performs a CI in this space, with the whole procedure being iterated to convergence.[143] Other procedures based on CI within a space of states selected by some perturbative estimate of their contribution have since been developed,[144, 145] with two of the more recent ones being Adaptive Sampling CI (ASCI)[146] and Heat-bath CI (HCI).[147]

2.4.3 Multiconfigurational SCF

Hartree–Fock is only accurate for states that can be well represented by a single Slater determinant. Multiconfigurational SCF (MCSCF) methods such as the Complete Active Space SCF method (CASSCF) aim to provide a mean-field treatment of multireference systems.[29, 30]

The CASSCF procedure optimises the orbitals on which a CASCI wavefunction

$$|\Psi\rangle = \sum_I C_I |\Phi_I\rangle \tag{2.4.3.1}$$

is built, where C_I are linear expansion coefficients for states $|\Phi_I\rangle$ spanning the active space.[29] If the orbital rotations are parametrised by the general one-body operator $\hat{\kappa}$,[30, 76] the CASSCF wavefunction can be written

$$|\Psi\rangle = \exp\left(-\hat{\kappa}\right) \sum_I C_I |\Phi_I\rangle \tag{2.4.3.2}$$

In the CASSCF method, an active space is defined by specifying a number of active orbitals and a number of electrons occupying them. The complete set of wavefunctions with the specified orbital occupations then forms the active space, within which the linear coefficients are optimised.[30, 76]

This space scales combinatorially (*i.e.* exponentially) with the number of orbitals, so the choice of active space requires careful consideration of the chemical system being modelled, so as to capture any strong correlation without increasing the cost beyond what is computationally feasible. For example, a complete active space constructed from 2 electrons in 4 spin-orbitals will contain 6 possible SDs, while 2 in 8 spin-orbitals will generate 28 SDs.

Usually CASSCF is formulated in spatial orbitals, with a specified projected spin value. For example, a CASSCF (2,2) calculation (i.e. an active space of 2 electrons in 2 orbitals) with a $M_S = 0$ will have 4 determinants in the active space. Although the determinants in this space are not generally spin eigenfunctions, the three singlet states and one triplet will be resolved by the 4×4 matrix diagonalisation that corresponds to performing FCI within this space.

The CASSCF method preserves the invariance of the energy to rotations among the orbitals within each of the core, active, and virtual spaces. A restricted active space (RAS) method defined with some limited set of SDs, not spanning the full space of functions with the desired active orbital occupations and are not guaranteed to preserve the orbital invariance.[148, 149] In strongly correlated

systems, such as in the intermediate regime in a bond dissociation, this orbital invariance becomes important in order to obtain smooth energy curves.

2.4.4 Many-Body Perturbation Theory

The first method going beyond mean-field SCF methods to calculate electron correlation in a size consistent manner is perturbation theory.

Consider a Hamiltonian of the form

$$\hat{H} = \hat{H}_0 + \hat{V} \tag{2.4.4.1}$$

where the eigenfunctions $|\Phi_i\rangle$ of $\hat{H}_0$ are known, with known eigenvalues $E_i^{(0)}$.

$$\hat{H}_0 |\Phi_i\rangle = E_i^{(0)} |\Phi_i\rangle \tag{2.4.4.2}$$

The traditional Rayleigh–Schrödinger approach to perturbation theory (RSPT) writes an interacting Hamiltonian

$$\hat{H}_1 = \hat{H}_0 + \lambda \hat{V} \tag{2.4.4.3}$$

where the range of λ from 0 to 1 corresponds to moving from the unperturbed to full Hamiltonian.[76, 150] The eigenfunctions and eigenvalues can be expanded in powers of λ to obtain terms in the RSPT perturbation series that converge to the exact answer, provided that $\hat{H}_0$ is a good approximation of $\hat{H}$.

While the RSPT is often the first to appear in pedagogical treatments,[76] there is an operator formalism that encapsulates the procedure of deriving terms in the perturbation series that offers several benefits for many-body problems. This 'many-body' perturbation theory (MBPT) simplifies the identification of terms that should be cancelled or retained in a size-extensive energy, exposes relationships to other perturbation theories such as Brillouin–Wigner PT, and also facilitates the extension to reference ('model') spaces of multiple states. For some small set of reference functions $\left|\Psi_i^{(0)}\right\rangle$, spanning the so-called "model space," a wave operator $\hat{\Omega}$ is defined to transform the reference functions to a

corresponding set of exact eigenfunctions $|\Psi_i\rangle$ of the full Hamiltonian $\hat{H}$, with exact energies E_i.

$$\hat{\Omega}\left|\Psi_i^{(0)}\right\rangle = |\Psi_i\rangle \tag{2.4.4.4}$$

$$\hat{H}\,|\Psi_i\rangle = E_i\,|\Psi_i\rangle \tag{2.4.4.5}$$

The model space projection operator $\hat{P}$ is defined to transform the exact eigenfunctions back to their corresponding model space functions

$$\hat{P}\,|\Psi_i\rangle = \left|\Psi_i^{(0)}\right\rangle \tag{2.4.4.6}$$

and its orthogonal complement is denoted $\hat{Q} = 1 - \hat{P}$.

Since $\left[\hat{H}_0, \hat{P}\right] = 0$,

$$\begin{aligned}
\hat{\Omega}\hat{P}E_i\,|\Psi_i\rangle &= \hat{\Omega}\hat{P}\left(\hat{H}_0 + \hat{V}\right)|\Psi_i\rangle \\
&= \hat{\Omega}\hat{P}\hat{H}_0\,|\Psi_i\rangle + \hat{\Omega}\hat{P}\hat{V}\,|\Psi_i\rangle \\
&= \hat{\Omega}\hat{H}_0\hat{P}\,|\Psi_i\rangle + \hat{\Omega}\hat{P}\hat{V}\,|\Psi_i\rangle \\
&= \hat{\Omega}\hat{H}_0\hat{P}\,|\Psi_i\rangle + \hat{\Omega}\hat{P}\hat{V}\hat{\Omega}\hat{P}\,|\Psi_i\rangle \\
&= \left(\hat{\Omega}\hat{H}_0 + \hat{\Omega}\hat{P}\hat{V}\hat{\Omega}\right)\hat{P}\,|\Psi_i\rangle \\
&= E_i\hat{\Omega}\hat{P}\,|\Psi_i\rangle \\
&= E_i\,|\Psi_i\rangle \\
&= \left(\hat{H}_0 + \hat{V}\right)|\Psi_i\rangle \\
&= \left(\hat{H}_0 + \hat{V}\right)\hat{\Omega}\hat{P}\,|\Psi_i\rangle \\
&= \left(\hat{H}_0\hat{\Omega} + \hat{V}\hat{\Omega}\right)\hat{P}\,|\Psi_i\rangle
\end{aligned} \tag{2.4.4.7}$$

and since the model functions span the entire model space, the generalised Bloch equation is obtained,[151]

$$\begin{aligned}
\left(\hat{H}_0\hat{\Omega} + \hat{V}\hat{\Omega}\right)\hat{P} &= \left(\hat{\Omega}\hat{H}_0 + \hat{\Omega}\hat{P}\hat{V}\hat{\Omega}\right)\hat{P} \\
\hat{H}_0\hat{\Omega}\hat{P} + \hat{V}\hat{\Omega}\hat{P} &= \hat{\Omega}\hat{H}_0\hat{P} + \hat{\Omega}\hat{P}\hat{V}\hat{\Omega}\hat{P} \\
\left[\hat{\Omega}, \hat{H}_0\right]\hat{P} &= \hat{V}\hat{\Omega}\hat{P} - \hat{\Omega}\hat{P}\hat{V}\hat{\Omega}\hat{P}
\end{aligned} \tag{2.4.4.8}$$

$\hat{\Omega}$ can be expanded in orders of $\hat{V}$

$$\hat{\Omega} = 1 + \hat{\Omega}^{(1)} + \hat{\Omega}^{(2)} + \dots \tag{2.4.4.9}$$

where $\hat{\Omega}^{(n)}$ represents the sum of terms in $\hat{\Omega}$ in which $\hat{V}$ appears n times. The generalised Bloch equation at each order of $\hat{V}$ is then

$$\begin{aligned}
\left[\hat{\Omega}^{(1)}, \hat{H}_0\right] \hat{P} &= \hat{V}\hat{P} - \hat{P}\hat{V}\hat{P} \\
&= \left(1 - \hat{P}\right) \hat{V}\hat{P} && (2.4.4.10) \\
\left[\hat{\Omega}^{(2)}, \hat{H}_0\right] \hat{P} &= \hat{V}\hat{\Omega}^{(1)}\hat{P} - \hat{\Omega}^{(1)}\hat{P}\hat{V}\hat{P} - \hat{P}\hat{V}\hat{\Omega}^{(1)}\hat{P} \\
&= \left(1 - \hat{P}\right) \hat{V}\hat{\Omega}^{(1)}\hat{P} - \hat{\Omega}^{(1)}\hat{P}\hat{V}\hat{P} && (2.4.4.11) \\
\left[\hat{\Omega}^{(3)}, \hat{H}_0\right] \hat{P} &= \hat{V}\hat{\Omega}^{(2)}\hat{P} - \hat{\Omega}^{(2)}\hat{P}\hat{V}\hat{P} - \hat{\Omega}^{(1)}\hat{P}\hat{V}\hat{\Omega}^{(1)}\hat{P} - \hat{P}\hat{V}\hat{\Omega}^{(2)}\hat{P} \\
&= \left(1 - \hat{P}\right) \hat{V}\hat{\Omega}^{(2)}\hat{P} - \hat{\Omega}^{(2)}\hat{P}\hat{V}\hat{P} - \hat{\Omega}^{(1)}\hat{P}\hat{V}\hat{\Omega}^{(1)}\hat{P} && (2.4.4.12)
\end{aligned}$$

At order n in $\hat{V}$, the general expression is

$$\left[\hat{\Omega}^{(n)}, \hat{H}_0\right] \hat{P} = \left(1 - \hat{P}\right) \hat{V}\hat{\Omega}^{(n-1)}\hat{P} - \sum_{k=1}^{n-1} \hat{\Omega}^{(n-k)}\hat{P}\hat{V}\hat{\Omega}^{(k-1)}\hat{P} \tag{2.4.4.13}$$

These equations, which are valid for the model space $\hat{P}$, are the Rayleigh–Schrödinger expansion for the perturbed wavefunction.[9, 150] This shows a general feature of perturbation theory, that the expansion consists of a series of connected terms with disconnected terms (also called 'renormalisation' terms) subtracted out.

A "resolvent" operator $\hat{R}$ may be defined in the orthogonal space by

$$\hat{R}\left(E_0 - \hat{H}_0\right) = \hat{Q}, \qquad \hat{R}\hat{Q} = \hat{Q} \tag{2.4.4.14}$$

The effect of this resolvent operator, applied at an intermediate step in a product of operators, is to introduce a denominator, dividing by the difference in energy eigenvalues of incoming lines and outgoing lines. For this reason, it is sometimes written

$$\hat{R} = \frac{1}{E_0 - \hat{H}_0} \tag{2.4.4.15}$$

The projectors $\hat{P}$ and $\hat{Q} = 1 - \hat{P}$ into and out of the (generally multi-dimensional) model space correspond to the projectors $|\Phi_0\rangle \langle\Phi_0|$ and $\sum_{i\neq 0} |\Phi_i\rangle \langle\Phi_i|$ appearing in the standard single-reference formulation of Rayleigh–Schrödinger perturbation theory.

Applied to time independent ground state molecular electronic structure theory, RSPT is most commonly applied in the Moller–Plesset partitioning of the Hamiltonian:[135]

$$\hat{H} = \hat{H}^{(0)} + \hat{H}^{(1)} = \hat{F} + \hat{G} \tag{2.4.4.16}$$

where $\hat{F}$ is the Fock operator, and $\hat{G}$ is the so-called 'fluctuation potential,' which is the remaining part of the 2-body Coulomb interaction that has not been integrated out and included in $\hat{F}$. If the Hartree–Fock solution well approximates the ground state, then this partitioning, in which the fluctuation potential is treated as the perturbation, leads to accurate energies at modest orders of perturbation theory. Contributions to the wavefunction and energy in increasing orders of $\hat{G}$ can be derived in turn:

$$E^{(1)} = \left\langle HF \middle| \hat{G} \middle| HF \right\rangle$$

$$\left|\Phi^{(1)}\right\rangle = \hat{R}\hat{G}\left|\Phi^{(0)}\right\rangle = \sum_{\substack{ij \\ ab}} \frac{g_{ij}^{ab}}{\varepsilon_i + \varepsilon_j - \varepsilon_a - \varepsilon_b} \left|\Phi_{ab}^{ij}\right\rangle$$

$$E^{(2)} = \left\langle HF \middle| \hat{G} \middle| \Phi^{(1)} \right\rangle = -\frac{1}{2} \sum_{\substack{ij \\ ab}} \frac{\left|g_{ij}^{ab}\right|^2}{\varepsilon_i + \varepsilon_j - \varepsilon_a - \varepsilon_b}$$

where $\left|\Phi_{ab}^{ij}\right\rangle = \hat{E}_{ab}^{ij} |HF\rangle$ is the state in which two electrons have been excited out of the Hartree–Fock determinant from orbitals a and b to orbitals i and j, and $g_{ij}^{ab} = \left\langle \Phi_{ab}^{ij} \middle| \hat{G} \middle| HF \right\rangle$ is a matrix element of $\hat{G}$. This gives the simplest perturbation correction to the Hartree–Fock energy, the second order Moller–Plesset (MP2) energy correction.

$$E_{MP2} = E_{HF} + E^{(2)} = E_{HF} - \frac{1}{2} \sum_{\substack{ij \\ ab}} \frac{\left|g_{ij}^{ab}\right|^2}{\varepsilon_i + \varepsilon_j - \varepsilon_a - \varepsilon_b} \tag{2.4.4.17}$$

The second-order correction to the wavefunction is given by

$$\left|\Phi^{(2)}\right\rangle = \hat{R}\hat{G}\hat{R}\hat{G}\left|\Phi^{(0)}\right\rangle - E^{(1)}\hat{R}\hat{G}\left|\Phi^{(0)}\right\rangle \tag{2.4.4.18}$$

These and higher order contributions become tedious to derive and enumerate. The systematic identification of connected terms that contribute at higher orders in the fluctuation potential is facilitated by diagrammatic notation.

2.4.5 Diagrammatic Notation

Feynmann's original time-dependent diagrammatic notation for perturbation theory was adapted for time independent problems in nuclear structure theory by Goldstone,[152] before later being adopted by the electronic structure community. A comprehensive pedagogical treatment of these techniques can be found in the textbook of Shavitt and Bartlett.[85] Tensors are represented as vertices, with lines above and below to represent quasiparticle creation and annihilation operators, respectively. An arrow entering and leaving a vertex indicates the scattering of an electron, i.e. an elementary annihilation operator and an elementary creation operator. Where a vertex represents a many-body interaction, it will consist of multiple nodes, connected with a line that may be dashed or solid, depending on the interaction being depicted.

2.4.5.1 Time ordering

Even for time-independent problems, it is necessary to keep track of the relative ordering of operators being applied to a state. The standard formalism for diagrams for perturbation theory and coupled cluster orients the time axis pointing upwards on the page, as in figure 2.6.[85] Alternative presentations may show time proceeding from right to left, as in the order in which operators are applied to a ket state,[33] but all diagrams in this thesis shall employ the vertical time axis.

The state at a given time is represented by the lines that cross an imaginary horizontal line at that time coordinate. The (Fermi) vacuum is represented by

Figure 2.6: Time ordering proceeds upwards in most presentations of Goldstone diagrams

nothing, i.e. a time coordinate at which a horizontal line could be drawn that does not cross any lines in a diagram.

2.4.5.2 Particle and hole lines

Lines representing an electron in a particle orbital (defined relative to a Fermi vacuum) are directed upwards, while electrons in hole orbitals are represented by downward-directed arrows (see figure 2.7). This notation reframes scattering of electrons as creation and destruction of electrons and holes. For example, an excitation of an electron from a hole orbital to a particle orbital is clearly seen as a creation of a particle-hole pair. Scattering within the occupied space or within the virtual space preserves quasiparticle number, which is reflected in the diagram.

In perturbation theory diagrams, the resolvent operator $\hat{R} = \left(E_0 - \hat{H}_0\right)^{-1}$ will be represented by a horizontal line at a given time, between the action of two other operators in the time-ordered product. In time-independent problems, a resolvent results in division by an energy denominator, given by the sum of orbital energy eigenvalues for any particle lines that cross the resolvent line, minus the corresponding sum for any hole lines. Diagrams for many-body perturbation theory and especially coupled cluster are often drawn with resolvent lines omitted, instead assuming that a resolvent line is implied in every interval between scattering events.[85]

In the spin-free formalism, we further specify a line to refer to the singly-occupied (active) orbitals by marking it with a skeleton arrowhead. Being a subset of the particle orbitals, the active orbitals will always be referred to with upward-directed skeleton arrows.

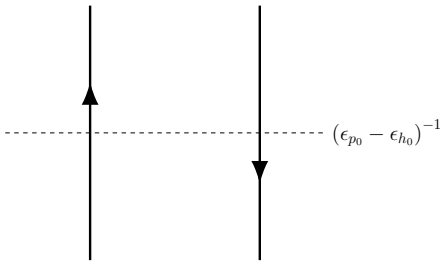

Figure 2.7: Particle lines are directed upwards, while hole lines are directed downwards. The resolvent line represents the action of $\left(E_0 - \hat{H}_0\right)^{-1}$, introducting a denominator of zero-order energy differences

2.4.5.3 Vertices

An operator comprised of some annihilation and some creation operators will be represented by a vertex at which incoming lines (for the annihilation operators) and outgoing lines (for creation operators) meet. In Goldstone diagrams, the vertices representing 2- or higher-body operators have a node for each particle involved in the scattering process. At each node, there is one line entering and one line leaving, representing the propagation of one electron before and after the interaction. An interaction is represented by a horizontal line, either between two nodes as in the fluctuation potential, or between a node and the mean field (represented by an x), as in the Fock operator, shown in figure 2.8.

Hugenholtz diagrams "collapse" vertices down to one node, reducing the number of distinct diagrams by exploiting the indistinguishability of electrons. Since the spin-summation procedure requires keeping track of which particle is which, our diagrammatic construction will use the more explicit Goldstone diagrams.

2.4.5.4 Contractions

When the indices corresponding to two lines are contracted together, the diagram is drawn with those two lines joined together into one, as in figure 2.9. If a tensor represents an operator not in normal order, then it may be able to contract with itself. This will lead to a diagram in which a vertex may have lines that loop round onto itself. Unless otherwise stated, all tensors hereon are considered

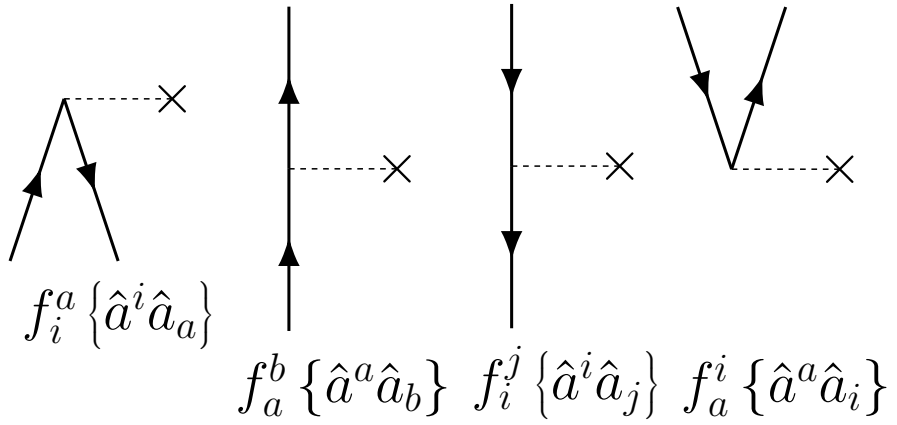

Figure 2.8: Diagrams representing Fock matrix elements

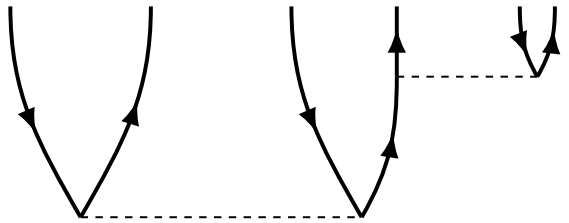

Figure 2.9: Diagram representing the contracted term $g_{ad}^{ij} g_{bc}^{dk} \left\{\hat{a}^a \hat{a}^b \hat{a}^c \hat{a}_k \hat{a}_j \hat{a}_i\right\}$

to correspond to operators in normal order, and so no contraction lines will appear from a vertex to itself.

2.4.5.5 Open diagrams

When there are lines that enter or leave the top or bottom of a diagram, it represents an initial or final state that is not the vacuum. It is sometimes useful, particularly in the spin summation procedure, to consider the operators that create such a state out of the vacuum, and to keep track of which particle in the state corresponds to which line in the diagram. This can be done by including external "ghost" vertices at the ends of the diagram, as illustrated in figure 2.10.

These will not be included in later diagrams, but will be implied by the order (from left to right) of outgoing and incoming legs of the diagram.

2.4.5.6 Loops and phase factors

The anticommutation relations lead to a factor of -1 for each loop. In a spin-summed theory, a factor of 2 is also obtained for each loop.

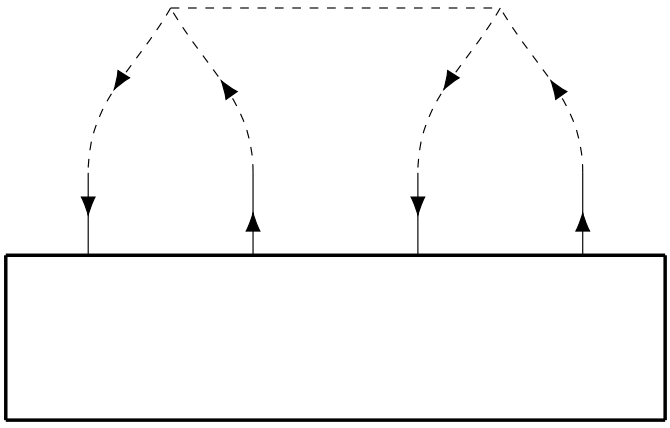

Figure 2.10: Diagram representing the pp-hh terms of the doubles residual equations, with the 'ghost' tensor drawn in to represent its projection onto a doubly excited state manifold.

For example, contributions to the MP2 energy from direct and exchange interactions are represented by the diagrams in figure 2.11. In a spin-orbital based theory, these come with opposite signs but equal magnitude. Using antisymmetrised Coulomb integrals automatically accounts for this and similar structures appearing in other more complicated diagrams, allowing the use of the simpler Hugenholtz diagrams.

When the spins are summed over, it is not trivial to keep track of which of the two modes of contraction (direct or exchange) with a 2-body vertex will introduce an extra factor of 2. In the simple example of the MP2 energy, the direct contribution carries a factor of $+4$, while the exchange contribution has -2. Although it is common for exchange contributions to appear with a factor of $-1/2$ compared to the corresponding direct contribution, it is not always easy to determine this *a priori* for more complicated diagrams, particularly when open shells are involved. We therefore do not use antisymmetrized 2-body integrals, but instead use the bare Coulomb integrals, and do not calculate the corresponding two-body antisymmetrised amplitudes for ourselves,[65] but instead allow each contribution to be evaluated separately in the overall spin summation.

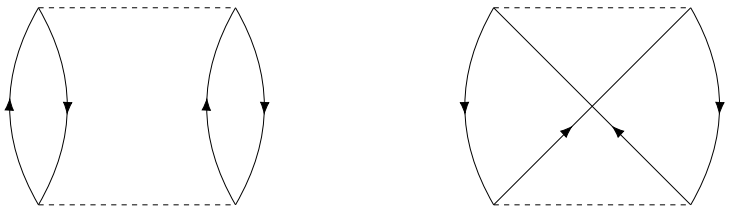

Figure 2.11: Direct ($\frac{v_{rs}^{ab}v_{ab}^{rs}}{\epsilon_r+\epsilon_s-\epsilon_a-\epsilon_b}$) and exchange ($\frac{v_{rs}^{ab}v_{ab}^{sr}}{\epsilon_r+\epsilon_s-\epsilon_a-\epsilon_b}$) MP2 energy diagrams

2.4.5.7 Linked and Connected diagrams

Categorising diagrams as linked/uninked, connected/disconnected, and open/closed (see figure 2.12) will be useful in determining to which equations a diagram contributes, and whether or not its contribution is size extensive.

A closed diagram is one in which no particle or hole lines are left uncontracted; a diagram in which there are uncontracted lines is called open. Disconnected diagrams are those that contain more than one smaller diagram without a line connecting them; connected diagrams are those with only one such component. An unlinked diagram is a disconnected diagram containing one or more closed components; a linked diagram may be connected or disconnected, but contains no closed components.

It will be shown that the unlinked diagrams cancel out of the perturbation series for the exact wavefunction, according to the linked diagram theorem.[9] This property should be retained in an approximate method in order for it to yield a size-extensive and size-consistent energy.

2.4.6 The Factorisation Theorem

Any two diagrams with the same vertices and connectivity, differing only in their relative ordering, will have the same numerators in each of their corresponding terms. The factorisation theorem then need only consider the denominators arising in each diagram by application of the resolvent between every possible pair of vertices. The factorisation theorem states that the (normal-ordered) product of two connected diagrams is equal to the sum of all the disconnected diagrams composed of the two separate diagrams, with all possible orderings

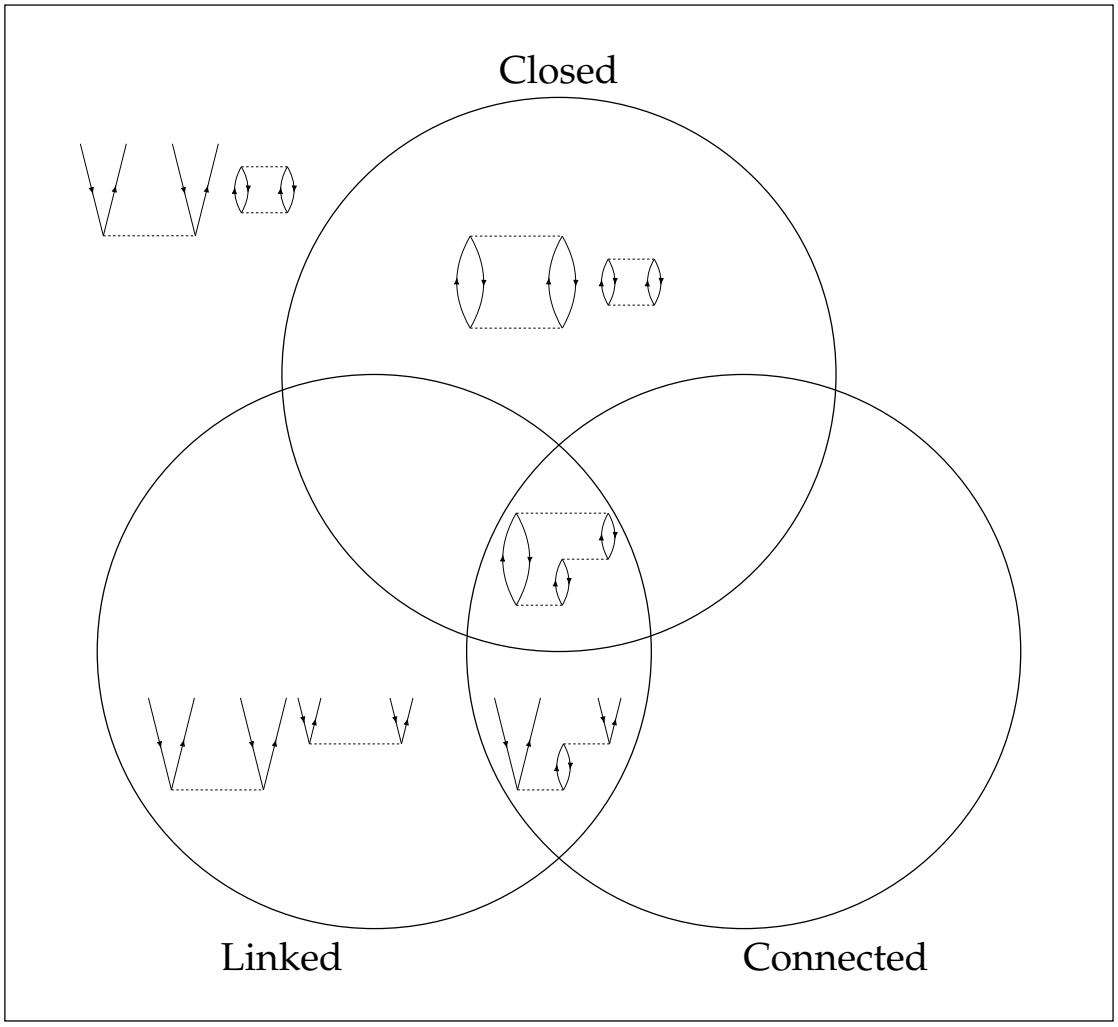

Figure 2.12: Examples of different types of Goldstone diagram, illustrating the definitions of closed, linked, and connected

of the vertices in one diagram relative to the other.[153] The factorisation of diagrams with two disconnected parts A and B:

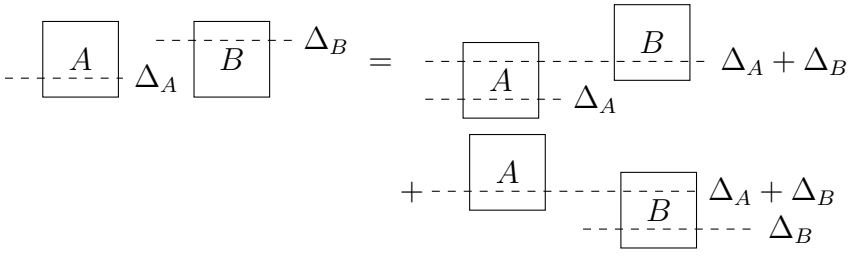

is seen in the denominators

$$\frac{1}{\Delta_A \Delta_B} = \frac{\Delta_B + \Delta_A}{\Delta_A \left(\Delta_A + \Delta_B\right) \Delta_B} = \frac{1}{\Delta_A \left(\Delta_A + \Delta_B\right)} + \frac{1}{\left(\Delta_A + \Delta_B\right) \Delta_B} \qquad (2.4.6.1)$$

If the two diagrams are respectively associated with matrix elements M_A

and M_B, and normal-ordered second quantized operators $\hat{o}_A$ and $\hat{o}_B$, then each diagram separately represents the expressions $\frac{M_A}{\Delta_A}\hat{o}_A$ and $\frac{M_B}{\Delta_B}\hat{o}_B$. The factorisation theorem has given us that the total contribution of disconnected diagrams consisting of diagrams A and B is $\frac{M_A M_B}{\Delta_A \Delta_B}\{\hat{o}_A\hat{o}_B\}$ The operator product is normal-ordered, as the disconnected diagrams specify no contractions between the two parts. It can be shown inductively that the factorisation theorem also holds for products of more than two diagrams.[85]

Where indices coincide in separate parts of a diagram, there will be some terms that violate the Pauli exclusion principle, where a particle or hole state could be occupied in both diagrams simultaneously. To avoid contributions from these unphysical diagrams, the summations can be carried out with the indices restricted not to coincide. These exclusion-principle-violating (EPV) terms will also appear in the connected diagrams generated by attaching the two diagrams together by the repeated line, but with the opposite sign. It turns out that including the EPV terms in both expressions with unrestricted summations means that they cancel out and their effect can be ignored.[85]

Any unlinked diagram in a Rayleigh–Schrödinger perturbation series will appear along with every reordering of the vertices, which by the factorisation theorem will amount to the multiplication by the disconnected component. The combined diagram will also appear with a sign change as a renormalisation term, and so will cancel out of the overall expression. This leads to the linked diagram theorem, which states that the full expansion of the wavefunction contains only linked diagrams.[152] The energy obtained by an approximate method is size extensive if it also contains only linked diagrams.

2.4.7 Coupled Cluster

To correctly obtain a multiplicatively separable wavefunction, as required to achieve size consistency, the treatment of dynamic correlation should include products of excitations. Unlike configuration interaction, coupled cluster retains

this property even when truncating the ansatz, as the products of disconnected excitations are generated by the exponential.

2.4.7.1 The exact wavefunction

The exact wavefunction is expressed as

$$|\Psi\rangle = \hat{\Omega}\,|\Phi_0\rangle$$

for some wave operator $\hat{\Omega}$ that preserves the size extensivity of the reference state $|\Phi_0\rangle$.

If the excitations $\hat{\tau}$ included in $\hat{T}$ are nilpotent ($\hat{\tau}_I^2 = 0$) and all commute with one another ($\hat{\tau}_I\hat{\tau}_J = \hat{\tau}_J\hat{\tau}_I$), then an exponential form of the wave operator can be seen to arise naturally as a product of correlating operators $(1 + \hat{\tau})$:

$$\begin{aligned}
\hat{\Omega} &= \prod_{I=1}^{n} (1 + \hat{\tau}_I) \\
&= 1 + \sum_{I=1}^{n} \hat{\tau}_I + \sum_{I=1}^{n} \sum_{J=I+1}^{n} \hat{\tau}_I\hat{\tau}_J + \sum_{I=1}^{n} \sum_{J=I+1}^{n} \sum_{K=J+1}^{n} \hat{\tau}_I\hat{\tau}_J\hat{\tau}_K + \dots \\
&= 1 + \sum_{I=1}^{n} \hat{\tau}_I + \frac{1}{2!} \sum_{I=1}^{n} \sum_{J=1}^{n} \hat{\tau}_I\hat{\tau}_J + \frac{1}{3!} \sum_{I=1}^{n} \sum_{J=1}^{n} \sum_{K=1}^{n} \hat{\tau}_I\hat{\tau}_J\hat{\tau}_K + \dots \\
&= 1 + \sum_{I=1}^{n} \hat{\tau}_I + \frac{1}{2!} \left(\sum_{I=1}^{n} \hat{\tau}_I \right)^2 + \frac{1}{3!} \left(\sum_{I=1}^{n} \hat{\tau}_I \right)^3 + \dots \\
&= \sum_{k=0}^{\infty} \frac{\hat{T}^k}{k!} = \mathrm{e}^{\hat{T}}
\end{aligned} \tag{2.4.7.1}$$

where $\hat{T} = \sum_{I=1}^{n} \hat{\tau}_I$.

If every possible excitation from the reference state is included in the cluster operator, then the FCI energy will be recovered. Such a "Full Coupled Cluster" would have the same number of amplitudes as the linear expansion coefficients in FCI, and so would not provide any computational benefit (in fact it would simply amount to an FCI calculation with a vastly increased prefactor in the computation time). Although the CC ansatz offers no benefit for exact calculation, it does offer a starting point for approximate theories that are usually more accurate than other similarly-scaling methods such as truncated CI.[84]

2.4.7.2 A correctly-scaling approximate wavefunction

In the standard spin-orbital based theory, and orbital-based theories for closed shell systems, the cluster operator can be written

$$\hat{T} = \hat{T}_1 + \hat{T}_2 + \cdots = \sum_{\substack{r \\ a}} t_r^a \hat{a}^r \hat{a}_a + \sum_{\substack{r,s \\ a,b}} t_{rs}^{ab} \hat{a}^r \hat{a}^s \hat{a}_b \hat{a}_a + \cdots$$

where the excitations $\hat{\tau}_I = t^I \hat{X}_I$ included in the cluster operator have been grouped into excitation levels from 1 to N, where the number N of electrons is the maximum order of excitation that can appear in the FCI expansion of the wavefunction.

A physically motivated approximate wavefunction can be obtained starting from this expression for the exact wavefunction, by truncating the cluster operator to contain only certain sets of excitations. The Brillouin condition states that including only single excitations would not change the Hartree–Fock wavefunction, as an exponential of a general singles excitation amounts to performing orbital rotations (Thouless' theorem), with respect to which the HF wavefunction is already optimised.[154]

The first CC method capturing electron correlation is the coupled cluster method with double excitations (CCD), which was historically also called the Coupled Pair Many-Electron Theory (CPMET).[21, 155] After this, progressively more accurate methods are obtained by including excitations up to a given level, starting from the coupled cluster with single and double excitations (CCSD). Including triples, quadruples, etc. constitutes the CCSDT, CCSDTQ, etc. methods, which are highly accurate, but generally too expensive for widespread application.

This form of the wave operator is equivalent to the sum of all linked diagrams that can be generated by repeated application of the Hamiltonian onto a reference state.[85] When the amplitudes are converged, it can be thought of as the infinite summation of the MP perturbation series. If the terms in the MP perturbation series are grouped by overall particle number, rather than by order in V, they

can be resummed to infinite order, yielding the familiar exponential ansatz of coupled cluster.

Goldstone's diagrammatic notation used in MBPT is extended to include diagrams for the coupled cluster amplitudes. Whereas the two-electron integrals were depicted as a vertex of two nodes connected by a dashed line, the amplitudes of a given level are depicted with a solid line.[85] This can be thought of as indicating that at convergence they will correspond to the sum of all diagrams up to infinite order with the same external form.

2.4.7.3 Coupled cluster equations

Having chosen an ansatz for the wave function, the Schrödinger equation, $\left(\hat{H} - E\right)|\Psi\rangle = 0$, is then solved in a space of dimension equal to the number of parameters (amplitudes). This space is a manifold of excited bra states $\langle\Phi_I| = \langle\Phi_0|\tilde{E}_I$, where the set of operators $\left\{\tilde{E}_I\right\}$ span the dual space of $\{E_I\}$ This means they are the Hermitian conjugate of a set of excitation operators $\tilde{E}^I$ spanning the same space as the operators $\hat{E}^I$ appearing in the cluster operator.

Directly projecting the Schrödinger equation onto the excited state manifold yields the coupled cluster equations in their energy-dependent, "unlinked" formulation

$$E = \langle\Phi_0|\hat{H}\mathrm{e}^{\hat{T}}|\Phi_0\rangle \tag{2.4.7.2}$$

$$0 = R_I = \langle\Phi_I|(\hat{H} - E)\mathrm{e}^{\hat{T}}|\Phi_0\rangle \tag{2.4.7.3}$$

The second term in this expression is the renormalisation term that serves to cancel the unlinked terms in the first, leaving a residual equation that contains only linked diagrams, and is therefore size-extensive, when all terms of a given order are included.

There is an alternative, "linked," formalism, in which the excited state manifold is transformed by pre-multiplying the Schrödinger equation by the inverse wave operator $\mathrm{e}^{-\hat{T}}$. A similarity transformed Hamiltonian can be written

$$\tilde{H} = \mathrm{e}^{-\hat{T}}\hat{H}\mathrm{e}^{\hat{T}} \tag{2.4.7.4}$$

which is an effective Hamiltonian for the reference state, and will be seen to contain only linked diagrams for each term in the cluster operator. The Baker–Campbell–Hausdorff (BCH) expansion of the similarity transformed Hamiltonian in nested commutators

$$\tilde{H} = \hat{H} + \left[\hat{H}, \hat{T}\right] + \frac{1}{2!}\left[\left[\hat{H}, \hat{T}\right], \hat{T}\right] + \frac{1}{3!}\left[\left[\left[\hat{H}, \hat{T}\right], \hat{T}\right], \hat{T}\right] + \ldots \tag{2.4.7.5}$$

terminates at fourth order in the amplitudes, as the Hamiltonian, being a 2-body operator, can contract with at most 4 instances of the cluster amplitudes. The nested commutators make explicit to the cancellation of terms that are unlinked.

The linked form of the coupled cluster equations can now be written

$$E = \langle \Phi_0 | \tilde{H} | \Phi_0 \rangle \tag{2.4.7.6}$$

$$0 = R_I = \langle \Phi_I | \tilde{H} | \Phi_0 \rangle \tag{2.4.7.7}$$

equivalent to

$$E_{CC}\delta_{0,I} = \left\langle \Phi_I \middle| \left(\hat{H}\mathrm{e}^{\hat{T}}\right)_C \middle| \Phi_0 \right\rangle$$

where the subscript C denoted only connected terms.

The linked formalism retains size-extensivity for each term in the equations, whereas the unlinked formalism is only size extensive when terms at each order are taken together.[76] This property is desirable but not essential, as when taken in their entirety the linked and unlinked equations are equivalent, giving the same amplitudes and energies as each other. The single-reference closed-shell and spin-unrestricted open-shell CC theories use cluster operators that mutually commute, and so are almost always implemented in the linked formalism.

Not only does coupled cluster preserve the size-extensivity and size-consistency of the reference, but it also preserves the invariance to orbital rotations within occupied and virtual spaces. This property is to be desired in a theoretical model for chemistry, and ideally would be preserved in a spin-free method for open shell systems.

The number of terms in the spin-adapted coupled cluster equations can often be reduced by a transformation of the projection manifold, such that the bra and ket states form a biorthogonal basis. The amplitudes that solve these equations will be unchanged, as the same equations are still being solved within the same space. It is usually the case that the equations are simplified if these bra states are constructed to form a biorthogonal basis with the ket states $|\{\Phi_I\rangle = \hat{E}^I |\Phi_0\rangle$:

$$\langle \Phi_I \,|\, \Phi_J \rangle = \left\langle \Phi_0 \,\middle|\, \tilde{E}_I \hat{E}^J \,\middle|\, \Phi_0 \right\rangle = \delta_I^J \tag{2.4.7.8}$$

This is automatically true when each state is a single SD constructed from orthogonal spin-orbitals. In a spin-adapted theory this is no longer the case, but the construction of the appropriate biorthogonal basis in general is not a trivial task. For a closed shell reference, the biorthogonal basis for up to double excitations can be constructed, but for triple and higher excitations this cannot be done, and the best that can be done is to reduce the off-diagonal elements to be as few as possible. For other CSF references, constructing an appropriate basis for the projection manifold is expected to be even more challenging, and has been left for future work.

2.4.7.4 Solution of CC equations

The working equations of coupled cluster may be written in a form $\mathbf{R}(\mathbf{t}) = 0$, where the amplitudes t_I to be found are those that set the residuals R_I to zero. Since these equations are in general highly non-linear, they must be solved by an iterative procedure.[76] Given some vector $\mathbf{t}^{(n)}$ of amplitudes at iteration n, a Taylor expansion for the residuals $\mathbf{R}$ may be made in small changes $\delta\mathbf{t}^{(n)}$ to the amplitudes.

$$\mathbf{R}\left(\mathbf{t}^{(n)} + \delta\mathbf{t}^{(n)}\right) = \mathbf{R}\left(\mathbf{t}^{(n)}\right) + \left.\frac{\partial \mathbf{R}}{\partial \mathbf{t}}\right|_{\mathbf{t}=\mathbf{t}^{(n)}} \delta\mathbf{t}^{(n)} + \mathcal{O}\left(\left(\delta\mathbf{t}^{(n)}\right)^2\right) \tag{2.4.7.9}$$

where $\frac{\partial \mathbf{R}}{\partial \mathbf{t}}$ is the Jacobian matrix of $\mathbf{R}(\mathbf{t})$. Neglecting terms of order $\mathcal{O}\left(\left(\delta \mathbf{t}^{(n)}\right)^2\right)$ and setting $\mathbf{R}\left(\mathbf{t}^{(n)} + \delta \mathbf{t}^{(n)}\right) = 0$ gives Newton's method,

$$\mathbf{t}^{(n+1)} = \mathbf{t}^{(n)} + \delta \mathbf{t}^{(n)} \tag{2.4.7.10}$$

$$\delta \mathbf{t}^{(n)} = -\left(\left. \frac{\partial \mathbf{R}}{\partial \mathbf{t}} \right|_{\mathbf{t}=\mathbf{t}^{(n)}} \right)^{-1} \mathbf{R}\left(\mathbf{t}^{(n)}\right) \tag{2.4.7.11}$$

There are usually very many amplitudes to be solved, so the coupled cluster Jacobian is a large matrix: for example in CCSD it will have dimensions scaling approximately as $N^4 \times N^4$. Inverting the Jacobian would need to be done at every iteration for these non-linear equations, and is therefore too expensive to be done directly.

Instead, a preconditioned quasi-Newton algorithm may be used, in which the inverse Jacobian is approximated by a much cheaper matrix. In a regime where the amplitudes are small (i.e. "weak correlation"), the off-diagonal elements in the CC Jacobian ($\frac{\partial R_I}{\partial t_J}, I \neq J$) will be much less significant than the diagonal elements.[156] Furthermore, the diagonal part of the CC Jacobian may be expected in this case to be dominated by the Fock operator, with negligible contribution from the fluctuation potential.[76]

$$\frac{\partial R_I}{\partial t_I} \approx \sum_{p \in \{\mathrm{occ}, I\}} \epsilon_{p \in \{\mathrm{occ}, 0\}} - \sum_0 \epsilon_p = \Delta_I \tag{2.4.7.12}$$

where Δ_I is the difference between sum of occupied canonical Hartree–Fock orbital energies ϵ in state I and the reference state. The inverse CC Jacobian can then be approximated as the reciprocal of these energy denominators, of which only $O(N^4)$ need to be calculated.

$$\delta t_I^{(n)} = -\frac{R_I\left(\mathbf{t}^{(n)}\right)}{\Delta_I} \tag{2.4.7.13}$$

The scheme based on this iteration directly corresponds to a summation of terms that generate a given overall excitation, up to infinite order in the Møller–Plesset perturbation series (equation 2.4.4.13).[21, 156]

Two assumptions have been made in approximating the inverse CC Jacobian with a perturbative quasi-Newton preconditioner: firstly that the CC Jacobean

is nearly diagonal, and secondly that the diagonal part is primarily from the Fock matrix, with negligible contribution from the fluctuation potential. These two approximations are related to one another, and together can no longer be expected to hold in a strongly correlated regime.

For an open shell reference such as that obtained by Restricted Open-shell Hartree–Fock theory, there may not even be a uniquely-defined Fock matrix in spatial orbital basis from which to take the energy denominators. Nevertheless, a pseudo-Fock matrix preconditioner may be constructed, with the understanding that convergence may consequently be slow, unstable, or not achieved at all.

$$f_q^p = h_q^p + \sum_{i \in \{\text{core}\}} 2g_{qi}^{pi} - g_{iq}^{pi} + \sum_{i \in \{\text{active}\}} g_{qi}^{pi} \tag{2.4.7.14}$$

Using such a crude preconditioner is a more serious deficiency than the previous approximations to the inverse CC Jacobian, but it turns out not to be fatal to orbital-based coupled cluster calculations. Stable convergence may be attained in many more situations than the standard perturbative quasi-Newton method by employing some regularisation techniques, which are outlined in the following sections.

2.4.7.5 Level Shifts

In strongly correlated systems, the CC Jacobean may become singular. Even in cases where the true inverse exists, it may be that the energy denominators in the (pseudo-)Fock matrix preconditioner become pathologically small. There are several different ways to regularise this problem,[157, 158] one of the simplest of which is to add a level shift to the denominator in each amplitude update.[76]

$$\delta t_I^{(n)} = -\frac{R_I\left(\mathbf{t}^{(n)}\right)}{\Delta_I + \Delta} \tag{2.4.7.15}$$

This is equivalent to a procedure which was originally developed to improve convergence in Hartree–Fock calculations.[159] The regularisation parameter Δ corresponds to effectively shifting the occupied orbitals down in energy and the virtual orbitals up. Δ can be chosen to be the same for all excitations I, but for

double, triple, etc. excitations ($k(I) = 2, 3, \dots$) an alternative is correspondingly to multiply it by the excitation level $k(I)$. This guarantees that if a shift of Δ is large enough to avoid zero denominators for the singles, then a shift of 2Δ will be large enough for the doubles, and so on.

$$\delta t_I^{(n)} = -\frac{R_I\left(\mathbf{t}^{(n)}\right)}{\Delta_I + k(I)\Delta} \tag{2.4.7.16}$$

The level shift effectively decreases the quasi-Newton step size, making it more likely that the procedure will converge, at the cost of an increased number of iterations. While each iteration of the perturbative quasi-Newton method described previously corresponds directly to introducing an additional order in the perturbation, this is no longer the case when a level shift has been added. In a finite-order perturbative method such as CASPT2, the level shift therefore has a significant, and essentially arbitrary, effect on the energy.[158, 160] However, for coupled cluster equations that are converged to all orders of perturbation theory, the amplitudes solve the same residual equations regardless of level shift, and so can still be said to correspond to the same partial infinite sum of the perturbation series.

2.4.7.6 Direct Inversion in the Iterative Subspace

A powerful method for forcing convergence in difficult cases, again developed originally to accelerate SCF convergence of Hartree–Fock calculations, is Direct Inversion in the Iterative Subspace (DIIS).[161, 162] The amplitude update $\delta\mathbf{t}^{(n)}$ is calculated as before, but instead of being added directly, the amplitudes are updated using a linear combination of n previous sets of amplitudes, according to a set of weights w_k.

$$\mathbf{t}^{(n+1)} = \sum_{k=1}^{n} w_k \left(\mathbf{t}^{(k)} + \delta\mathbf{t}^{(k)}\right) \tag{2.4.7.17}$$

where the total weights sum to 1. The weights are determined by using an error vector that is to be minimised, which can be either the vector of residuals R_I or the calculated amplitude updates δt_I. Minimising the norm of the average error

vector $\tilde{\delta\mathbf{t}} = \sum_{k=1}^{n} w_k \delta\mathbf{t}^{(k)}$ subject to the constraint $\sum_{k=1}^{n} w_k = 1$ is done by inverting an $(n+1) \times (n+1)$ matrix, according to the method of Lagrange multipliers.[76]

$$\begin{pmatrix} \langle\delta\mathbf{t}^{(1)}|\delta\mathbf{t}^{(1)}\rangle & \langle\delta\mathbf{t}^{(1)}|\delta\mathbf{t}^{(2)}\rangle & \cdots & \langle\delta\mathbf{t}^{(1)}|\delta\mathbf{t}^{(n)}\rangle & -1 \\ \langle\delta\mathbf{t}^{(2)}|\delta\mathbf{t}^{(1)}\rangle & \langle\delta\mathbf{t}^{(2)}|\delta\mathbf{t}^{(2)}\rangle & \cdots & \langle\delta\mathbf{t}^{(2)}|\delta\mathbf{t}^{(1)}\rangle & -1 \\ \vdots & \vdots & \ddots & \vdots & \vdots \\ \langle\delta\mathbf{t}^{(n)}|\delta\mathbf{t}^{(1)}\rangle & \langle\delta\mathbf{t}^{(n)}|\delta\mathbf{t}^{(2)}\rangle & \cdots & \langle\delta\mathbf{t}^{(n)}|\delta\mathbf{t}^{(n)}\rangle & -1 \\ -1 & -1 & \cdots & -1 & 0 \end{pmatrix} \begin{pmatrix} w_k \\ w_k \\ \vdots \\ w_k \\ \lambda \end{pmatrix} = \begin{pmatrix} 0 \\ 0 \\ \vdots \\ 0 \\ 1 \end{pmatrix}$$

Usually the sum is restricted to include a constant number of the most recent iterations, running from $k = n - d + 1$ up to $k = n$. The subspace size d is a parameter that can be increased to obtain more stable convergence at the expense of memory needed to store a larger number of previous amplitudes.

2.4.8 Multireference CC methods

Some systems require multiple determinants in the reference state:

$$|\Psi_0\rangle = \sum_I c^{(I)} |\Phi_I\rangle \tag{2.4.8.1}$$

Whether this linear combination is symmetry-determined, as a single CSF, or variationally optimised as a MCSCF wavefunction, the incorporation of dynamical correlation will require some additional considerations.

A "genuine" multireference CC (MRCC) method may be considered as one in which the linear coefficients $c^{(I)}$ in the model space (of dimension $d > 1$) are to be determined, as well as the amplitudes that define the wave operator.[6, 7] A "state-universal" (SU) method is one in which an effective Hamiltonian is formulated and diagonalised in the entire model space, in order to obtain a balanced treatment of all of the reference functions. A "state-specific" (SS) approach, in contrast, targets just a single state in the model space.

Further to all these particle number-conserving, or "Hilbert Space" MRCC approaches, are those for which the cluster operator is not restricted to conserve particle number.

2.4.8.1 Jeziorski–Monkhorst approaches

The Jeziorski–Monkhorst ansatz applies a separate wave operator to each of the d model space functions:[34]

$$|\Psi\rangle = \sum_I c^{(I)} \hat{\Omega}^{(I)} |\Phi_I\rangle \tag{2.4.8.2}$$

Projecting the Schrödinger equation onto the states $\langle\Phi_A|$ orthogonal to the model space:

$$0 = \sum_I \left\langle \Phi_A \middle| \left(\hat{H} - E\right) \hat{\Omega}^{(I)} \middle| \Phi_I \right\rangle c^{(I)} \tag{2.4.8.3}$$

the initial idea was to solve for the entire space obtained from all of the model functions, in a multistate approach.[34] If a single state is sought, the challenge arises to obtain a set of equations that has the same number of linearly independent equations, defined by the projection manifold $\mathrm{span}\left(\{\langle\Phi_A|\}\right)$ as there are parameters defining the wave operators $\hat{\Omega}^{(I)}$.[4, 6] If each wave operator takes the traditional exponential form $\hat{\Omega}^{(I)} = \mathrm{e}^{\hat{T}^{(I)}}$, then at first glance the correct number of parameters would seem to be obtained by defining the projection manifold as that generated by all the excitations for which there is an amplitude in the cluster operators $\hat{T}^{(I)}$. However, since there are excited states that can be reached from multiple model space functions, there are not generally enough independent equations to uniquely define the amplitudes. The excess amplitudes may be described as redundant.[6, 34]

One approach to obtaining enough equations to uniquely define the amplitudes is by noting that each term in the sum in equation 2.4.8.3 can be set independently to zero, and this would be a sufficient condition to satisfy the Schrödinger equation.[35]

$$0 = \left\langle \Phi_A \middle| \left(\hat{H} - E\right) \mathrm{e}^{\hat{T}^{(I)}} \middle| \Phi_I \right\rangle \qquad \forall I \tag{2.4.8.4}$$

The fact that these so-called "sufficiency conditions" are more stringent than strictly necessary reflects the fact that additional constraints are being placed on the amplitudes to find a unique solution to the otherwise underdetermined set

of equations.[6] The full orthogonal space spanned by $\{\langle\Phi_A|\}$ is larger than the number of amplitudes in any one truncated cluster operator, and so equation 2.4.8.4 cannot in general be solved. A truncated excitation manifold of functions $\left\langle\Phi_A^{(I)}\right|$ can be defined for each model space function, using the excitations that appear only in each truncated cluster operator.[34] Since there is now no longer a single projection manifold within which the Schrödinger equation is satisfied, it is said that these JM-formulated multireference coupled cluster theories do not satisfy the "proper residual condition."[35, 163]

There are four commonly considered multireference coupled cluster theories derived by applying sufficiency conditions in the J–M ansatz after different manipulations of the Schrödinger equation.[6, 35] The most straightforward of these is the Brillouin–Wigner MRCC (BW-MRCC),[164, 165] whose amplitude equations are simply those obtained when equation 2.4.8.4 is projected onto the excitation manifold for each I:

$$0 = \sum_I \left\langle\Phi_A\right| \left(\hat{H} - E\right) \mathrm{e}^{\hat{T}^{(I)}} \left|\Phi_I\right\rangle c^{(I)} \tag{2.4.8.5}$$

$$\Longleftarrow \qquad 0 = \left\langle\Phi_A^{(I)}\right| \left(\hat{H} - E^{(I)}\right) \mathrm{e}^{\hat{T}^{(I)}} \left|\Phi_I\right\rangle \tag{2.4.8.6}$$

Since the energy E for the state in question appears, this is a state-specific MRCC.

By replacing the energy E of a specific state with a model space effective Hamiltonian defined by

$$H_{\mathrm{eff}}{}_I^J = \left\langle\Phi_J\right| \hat{H}\mathrm{e}^{\hat{T}^{(I)}} \left|\Phi_I\right\rangle = \left\langle\Phi_J\right| \mathrm{e}^{-\hat{T}^{(I)}} \hat{H}\mathrm{e}^{\hat{T}^{(I)}} \left|\Phi_I\right\rangle$$

a set of MRCC equations can be obtained which contain no reference to a specific state, and so may be described as state-universal.[6]

$$0 = \sum_I \left(\left\langle\Phi_A^{(I)}\right| \hat{H}\mathrm{e}^{\hat{T}^{(I)}} \left|\Phi_I\right\rangle - \sum_J \left\langle\Phi_A^{(J)}\right| \mathrm{e}^{\hat{T}^{(J)}} \left|\Phi_J\right\rangle H_{\mathrm{eff}}{}_I^J \right) c^{(I)} \tag{2.4.8.7}$$

$$\Longleftarrow \qquad 0 = \left\langle\Phi_A^{(I)}\right| \hat{H}\mathrm{e}^{\hat{T}^{(I)}} \left|\Phi_I\right\rangle - \sum_J \left\langle\Phi_A^{(J)}\right| \mathrm{e}^{\hat{T}^{(J)}} \left|\Phi_J\right\rangle H_{\mathrm{eff}}{}_I^J \tag{2.4.8.8}$$

Solving these SU-MRCC equations will give amplitudes to give a correlated wavefunction corresponding to any of the reference states in the model space. This state universality comes with the drawback of serious convergence issues

when so-called "intruder states" appear.[6, 166] Even for model space functions that are well-separated, it may be the case that a correlated wavefunction approaches another reference wavefunction, leading to a failure in the perturbative treatment on which the method is based, and consequent issues with convergence. The separation between model states may not be preserved when following potential energy surfaces across molecular geometries, or external states that were previously high in energy may drop down and become intruders, again hindering convergence.[166]

Two other formulations of MRCC in the J–M ansatz may be obtained by inserting a resolution of the identity, separating out the model space and the orthogonal space.[61, 62]

$$\hat{1} = \sum_J \mathrm{e}^{\hat{T}^{(I)}} \left|\Phi_J\right\rangle \left\langle\Phi_J\right| \mathrm{e}^{-\hat{T}^{(I)}} + \sum_B \mathrm{e}^{\hat{T}^{(I)}} \left|\Phi_B\right\rangle \left\langle\Phi_B\right| \mathrm{e}^{-\hat{T}^{(I)}} \tag{2.4.8.9}$$

Modifying the Schrödinger equation in this way before applying the sufficiency conditions yields the size-extensive formulation known as Mukherjee-MRCC (Mk-MRCC)

$$\begin{aligned}
0 &= \sum_I \left\langle \Phi_A \right| \left(\hat{H} - E\right) \mathrm{e}^{\hat{T}^{(I)}} \left| \Phi_I \right\rangle c^{(I)} \\
&= \sum_I \sum_J \left\langle \Phi_A \right| \mathrm{e}^{\hat{T}^{(I)}} \left| \Phi_J \right\rangle \left\langle \Phi_J \right| \mathrm{e}^{-\hat{T}^{(I)}} \left(\hat{H} - E\right) \mathrm{e}^{\hat{T}^{(I)}} \left| \Phi_I \right\rangle c^{(I)} \\
&\quad + \sum_I \sum_B \left\langle \Phi_A \right| \mathrm{e}^{\hat{T}^{(I)}} \left| \Phi_B \right\rangle \left\langle \Phi_B \right| \mathrm{e}^{-\hat{T}^{(I)}} \left(\hat{H} - E\right) \mathrm{e}^{\hat{T}^{(I)}} \left| \Phi_I \right\rangle c^{(I)} \\
&= \sum_I \sum_J \left\langle \Phi_A \right| \mathrm{e}^{\hat{T}^{(J)}} \left| \Phi_I \right\rangle \left\langle \Phi_I \right| \mathrm{e}^{-\hat{T}^{(J)}} \hat{H} \mathrm{e}^{\hat{T}^{(J)}} \left| \Phi_J \right\rangle c^{(J)} \\
&\quad - \sum_I E \left\langle \Phi_A \right| \mathrm{e}^{\hat{T}^{(I)}} \left| \Phi_I \right\rangle c^{(I)} \\
&\quad + \sum_I \sum_B \left\langle \Phi_A \right| \mathrm{e}^{\hat{T}^{(I)}} \left| \Phi_B \right\rangle \left\langle \Phi_B \right| \mathrm{e}^{-\hat{T}^{(I)}} \hat{H} \mathrm{e}^{\hat{T}^{(I)}} \left| \Phi_I \right\rangle c^{(I)} \\
&= \sum_I \left(\sum_J \left\langle \Phi_A \right| \mathrm{e}^{\hat{T}^{(J)}} \left| \Phi_J \right\rangle H_{\mathrm{eff}}{}_I^J c^{(J)} - \left\langle \Phi_A \right| \mathrm{e}^{\hat{T}^{(I)}} \left| \Phi_I \right\rangle E c^{(I)} \right. \\
&\qquad \left. + \sum_B \left\langle \Phi_A \right| \mathrm{e}^{\hat{T}^{(I)}} \left| \Phi_B \right\rangle \left\langle \Phi_B \right| \mathrm{e}^{-\hat{T}^{(I)}} \hat{H} \mathrm{e}^{\hat{T}^{(I)}} \left| \Phi_I \right\rangle c^{(I)} \right) \\
\Longleftarrow \qquad 0 &= \sum_J \left\langle \Phi_A^{(J)} \right| \mathrm{e}^{\hat{T}^{(J)}} \left| \Phi_J \right\rangle H_{\mathrm{eff}}{}_I^J c^{(J)} - \left\langle \Phi_A^{(I)} \right| \mathrm{e}^{\hat{T}^{(I)}} \left| \Phi_I \right\rangle E c^{(I)} \\
&\quad + \sum_B \left\langle \Phi_A^{(I)} \right| \mathrm{e}^{\hat{T}^{(I)}} \left| \Phi_B \right\rangle \left\langle \Phi_B \right| \mathrm{e}^{-\hat{T}^{(I)}} \hat{H} \mathrm{e}^{\hat{T}^{(I)}} \left| \Phi_I \right\rangle c^{(I)}
\end{aligned}$$

The single-root MRCC method uses the same resolution of the identity, while also using the effective Hamiltonian instead of the energy.[6, 62]

$$
\begin{aligned}
0 &= \sum_I \left(\left\langle \Phi_A \middle| \hat{H} \mathrm{e}^{\hat{T}^{(I)}} \middle| \Phi_I \right\rangle - \sum_J \left\langle \Phi_A \middle| H_{\mathrm{eff}}{}_I^J \mathrm{e}^{\hat{T}^{(I)}} \middle| \Phi_I \right\rangle \right) c^{(I)} \\
&= \sum_I \sum_J \left(\left\langle \Phi_A \middle| \mathrm{e}^{\hat{T}^{(J)}} \middle| \Phi_J \right\rangle H_{\mathrm{eff}}{}_I^J c^{(J)} - \left\langle \Phi_A \middle| \mathrm{e}^{\hat{T}^{(I)}} \middle| \Phi_I \right\rangle H_{\mathrm{eff}}{}_I^J c^{(I)} \right) \\
&+ \sum_I \sum_B \left(\left\langle \Phi_A \middle| \mathrm{e}^{\hat{T}^{(I)}} \middle| \Phi_B \right\rangle \left\langle \Phi_B \middle| \mathrm{e}^{-\hat{T}^{(I)}} \hat{H} \mathrm{e}^{\hat{T}^{(I)}} \middle| \Phi_I \right\rangle c^{(I)} \right) \\
\Longleftarrow \qquad 0 &= \sum_J \left\langle \Phi_A^{(J)} \middle| \mathrm{e}^{\hat{T}^{(J)}} \middle| \Phi_J \right\rangle H_{\mathrm{eff}}{}_I^J c^{(J)} - c^{(I)} \sum_J \left\langle \Phi_A^{(J)} \middle| \mathrm{e}^{\hat{T}^{(J)}} \middle| \Phi_J \right\rangle H_{\mathrm{eff}}{}_I^J \\
&+ \sum_B \left\langle \Phi_A^{(I)} \middle| \mathrm{e}^{\hat{T}^{(I)}} \middle| \Phi_B \right\rangle \left\langle \Phi_B \middle| \mathrm{e}^{-\hat{T}^{(I)}} \hat{H} \mathrm{e}^{\hat{T}^{(I)}} \middle| \Phi_I \right\rangle c^{(I)}
\end{aligned}
$$

Although the equations for the latter two methods do not contain the energy of the target state, they do contain the coefficients of one specific model space function $c^{(I)}$, and so they are both state-specific MRCC methods.[6, 35]

Using sufficiency conditions as in the previous approaches constitutes an increase in the number of equations to give a unique solution for the redundant set of amplitudes. The alternative is to reduce the number of amplitudes to be the same as the number of linearly independent excited state wavefunctions in the projection manifold. The MRexpT method of Hanrath achieves this by defining a cluster operator wherein each amplitude is uniquely identified with an excited state in the projection manifold, regardless of whether it is precisely the state generated out of any individual model space function by the corresponding excitation.[163, 167]

$$
|\Psi\rangle = \sum_I c^{(I)} \mathrm{e}^{\hat{T}(I)} |\Phi_I\rangle \tag{2.4.8.10}
$$

$$
\hat{T}(I) = \mathrm{e}^{-\mathrm{i}\arg\left(c^{(I)}\right)} \sum t_{\hat{\tau}^A(I)|I\rangle} \hat{\tau}^A(I) \tag{2.4.8.11}
$$

To avoid states of multiple parentage cancelling each other out and leaving their combined amplitude undetermined, the relative phase of the model space coefficients is cancelled out of the leading term in the exponential.[163] Since each term is projected onto only those excitations that reach an excited state manifold that is shared across all model space functions, the MRexpT method also satisfies

the proper residual condition, although it is not size-extensive, and suffers from orbital invariance problems common to many J–M-based methods.[5, 163]

2.4.8.2 Internally contracted approaches

In contrast to using the J–M ansatz of a separate wave operator for each model space function, another approach is to contract the coefficients with the model space functions before applying a single wave operator.[5, 57, 66–68]

$$|\Psi\rangle = \hat{\Omega} \sum_I c^{(I)} |\Phi_I\rangle$$

In these, "internally contracted," approaches, the intruder state problem is much less serious, but there can still be redundant amplitudes due to spectating excitations and states of multiple parentage.

A set of linearly independent amplitudes can be found in analogy to Löwdin's canonical orthogonalisation procedure.[68, 69, 168] The overlap matrix (metric) of the excitation manifold can be constructed

$$S_J^I = \left\langle \Phi \middle| \hat{\tau}_J \hat{\tau}^I \middle| \Phi \right\rangle \tag{2.4.8.12}$$

where $|\Phi\rangle$ is the (multiconfigurational) reference state. If $\mathbf{U}$ is the matrix which diagonalises $\mathbf{S}$, then truncating the diagonal matrix $\mathbf{\Lambda}$ to contain only those eigenvalues of $\mathbf{S}$ above a numerical threshold ϵ yields a transformation $\mathbf{X}$ that can be applied to the excitations to obtain a reduced number that are linearly independent.[68]

$$\mathbf{U}^\dagger \mathbf{S} \mathbf{U} = \mathbf{\Lambda} \tag{2.4.8.13}$$

$$X_J^I = U_K^I \left(\Lambda_J^K\right)^{-1/2} \qquad \left(\Lambda_J^K > \epsilon, K = J\right) \tag{2.4.8.14}$$

$$\tilde{\tau}^I = X_J^I \hat{\tau}^J \tag{2.4.8.15}$$

Evangelista and Gauss observed in some small calculations that there tended to be a large difference in order of magnitude between about $2/3$ of the eigenvalues which should be retained ($\lambda \gtrsim 10^{-9}$) and the remaining $1/3$ which were nearly zero ($\lambda \lesssim^{-14}$), and so they heuristically chose a threshold of $\epsilon = 10^{-9}$, but

acknowledged that a systematic procedure for choosing ϵ would be preferable.[68] Hanauer and Köhn noted that size extensivity of icMRCC depends on a generalised normal ordering[47] with respect to the reference of the redundant excitations that are eliminated.[71]

The use of a single projection manifold spanned by excitations from all of the reference determinants leads to an orbitally invariant theory, thanks to the satisfaction of the proper residual condition.[68, 72]

In general, operators will need to be included that excite electrons from core orbitals into active orbitals, as well as active to virtual. These will not commute, and will lead to a non-terminating BCH expansion of the similarity transformed Hamiltonian.

However, the ic-MRCC method involves not only solving for the amplitudes in the cluster operator, but also optimisation of the linear contraction coefficients within the model space. In the case that the model space contains every possible determinant with the active orbitals singly occupied (a "complete model space"), then the ic-MRCC energy is fully invariant to orbital rotations.[57, 68] In this case, exclusion of internal excitations within the model space amounts to the (orbitally-invariant) neglect of relaxation to the reference in the presence of dynamic correlation. Since a CASSCF reference may be considered already to have included the orbital relaxition in response to static correlation, this effect is often considered small enough to ignore, avoiding the excessive complications introduced by active-active excitations.[5, 57]

2.4.8.3 Fock Space Coupled Cluster

Cluster operators can be included that do not necessarily conserve particle number, in so-called 'Fock Space' MRCC methods.[36, 38, 39] These methods use a 'Valence Universal' wave operator, appropriate for states with any number of particles (relative to the true vacuum) or quasiparticles (e.g. attached or ionised electrons, or particle-hole excitations relative to a Fermi vacuum). A cluster operator $\hat{S}$ can be decomposed into n-body parts $\hat{S}_n$, of which each part has

contributions that can be labelled by the numbers (k, l) of annihilation operators in the active particle (k) and hole (l) orbitals.

$$\hat{S} = \hat{S}_1 + \hat{S}_2 + \ldots + \hat{S}_n \tag{2.4.8.16}$$

$$\hat{S}_n = \hat{S}_n^{(0,0)} + \hat{S}_n^{(1,0)} + \hat{S}_n^{(0,1)} + \hat{S}_n^{(1,1)} + \ldots \tag{2.4.8.17}$$

The FSCC equations are solved in a hierarchy of (k, l) sectors of Fock space with increasing particle and hole numbers. The amplitudes of a given (k, l) valence appear in the equations in higher-valence subspaces, giving the so-called Subspace Embedding Conditions for this hierarchical solution scheme.[6, 37, 169] More generally, the equations in different valence sectors of Fock space may be decoupled by a sequence of similarity transforms of the Hamiltonian.[6, 38, 170–172]

Some formulations of FSCC have long employed a normal-ordered exponential ansatz that was introduced by Lindgren.[9, 173] There has been work by Nooijen, and more recently Mukherjee and coworkers, to derive the appropriate similarity transformations of the Hamiltonian when the exponential is replaced by its normal ordered form, but the contractions that can appear on both sides of the Hamiltonian lead to a series of terms that generally has no closed form.[44, 174] We will now consider this form of the wave operator in the state-specific, general single-reference context.

3

Normal-Ordered Exponential Coupled Cluster

This chapter contains work that was published in the Faraday Discussions paper:

Gunasekera, A. D. *et al.* Multi-reference coupled cluster theory using the normal ordered exponential ansatz. *Faraday Discuss.* **254,** 170–190. doi:10.1039/D4FD00044G (6th Nov. 2024)

Spin-adapted excitations involving singly-occupied orbitals will not commute in general, and so the BCH expansion (equation 2.4.7.5) for the similarity-transformed Hamiltonian will no longer terminate. To avoid the terms that appear in the wave operator with amplitudes contracted together up to infinite order, Lindgren's normal-ordered exponential (NOE) form of the coupled-cluster wave operator[9] can be used.

We have developed a general single-reference formalism that can be used to apply a normal-ordered exponential *ansatz* on a high- or low-spin reference, while maintaining a spin-free cluster operator. With no closed-form similarity transformed Hamiltonian generally available for this form of the wave operator, we have adapted the unlinked formalism of traditional CC, explicitly introducing the renormalisation terms that cancel unlinked diagrams in the CC equations.

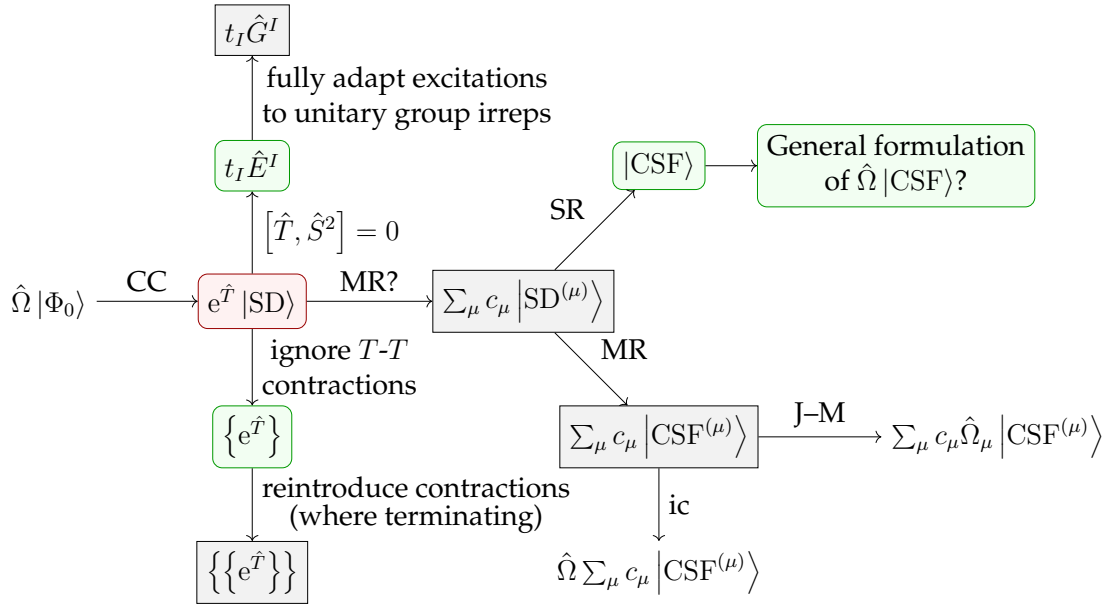

Figure 3.1: The choices made in the general single-reference NOECC *ansatz*

In truncating this theory to the lowest one or two orders in the amplitudes for computational feasibility, we have employed a careful procedure to avoid introducing spurious higher-order terms and minimise the size-extensivity error. In the cluster operator, we include all possible excitations from the first-order interacting space, including any active-active excitations, compatible with intermediate normalisation thanks to the single-reference nature of this framework. While this also avoids the issue of states of multiple parentage, there are still redundancies due to spectating excitations, which are not fatal to convergence with appropriate numerical methods, but lead to a non-uniqueness of the solutions which should be dealt with in the future.

3.1 The normal-ordered exponential

The traditional coupled cluster wavefunction for a cluster operator containing terms that mutually commute is written as an exponential wave operator applied to the reference determinant

$$|\Psi\rangle = e^{\hat{T}} |\Phi_0\rangle \tag{3.1.0.1}$$

The appropriate generalisation for an open-shell CSF reference state $|\Phi_0\rangle$ is Lindgren's normal-ordered exponential coupled-cluster (NOECC) wave operator

$$|\Psi\rangle = \{\mathrm{e}^{\hat{T}}\}\,|\Phi_0\rangle \tag{3.1.0.2}$$

where braces indicate normal-ordering with respect to the closed-shell vacuum. The normal-ordered exponential form excludes contractions between cluster operators and properly parametrises independent correlation processes according to the factorisation theorem[9]. Without normal-ordering, contractions among active-to-active excitations in the cluster operator, such as $\hat{T}^u_t$ and $\hat{T}^{uy}_{tx}$, would give rise to non-terminating working equations. Normal-ordering ensures that the energy and amplitude equations terminate at finite order in the cluster operators. The order at which the equations terminate is $4 + \min(n, 2N_r)$, where n is the number of active orbitals and N_r is the maximum rank of the excitation operators. When applied to a closed-shell reference, $\{\mathrm{e}^{\hat{T}}\} = \mathrm{e}^{\hat{T}}$ and NOECC is equivalent to the standard coupled-cluster ansatz.

The exact wave operator, consisting of all linked diagrams up to infinite order in the perturbation, is expressed as a normal ordered exponential, according to an analagous argument to the derivation of the standard CC *ansatz*. Let $T = \sum_k T^{(k)}$, where $T^{(k)}$ consists of only open, connected diagrams of order k in the perturbation. In the wave operator Ω, the terms $\Omega^{(k)}$ of order k in the perturbation are, according to the factorisation theorem,

$$\Omega^{(2)} = T^{(2)} + \frac{1}{2}\left\{T^{(1)}T^{(1)}\right\} \tag{3.1.0.3}$$

$$\Omega^{(3)} = T^{(3)} + \left\{T^{(1)}T^{(2)}\right\} + \frac{1}{3!}\left\{\left(T^{(1)}\right)^3\right\} \tag{3.1.0.4}$$

and generally

$$\Omega^{(l)} = \sum\left\{\prod_k \frac{\left(T^{(k)}\right)^{n_k}}{n_k!}\right\} \tag{3.1.0.5}$$

with $\sum_k k n_k = l$ The overall wave operator $\Omega = \sum_{l=0}^{\infty}\Omega^{(l)}$ can be identified[9] as

$$\Omega = \sum_{n=0}^{\infty}\left\{\frac{T^N}{n!}\right\} = \left\{\mathrm{e}^T\right\} \tag{3.1.0.6}$$

This *ansatz*, with its origins in the factorisation theorem,[153] better aligns with the physical motivation for coupled cluster as modelling independent excitation events. An amplitude tensor contracted to another amplitude tensor would constitute a connected cluster that should properly be included only at a higher truncation level. The choice to take the exponential in normal order ensures that there are no contractions among cluster operators, so the working equations terminate at finite order in the cluster amplitudes even when active-to-active excitations are included.

Single CSF references are invariant with respect to rotations among the doubly-occupied orbitals, but not in general among the open-shell (active) orbitals. We include purely active-to-active excitations in our cluster operator, since these are required to fully allow for correlation-induced orbital relaxation of the CSF reference. Using a model space consisting of a single function means that active-active excitations are no longer "internal," and so are compatible with intermediate normalisation. The normal-ordered *ansatz* allows the inclusion of these otherwise problematic excitations.

3.2 An 'unlinked' Coupled Cluster *ansatz*

Internally contracted MRCC can be formulated with linked equations because active-to-active excitations are excluded. Using a linked formalism for NOECC theory in an analogous way to the standard theory would require knowledge of the inverse wave operator $\{e^{\hat{T}}\}^{-1}$, which is non-trivial[43]. Several attempts have been made to construct linked equations equivalent to a similarity transformed Hamiltonian by other means. The work by Mukherjee *et al.* uses the Bloch formalism

$$\hat{H}\{\mathrm{e}^{\hat{T}}\}|\Phi_0\rangle = \{\mathrm{e}^{\hat{T}}\}\hat{H}_{\text{eff}}|\Phi_0\rangle \tag{3.2.0.1}$$

where $\hat{H}_{\text{eff}}$ is an effective Hamiltonian in the reference space $|\Phi_0\rangle$ with the same eigenenergy as the target space $\{\mathrm{e}^{\hat{T}}\}|\Phi_0\rangle$. By applying Wick's theorem to factor out $\{\mathrm{e}^{\hat{T}}\}$ they obtain a rigorous expression for the effective Hamiltonian as an

infinite series, along with a hierarchy of finite order approximations of increasing accuracy[174, 175]. Intermediate normalisation $\hat{P}\{\mathrm{e}^{\hat{T}}\}\hat{P} = \hat{P}$ is not imposed since it is in general incompatible with size-extensivity, which requires $(1-\hat{P})\hat{H}_{\text{eff}}\hat{P} = 0$, where $\hat{P}$ projects onto the reference space[169, 173].

Our approach is much simpler. Recognising that for the single-reference case intermediate normalisation can be imposed, we use the unlinked form. The unlinked energy and amplitude equations are given by

$$E = \langle\Phi_0|\hat{H}\{\mathrm{e}^{\hat{T}}\}|\Phi_0\rangle \tag{3.2.0.2}$$

$$R_I = \langle\Phi_I|(\hat{H} - E)\{\mathrm{e}^{\hat{T}}\}|\Phi_0\rangle \tag{3.2.0.3}$$

where the cluster excitations $\hat{E}_I$ are chosen so that the projection manifold $\langle\Phi_I| = \langle\Phi_0|\,\hat{E}_I^\dagger$ is the first-order interacting space. The unlinked residual equations can be rewritten as

$$R_I = \langle\Phi_I|\hat{H}\{\mathrm{e}^{\hat{T}}\}|\Phi_0\rangle - \langle\Phi_I|\{\mathrm{e}^{\hat{T}}\}|\Phi_0\rangle\, E \tag{3.2.0.4}$$

$$= \langle\Phi_I|\hat{H}\{\mathrm{e}^{\hat{T}}\}|\Phi_0\rangle - \langle\Phi_I|\{\mathrm{e}^{\hat{T}}\}|\Phi_0\rangle\,\langle\Phi_0|\hat{H}\{\mathrm{e}^{\hat{T}}\}|\Phi_0\rangle \tag{3.2.0.5}$$

A proof that Eq. 3.2.0.5 is equivalent to a connected form of the residual equations and that the formulation is therefore size extensive is provided in section 3.5. For NOECC with up to N_r-order excitations and n active orbitals, the equations will terminate, but at a high order in $\hat{T}$ of $4 + \min(n, 2N_r)$, so we presently study truncated equations. Naively truncating the exponential in the unlinked formalism to obtain a lower-cost approximation would result in non-size extensive equations. However, the size-extensivity error can be kept small by retaining all terms in Eq. 3.2.0.5 up to a given power in the amplitudes (see section 3.5). Specifically, the linearised equations (l-NOECC) are:

$$E = \langle\Phi_0|\hat{H}\{1 + \hat{T}\}|\Phi_0\rangle \tag{3.2.0.6}$$

$$R_I = \langle\Phi_I|\hat{H}\{1 + \hat{T}\}|\Phi_0\rangle - \langle\Phi_I|\{\hat{T}\}|\Phi_0\rangle\,\langle\Phi_0|\hat{H}|\Phi_0\rangle \tag{3.2.0.7}$$

and the quadratic equations (q-NOECC) are:

$$E = \langle \Phi_0 | \hat{H} \{ 1 + \hat{T} + \frac{1}{2} \hat{T}^2 \} | \Phi_0 \rangle \tag{3.2.0.8}$$

$$R_I = \langle \Phi_I | \hat{H} \{ 1 + \hat{T} + \frac{1}{2} \hat{T}^2 \} | \Phi_0 \rangle - \langle \Phi_I | \{ \hat{T} \} | \Phi_0 \rangle \langle \Phi_0 | \hat{H} \{ 1 + \hat{T} \} | \Phi_0 \rangle - \langle \Phi_I | \{ \frac{1}{2} \hat{T}^2 \} | \Phi_0 \rangle \langle \Phi_0 | \hat{H} | \Phi_0 \rangle \tag{3.2.0.9}$$

Since standard CCD only includes terms up to quadratic in the amplitudes, our truncated q-NOECCD method exactly replicates closed-shell CCD, and q-NOECCSD differs from CCSD only by neglecting third- and fourth-order terms involving singles amplitudes and the failure to cancel the disconnected $\langle \Phi_I | \{ \hat{T} \} | \Phi_K \rangle \langle \Phi_K | \hat{H} \{ \hat{T} \} | \Phi_0 \rangle$ term in the residual equation, where $|\Phi_K\rangle$ is a singly excited state and $|\Phi_I\rangle$ is doubly excited.

Our unlinked formulation explicitly imposes intermediate normalisation. It therefore allows for the possibility to include purely active-to-active excitations in the cluster operator that would formally break intermediate normalisation, since the amplitudes that would violate intermediate normalisation are necessarily zero at convergence.

3.3 Choice of cluster Operator

We choose the cluster operator so that it generates the entire first-order interacting space out of the reference state. For excitations from core orbitals to virtual, this leads to the usual inclusion of singles and doubles as in standard CCSD approaches. We also include core-to-active, active-to-virtual, and active-to-active excitations in both the singles and doubles. The active-to-active excitations are important to allow the possibility of correlation-induced orbital relaxation of the reference state. The Goldstone diagrams for the general excitation operators for NOECCSD are depicted in Figure 3.2. For reference states with only one active orbital, we exclude purely active-to-active excitations in the singles and doubles.

The active-to-active amplitudes introduce spectator excitations, where a double excitation involves an electron being annihilated and created in the

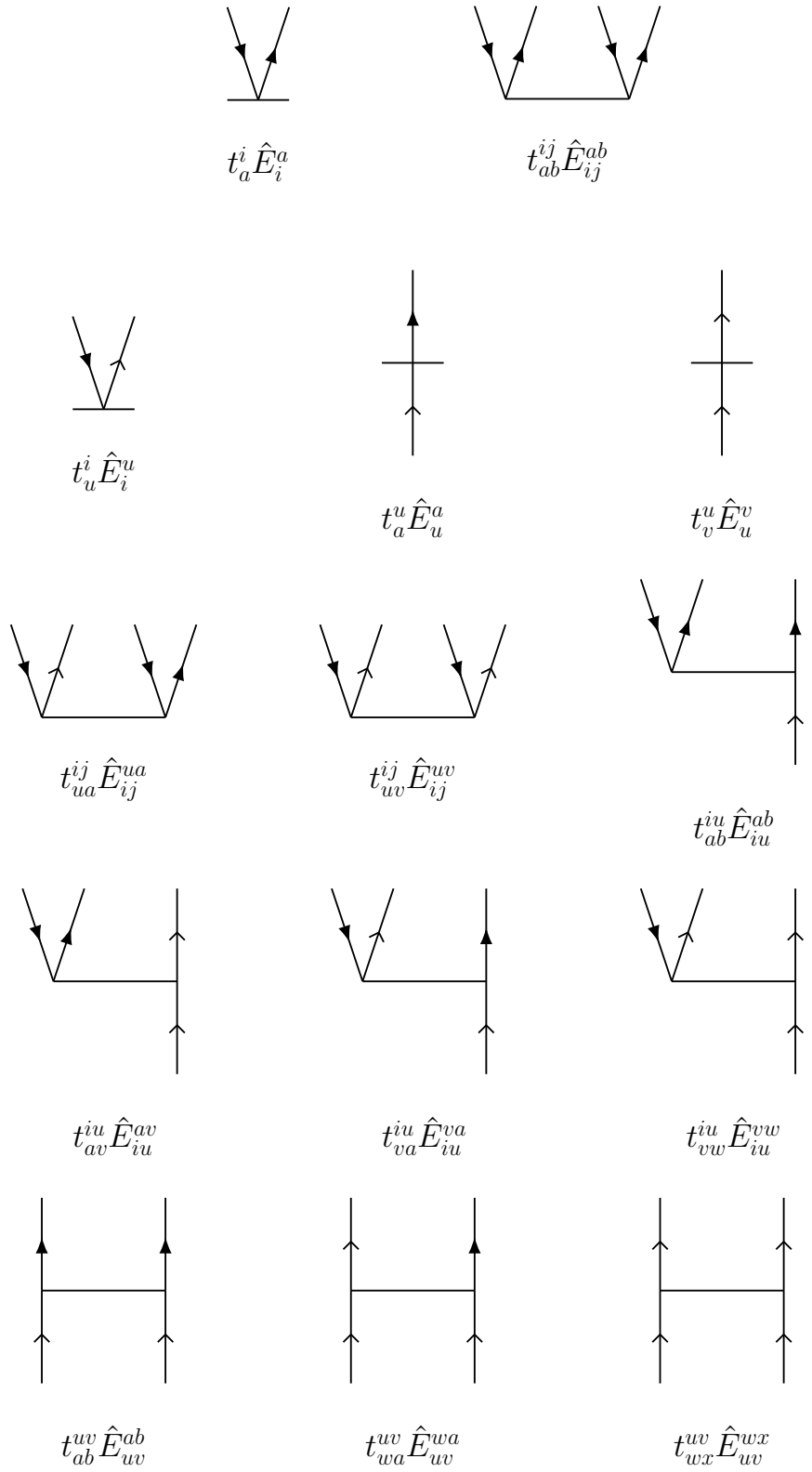

Figure 3.2: Goldstone diagrams for the singles and doubles amplitudes used in our NOECCSD. Core and virtual electrons are represented by solid arrows; active electrons are represented by skeleton arrows.

same active orbital and acts as a single excitation when applied to the reference. The same residual equation is therefore obtained by projection with either the single excitation $\hat{E}_p^q$ or the double excitation with a spectator $\hat{E}_{pu}^{qu}$, and there are an insufficient number of equations to uniquely determine the amplitudes[33, 34, 37, 169, 176].

In the linearised approximation l-NOECCSD, the redundant excitations are interchangeable and the infinite set of amplitudes that solve the residual equations all result in exactly the same energy. We have also observed that different amplitude solutions also yield nearly the same energies for the q-NOECCSD method, although we do not know to what extent this is true in general. Despite the fact that in the current formulation the equations contain redundant excitations and are under-determined, we find that it is always possible to converge the residual equations. Typically, convergence requires use of an appropriate level shift and the Direct Inversion in the Iterative Subspace (DIIS) technique[161]. It should be noted that, while spectator excitations are present, we choose to include these only at the ranks denoted by the ansatz, i.e. the NOECCSD cluster operator only includes one- and two-body operators, even though there may be higher rank operators that produce the same configuration from the reference.

3.4 Spin incompleteness of the projection manifold

For a given excited state generated from an open-shell reference, there may be other states of the same spin and orbital occupation that are not reached directly by excitations included in the cluster operator. Some formulations include the higher-body excitations required to generate these excited states and obtain a spin-complete projection manifold.[74] Including these will lead to computationally expensive terms in the NOECC equations that are not necessary to guarantee spin adaptation. We also expect that those higher-order excitations will be of much less significance that the ones generating the first-order interacting space.[120, 177] Herrmann and Hanrath found that although excluding spectators in spin-adapted CC treatments gave a significant spin-incompleteness error in the energy,

including them only up to the tensor rank was sufficient to remove it almost entirely, despite the excitation manifold not being fully spin-complete.[74]

In the NOECC formulation implemented in OCCSFrD, we do not include those higher-body excitations, and make no attempt at spin completeness of the excitation manifold. We do, however, include the spectator excitations up to the rank of the ansatz, which can mitigate almost all the spin incompleteness error.[74] This choice reflects the fact that coupled cluster methods are based on a description of dynamic correlation in which operators take precedence over the states generated. For single-reference cases the dominant spin-coupling is present in the CSF and the remaining dynamic correlation processes are contained within the first-order interacting space.

The success of traditional CCSD is attributable to the presence of operators spanning the entire first-order interacting space. For open shell and multi-reference cases, we may expect similar success using precisely those operators that span the first-order interacting space, regardless of whether that space is spin-complete or not. Analagously to traditional CC, the normal-ordered CC can in principle be systematically improved towards FCI by incorporating connected triples, quadruples, and higher excitations in the cluster operator, whether or not the projection manifold is spin-complete.

3.5 Connectedness of the residual equation

We demonstrate here that our working equations (Equation 3.2.0.5) are equivalent to a connected form of the residual equations. We also show that truncating our equations does introduce disconnected terms, but that size extensivity can be restored if the equations are taken to the full (finite) order at which they terminate. The proof uses a derivation found in Lindgren's paper[9] that extracts the connected terms from the product of the Hamiltonian and the normal ordered exponential form of the wave operator:

$$\hat{H}\{e^{\hat{T}}\} = \{\hat{H}\{e^{\hat{T}}\}\} + \{\hat{H}\overbrace{\{e^{\hat{T}}\}}\} \tag{3.5.0.1}$$

The contracted terms can be separated into products of the connected parts and the remaining cluster operators:

$$\begin{aligned}\left\{\hat{H}\overbrace{e^{\hat{T}}}\right\} &= \sum_{n=1}^{\infty}\frac{1}{n!}\{\hat{H}\overbrace{\{\hat{T}^n\}}\} \\ &= \sum_{n=1}^{\infty}\frac{1}{n!}\sum_{k=1}^{n}\binom{n}{k}\{(\hat{H}\,\hat{T}^k)_C\}\{\hat{T}^{n-k}\}\}\} \\ &= \sum_{(n-k)=0}^{\infty}\sum_{k=1}^{\infty}\frac{1}{k!}\frac{1}{(n-k)!}\{(\hat{H}\,\{\hat{T}^k\})_C\,\{\hat{T}^{n-k}\}\} \\ &= \sum_{k=1}^{\infty}\frac{1}{k!}\{(\hat{H}\,\{\hat{T}^k\})_C\,\{e^{\hat{T}}\}\} \end{aligned} \tag{3.5.0.2}$$

The first term of equation 3.5.0.1 corresponds to extending the sum to $k = 0$, leading to the classic result that[9, 33]

$$\hat{H}\{e^{\hat{T}}\} = \sum_{k=0}^{\infty}\frac{1}{k!}\{(\hat{H}\,\{\hat{T}^k\})_C\,\{e^{\hat{T}}\}\} = \{\{e^{\hat{T}}\}(\hat{H}\{e^{\hat{T}}\})_C\} \tag{3.5.0.3}$$

where the subscript C denotes connected terms. We have also used the fact that, within a normal ordered product, operators consisting of even numbers of creation and annihilation operators commute.

3.5.1 Size extensivity in the closed shell case

Our residual equation is

$$\begin{aligned} R_I &= \langle\Phi_I|\hat{H}\{e^{\hat{T}}\}|\Phi_0\rangle - \langle\Phi_I|\{e^{\hat{T}}\}|\Phi_0\rangle\,\langle\Phi_0|\hat{H}\{e^{\hat{T}}\}|\Phi_0\rangle \\ &= \langle\Phi_I|\{\{e^{\hat{T}}\}(\hat{H}\{e^{\hat{T}}\})_C\}|\Phi_0\rangle - \langle\Phi_I|\{e^{\hat{T}}\}|\Phi_0\rangle\,\langle\Phi_0|\hat{H}\{e^{\hat{T}}\}|\Phi_0\rangle \\ &= \langle\Phi_I|\{e^{\hat{T}}\}(\hat{H}\{e^{\hat{T}}\})_C|\Phi_0\rangle - \langle\Phi_I|\{\overbrace{e^{\hat{T}}\}(\hat{H}\{e^{\hat{T}}\})_C}|\Phi_0\rangle \\ &\quad - \langle\Phi_I|\{e^{\hat{T}}\}|\Phi_0\rangle\,\langle\Phi_0|\hat{H}\{e^{\hat{T}}\}|\Phi_0\rangle \end{aligned} \tag{3.5.1.1}$$

In the closed shell case, amplitudes cannot be contracted with from the right so the middle term is zero. The disconnected terms in $\langle\Phi_0|\hat{H}\{e^{\hat{T}}\}|\Phi_0\rangle$ will also

vanish. We then have

$$\begin{aligned} R_I &= \langle\Phi_I|\{e^{\hat{T}}\}(\hat{H}\{e^{\hat{T}}\})_C|\Phi_0\rangle - \langle\Phi_I|\{e^{\hat{T}}\}|\Phi_0\rangle\,\langle\Phi_0|(\hat{H}\{e^{\hat{T}}\})_C|\Phi_0\rangle \\ &= \sum_{K\neq 0}\langle\Phi_I|\{e^{\hat{T}}\}|\Phi_K\rangle\,\langle\Phi_K|(\hat{H}\{e^{\hat{T}}\})_C|\Phi_0\rangle \\ &= \langle\Phi_I|(\hat{H}\{e^{\hat{T}}\})_C|\Phi_0\rangle + \sum_{K\neq 0}\langle\Phi_I|\{e^{\hat{T}}-1\}|\Phi_K\rangle\,\langle\Phi_K|(\hat{H}\{e^{\hat{T}}\})_C|\Phi_0\rangle \end{aligned} \tag{3.5.1.2}$$

If $|\Phi_I\rangle$ is to be reached from $|\Phi_K\rangle$ using only excitations and $|\Phi_K\rangle \neq |\Phi_0\rangle$, then $|\Phi_K\rangle$ must be in the manifold spanned by the states $|\Phi_I\rangle$. If $|\Phi_K\rangle$ is an excited state that can only be reached from $|\Phi_0\rangle$, then $\langle\Phi_K|(\hat{H}\{e^{\hat{T}}\})_C|\Phi_0\rangle = R_K$. The disconnected terms vanish at convergence because they are comprised of smaller connected terms that are already solved in our equations. Solving our (not fully connected) equation is equivalent to solving the connected equation

$$0 = R_I = \langle\Phi_I|(\hat{H}\{e^{\hat{T}}\})_C|\Phi_0\rangle \tag{3.5.1.3}$$

3.5.2 The truncated residual equation

Expanding our equation (including disconnected terms) for R_I at each order in $\hat{T}$:

$$\begin{aligned} R_I^{(n)} =& \frac{1}{n!}\langle\Phi_I|\hat{H}\{\hat{T}^n\}|\Phi_0\rangle - \sum_{a=0}^{n}\frac{1}{a!}\langle\Phi_I|\{\hat{T}^a\}|\Phi_0\rangle\,\frac{1}{(n-a)!}\langle\Phi_0|\hat{H}\{\hat{T}^{(n-a)}\}|\Phi_0\rangle \\ =& \frac{1}{n!}\sum_{a=0}^{n}\binom{n}{a}\langle\Phi_I|\{\hat{T}^a\}\left(\hat{H}\{\hat{T}^{(n-a)}\}\right)_C|\Phi_0\rangle \\ & - \frac{1}{n!}\sum_{a=0}^{n}\binom{n}{a}\langle\Phi_I|\{\hat{T}^a\}|\Phi_0\rangle\,\langle\Phi_0|\hat{H}\{\hat{T}^{(n-a)}\}|\Phi_0\rangle \\ =& \frac{1}{n!}\sum_{a=0}^{n}\binom{n}{a}\sum_{K\neq 0}\langle\Phi_I|\{\hat{T}^a\}|\Phi_K\rangle\,\langle\Phi_K|\left(\hat{H}\{\hat{T}^{(n-a)}\}\right)_C|\Phi_0\rangle \end{aligned} \tag{3.5.2.1}$$

Our residual including terms up to order N is then

$$\begin{aligned} R_I^{[N]} =& \sum_{n=0}^{N}\frac{1}{n!}\sum_{a=0}^{n}\binom{n}{a}\sum_{K\neq 0}\langle\Phi_I|\{\hat{T}^a\}|\Phi_K\rangle\,\langle\Phi_K|\left(\hat{H}\{\hat{T}^{(n-a)}\}\right)_C|\Phi_0\rangle \\ =& \sum_{n=0}^{N}\frac{1}{n!}\Bigg(\langle\Phi_I|\left(\hat{H}\{\hat{T}^n\}\right)_C|\Phi_0\rangle \\ & + \sum_{a=1}^{n}\binom{n}{a}\sum_{K\neq 0}\langle\Phi_I|\{\hat{T}^a\}|\Phi_K\rangle\,\langle\Phi_K|\left(\hat{H}\{\hat{T}^{(n-a)}\}\right)_C|\Phi_0\rangle\Bigg) \end{aligned} \tag{3.5.2.2}$$

The disconnected terms on the right are no longer zero in general, as convergence of the other residuals will impose $R_K^{[N]} = 0$, rather than the lower-truncated residual equation $R_K^{[N-a]} = 0$. Our method is therefore not truly size-extensive.

We do however avoid the spurious higher-order disconnected terms that would arise if each exponential were independently truncated at order N:

$$\tilde{R}_I^{[N]} = \sum_{a=0}^{N} \frac{1}{a!} \langle \Phi_I | \hat{H} \{ \hat{T}^a \} | \Phi_0 \rangle - \sum_{a=0}^{N} \frac{1}{a!} \langle \Phi_I | \{ \hat{T}^a \} | \Phi_0 \rangle \sum_{b=0}^{N} \frac{1}{b!} \langle \Phi_0 | \hat{H} \{ \hat{T}^b \} | \Phi_0 \rangle \quad (3.5.2.3)$$

This does not affect the fact that the equations for closed shells terminate at 4th order in the the amplitudes. If our equations are truncated at 4th order, we do recover the full size extensive formulation of the theory without truncation. In the smaller connected components of the disconnected terms where $|\Phi_I\rangle$ can be reached from $|\Phi_K\rangle$ by application of $\{\hat{T}^a\}$, $R_K^{[N]}$ only has terms up to order $N - a$, so $R_K^{[N]} = R_K^{[N-a]}$ and our equation is equivalent to the connected form.

3.5.3 The general case

We first use the fact that the product of Hamiltonian and normal ordered wave operator $\hat{H}\{e^{\hat{T}}\}$ can be expressed as the product of $\{e^{\hat{T}}\}$ with a fully connected operator:

$$\hat{H}\{e^{\hat{T}}\} = \{e^{\hat{T}}\}\hat{\Lambda} \quad (3.5.3.1)$$

where $\hat{\Lambda}$ is a sum of fully connected terms. This result was first published by Mukherjee[174, 175], the proof for which is reproduced here. It is convenient to define the fully connected term $\tilde{H}_0 = (\hat{H}\{e^{\hat{T}}\})_C$ and the modified exponential $\{\tilde{e}^{\hat{T}}\} = \{e^{\hat{T}} - 1\}$.

Repeatedly applying Wick's theorem to equation 3.5.0.3 yields the relation obtained by Chakravarti, Sen, and Mukherjee[174, 175], that

$$\hat{H}\{e^{\hat{T}}\} = \{\{e^{\hat{T}}\}\tilde{H}_0\} = \{e^{\hat{T}}\}\hat{\Lambda} \quad (3.5.3.2)$$

where $\hat{\Lambda}$ is the sum of connected terms defined by

$$\hat{\Lambda} = \{\tilde{H}_0\} - \{(\{\tilde{e}^{\hat{T}}\}\tilde{H}_0)_C\} + \{(\{\tilde{e}^{\hat{T}}\}(\{\tilde{e}^{\hat{T}}\}\tilde{H}_0)_C)_C\} - \{(\{\tilde{e}^{\hat{T}}\}(\{\tilde{e}^{\hat{T}}\}(\{\tilde{e}^{\hat{T}}\}\tilde{H}_0)_C)_C)_C\} + \dots \quad (3.5.3.3)$$

Using this result, the residual equation can be written

$$R_I = \langle\Phi_I|\hat{H}\{e^{\hat{T}}\}|\Phi_0\rangle - \langle\Phi_I|\{e^{\hat{T}}\}|\Phi_0\rangle\langle\Phi_0|\hat{H}\{e^{\hat{T}}\}|\Phi_0\rangle \tag{3.5.3.4}$$

$$= \langle\Phi_I|\{e^{\hat{T}}\}\hat{\Lambda}|\Phi_0\rangle - \langle\Phi_I|\{e^{\hat{T}}\}|\Phi_0\rangle\langle\Phi_0|\{e^{\hat{T}}\}\hat{\Lambda}|\Phi_0\rangle \tag{3.5.3.5}$$

$$= \sum_{K\neq 0}\Big(\langle\Phi_I|\{e^{\hat{T}}\}|\Phi_K\rangle - \langle\Phi_I|\{e^{\hat{T}}\}|\Phi_0\rangle\langle\Phi_0|\{e^{\hat{T}}\}|\Phi_K\rangle\Big)\langle\Phi_K|\hat{\Lambda}|\Phi_0\rangle \tag{3.5.3.6}$$

$$= \langle\Phi_I|\hat{\Lambda}|\Phi_0\rangle + \sum_{K\neq 0}\Big(\langle\Phi_I|\{\tilde{e}^{\hat{T}}\}|\Phi_K\rangle - \langle\Phi_I|\{\tilde{e}^{\hat{T}}\}|\Phi_0\rangle\langle\Phi_0|\{\tilde{e}^{\hat{T}}\}|\Phi_K\rangle\Big)\langle\Phi_K|\hat{\Lambda}|\Phi_0\rangle \tag{3.5.3.7}$$

where the $K = 0$ terms cancel due to the intermediate normalisation condition $\langle\Phi_0|\{e^{\hat{T}}\}|\Phi_0\rangle = 1$. Assuming intermediate normalisation also gives that $\langle\Phi_0|\{\tilde{e}^{\hat{T}}\}|\Phi_K\rangle = 0$, so we can write

$$R_I = \langle\Phi_I|\hat{\Lambda}|\Phi_0\rangle + \sum_{K\neq 0}\langle\Phi_I|\{\tilde{e}^{\hat{T}}\}|\Phi_K\rangle\langle\Phi_K|\hat{\Lambda}|\Phi_0\rangle \tag{3.5.3.8}$$

As for the closed shell case, if $|\Phi_K\rangle$ cannot be reached from another excited state, then we have $\langle\Phi_K|\hat{\Lambda}|\Phi_0\rangle = R_K$, which vanishes at convergence.

Solving the residual Eq 3.2.0.5 is therefore equivalent to solving the fully connected equation

$$0 = R_I = \langle\Phi_I|\hat{\Lambda}|\Phi_0\rangle \tag{3.5.3.9}$$

The contribution of order $\hat{T}^n$ to the residual is

$$R_I^{(n)} = \sum_{K\neq 0}\sum_{c=0}^{n}\frac{1}{(n-c)!}\langle\Phi_I|\{T^{(n-c)}\}|\Phi_K\rangle\langle\Phi_K|\Lambda^{(c)}|\Phi_0\rangle \tag{3.5.3.10}$$

where $\Lambda^{(c)}$ is the sum of (connected) terms in Λ of order c with respect to $\hat{T}$. The residual truncated at order N is then

$$R_I^{[N]} = \sum_{n=0}^{N}R_I^{(n)} = \sum_{K\neq 0}\sum_{c=0}^{N}\sum_{a=0}^{N-c}\frac{1}{a!}\langle\Phi_I|\{T^a\}|\Phi_K\rangle\langle\Phi_K|\Lambda^{(c)}|\Phi_0\rangle \tag{3.5.3.11}$$

where the relabelling $a = (n-c)$ has been made inside the sum. Equivalently,

$$R_I^{[N]} = \sum_{K\neq 0}\sum_{a=0}^{N}\frac{1}{a!}\langle\Phi_I|\{T^a\}|\Phi_K\rangle\sum_{c=0}^{N-a}\langle\Phi_K|\Lambda^{(c)}|\Phi_0\rangle \tag{3.5.3.12}$$

$$= \sum_{K\neq 0}\sum_{a=0}^{N}\frac{1}{a!}\langle\Phi_I|\{T^a\}|\Phi_K\rangle\langle\Phi_K|\Lambda^{[N-a]}|\Phi_0\rangle \tag{3.5.3.13}$$

where $\Lambda^{[N-a]}$ indicates the sum of terms in Λ up to order $N-a$ in $\hat{T}$. Since we have not solved the connected equations $\langle \Phi_K | \Lambda^{[N-a]} | \Phi_0 \rangle = 0$ truncated to lower order, the truncation of our equations has once again introduced a size-extensivity error.

3.6 Formal scaling

The computation time required for each coupled cluster iteration scales with the number of core, active, and virtual orbitals. The formal scaling with the size of each of these spaces can be determined by analysis of the diagrams representing the tensor contractions: each particle or hole line appearing in a diagram represents an index over which the calculation will run, introducing a factor of n_c, n_a, or n_v into the computation time.

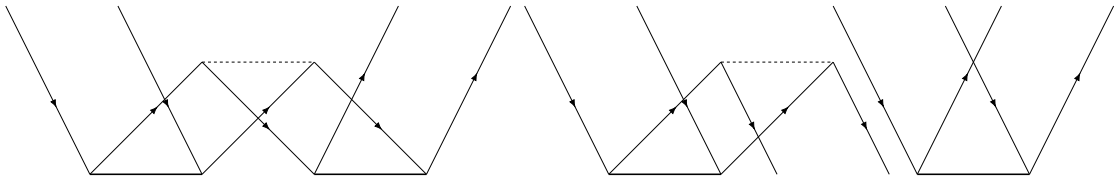

$$r_{p_0p_1}^{h_0h_1} = g_{h_2h_3}^{p_2p_3} t_{p_2p_3}^{h_0h_1} t_{p_0p_1}^{h_2h_3} = A_{h_2h_3}^{h_0h_1} t_{p_0p_1}^{h_2h_3} \qquad A_{h_2h_3}^{h_0h_1} = g_{h_2h_3}^{p_2p_3} t_{p_2p_3}^{h_0h_1} \qquad t_{p_4p_5}^{h_4h_5}$$

Figure 3.3: A diagram in the CCD and CCSD amplitude equations that will scale as N^8, and its factorisation into calculations scaling as N^6.

In traditional closed-shell formulations of CCSD, the most expensive term in the doubles amplitudes has contractions over four indices, with four indices uncontracted, for an overall N^8 scaling. When factorised in to the appropriate intermediates, this can be reduced to N^6,[85] as depicted in figure 3.3 The residual tensor $r_{p_0p_1}^{h_0h_1}$ has $\mathcal{O}\left(N_h^2 N_p^2\right)$ entries, each requiring $\mathcal{O}\left(N_h^2 N_p^2\right)$ operations, for an overall scaling of $\mathcal{O}\left(N_h^4 N_p^4\right) \sim \mathcal{O}\left(N^8\right)$. The intermediate tensor $A_{h_2h_3}^{h_0h_1}$ has $\mathcal{O}\left(N_h^4\right)$ entries, each requiring $\mathcal{O}\left(N_p^2\right)$ operations, for an overall scaling of $\mathcal{O}\left(N_h^4 N_p^2\right) \sim \mathcal{O}\left(N^6\right)$. Contracting this intermediate tensor with the amplitudes $t_{p_4p_5}^{h_4h_5}$, the $\mathcal{O}\left(N_h^2 N_p^2\right)$ entries in $r_{p_0p_1}^{h_0h_1}$ are then obtained with $\mathcal{O}\left(N_h^2\right)$ operations, for an overall scaling of $\mathcal{O}\left(N_h^4 N_p^2\right) \sim \mathcal{O}\left(N^6\right)$. If the intermediate A is stored in memory, these two contractions can be done separately, reducing the overall scaling from $\mathcal{O}\left(N^8\right)$ to $\mathcal{O}\left(N^6\right)$.

In general, a (factorised) closed shell CC treatment including excitations up to order X will scale per iteration as N^{2X+2}. A perturbative treatment of $(X+1)$-body excitations will introduce an additional factor of N. This arises from a basis transformation of the $(X+1)$-body perturbative amplitudes, which contain $\mathcal{O}\left(N^{2X+2}\right)$ entries. Since each index can be transformed in turn, this requires only $N\left(2X+2\right)$ additional operations, for an overall scaling of $\mathcal{O}\left(N^{2X+3}\right)$

3.6.1 NOECC

In our spin-adapted normal-ordered exponential CC, a similar diagrammatic analysis can be performed. Considering systems with a small number of open-shell orbitals ($N_a << N_c < N_v$), the most expensive terms will be the same as for the closed shell case. For an *ansatz* with up to X-body excitations, the most expensive terms will still scale as $\mathcal{O}\left(N^{2X+4}\right)$, or $\mathcal{O}\left(N^{2X+2}\right)$ with the proper factorisation. This is despite the fact that the amplitudes can appear up to 8th order in the full equations: the additional contractions are over the open-shell indices, which run only over the active orbitals, of which there are only $\mathcal{O}\left(1\right)$.

However, the open-shell NOECC equations have a combinatorial number of terms with respect to the number of open-shell orbitals, so there will be a prefactor that scales exponentially with the active orbital space.

4
The OCCSFrD Software Package

For systems requiring a multideterminantal reference state, it is well known that a spin-adapted coupled cluster method will use working equations with very many terms. This is the principal motivation for using an automated tool for deriving the equations. Equations with many thousands of terms may be generated while mitigating the impact of human error in their derivation.

Programs to automate the derivation of coupled cluster equations have become more and more prevalent as theories have been developed with more and more complicated formalisms. Kallay and Surjan's algorithm for solving general CC equations implemented a many-body approach and generated factorised equations.[178, 179] Kong's APG,[56] Köhn's GeCCo,[57] Evangelista's Wick&d,[58] Valeev's SeQuant,[59] among others, have been developed to implement various multireference or high-order CC theories that involve complicated equations.

An automated equation generator will also allow for extensions to higher levels of theory, and comparison between methods. The ability to implement different ansatze and generate equations for different systems is also a desirable feature of the software.

Not only is this equation generator intended as a tool for computation, but it also aims to aid interpretation of spin-adapted coupled cluster equations by

expressing them in a human-readable format. The fact that new equations need to be derived for each possible reference CSF makes it all the more important to be able to generate these equations automatically.

Having generated arbitrary spin-adapted open-shell coupled cluster equations, code must also be developed to solve them. The complications involved in solving spin-adapted, generally multi-determinantal, problems, were able to be addressed by developing our own in-house CC code. While greater efficiency may be possible in a compiled language such as C++ or Fortran, at this stage of method development, python was preferred for ease of implementation.

We developed a Python package for the automated generation of coupled cluster equations for arbitrary open shell configurations, which we have named Open-shell Coupled Cluster using a Spin-Free Diagrammatic construction (OCCSFrD). It implements two high-level functionalities: the generation of spin-free coupled cluster equations for arbitrary single CSF references, and the solution of those equations to obtain CC amplitudes and energies of accuracy comparable to traditional CC methods for single determinant references. The software is designed to interface with the PySCF package[180] for atomic orbital basis sets, integrals, and SCF calculations, and to use the numpy library for the mathematical manipulations, in particular numpy.einsum for applying the contractions in the CC equations.

4.1 Package Structure

A schematic for the structure of the OCCSFrD package is shown in figure 4.1.

OCCSFrD contains 5 modules:

- ansatz
- interface
- reference
- solve
- wick

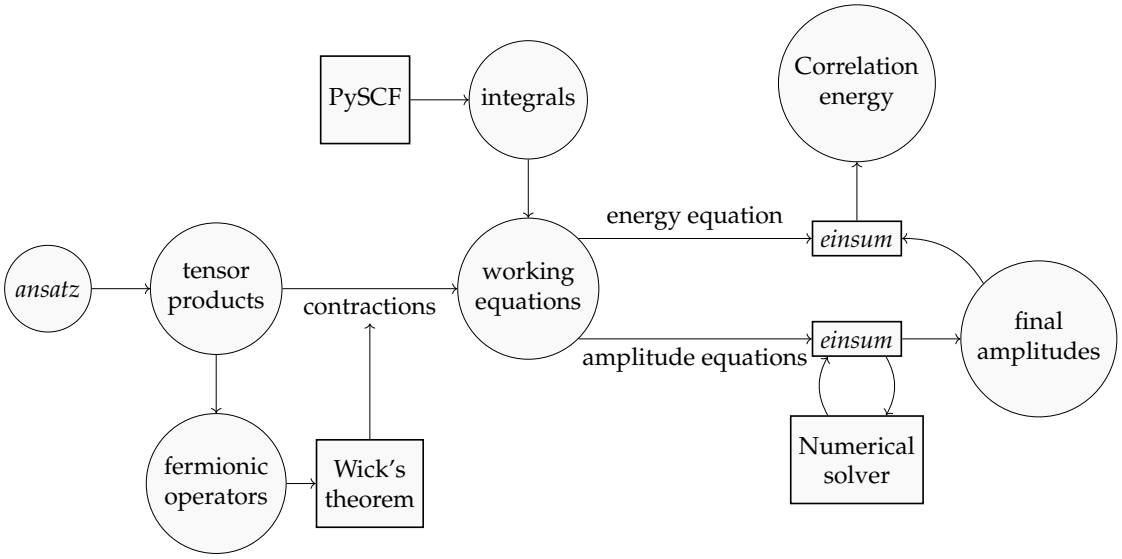

Figure 4.1: Schematic diagram to show the functions of the OCCSFrD package and how they relate to each other

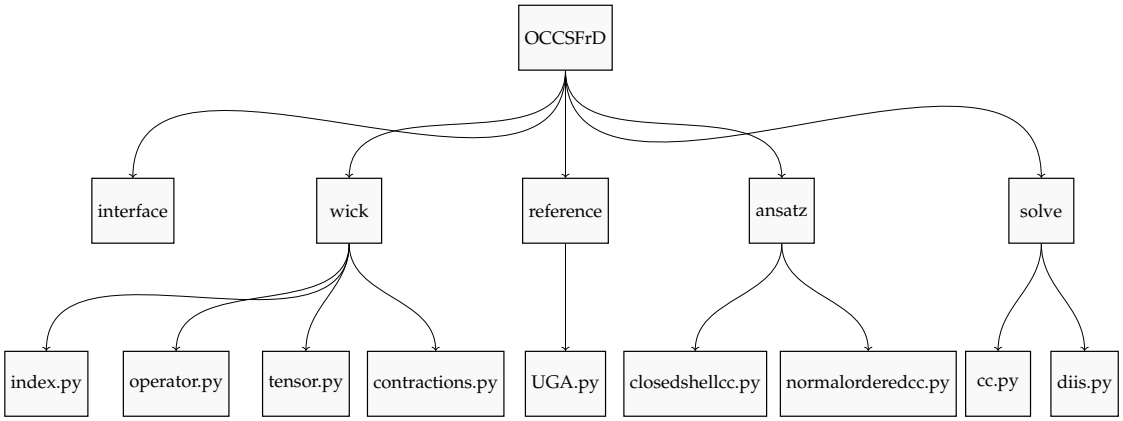

Figure 4.2: Schematic diagram to show the structure of the OCCSFrD package

The wick module contains the classes and routines for defining the tensor and operator algebras used in generating coupled cluster equations by Wick's theorem. It is organised into 4 python files:

- index.py
- operator.py
- tensor.py
- contractions.py

The reference module uses objects from the wick module to set up the creation

operators for an arbitrary reference configuration. UGA.py contains routines for constructing an arbitrary G–T basis function as a reference CSF.

The ansatz module contains classes and routine for setting up the normal ordered exponential or other many-body expression for the wave operator.

- closedshellcc
- normalorderedcc

The interface module deals with saving and loading the equations in a format in which they can be re-used for future calculations. It also contains routines to generate TeX code to display equations in a human-readable format, although all but the very simplest equations contain far too many terms for this to be practical under normal circumstances.

The solve module contains the actual CC solver for our general coupled cluster equations. The approach for this code was not to automate the generation of (for example) Fortran code, but instead to develop python code that could generalise the solution of CC equations to the range of possible equations generated by OCCSFrD.

4.2 Automated equation generator

We generate equations using an object-oriented Python code that carries out the construction of fully contracted terms using Wick's theorem in second quantization.

Features that were sought in the development of this equation generator included:

- The ability to deal with possibly large numbers of terms appearing in the equations
- Treating different reference systems using the same framework

- The ability to extend the ansatz to include higher excitations as well as different forms of the exponential (arbitrary truncation level, with or without contractions etc.)
- Recreating known results where available
- The ability to save the equations in a format enabling re-use on systems with the same reference configuration

The form of a reference CSF can be chosen by its GUGA vector. Specific linear combinations of CSFs may also be chosen. The purpose of the equation generator is to provide input for the fast routines in numpy.einsum, which will carry out the numerically intensive linear algebra steps involved in solving the equations.

Our CC equation generator uses a projective approach, where a residual tensor of a given shape is constructed as the sum of all possible contribution that would fully contract to a scalar with a tensor of the conjugate shape. Although it may be more efficient to use the many-body approach that constructs the appropriate tensors without requiring a projection, we have instead chosen this approach for its ease of application to general open shell cases.

To demonstrate this projective approach, consider an excited state given by $\left|\Phi^I\right\rangle = \hat{E}^I \left|\Phi_0\right\rangle$, where I indexes a general excitation operator $\hat{E}^I$ that is applied to reference state $\left|\Phi_0\right\rangle$. The residual R^I is the sum of all terms that will contract to a non-zero scalar when the Schrödinger equation is projected onto the excited (bra) state manifold $\left\langle\Phi_I\right| = \left\langle\Phi_0\right| \hat{E}_I$, where $\hat{E}_I = \left(\hat{E}^I\right)^\dagger$. It can be thought of as the partial derivative of the projected Schrödinger equation with respect to some arbitrary coefficients ϕ_I parametrising the excited state manifold:

$$R^I = \frac{\partial}{\partial \phi_I} \left\langle \Phi_0 \middle| \phi_I \hat{E}^I \left[\left(\hat{H} - E\right)\hat{\Omega}\right]_{l,q,\ldots} \middle| \Phi_0 \right\rangle \tag{4.2.0.1}$$

where the subscript $l, q, \ldots$ indicates a possible truncation of the equations to linear, quadratic, *etc.* level overall in the amplitudes.

For example, consider a doublet with one open-shell electron, with spin α, in an orbital labelled t. One contribution r^{iu}_{ab} to the residual R^{iu}_{ab} comes from the

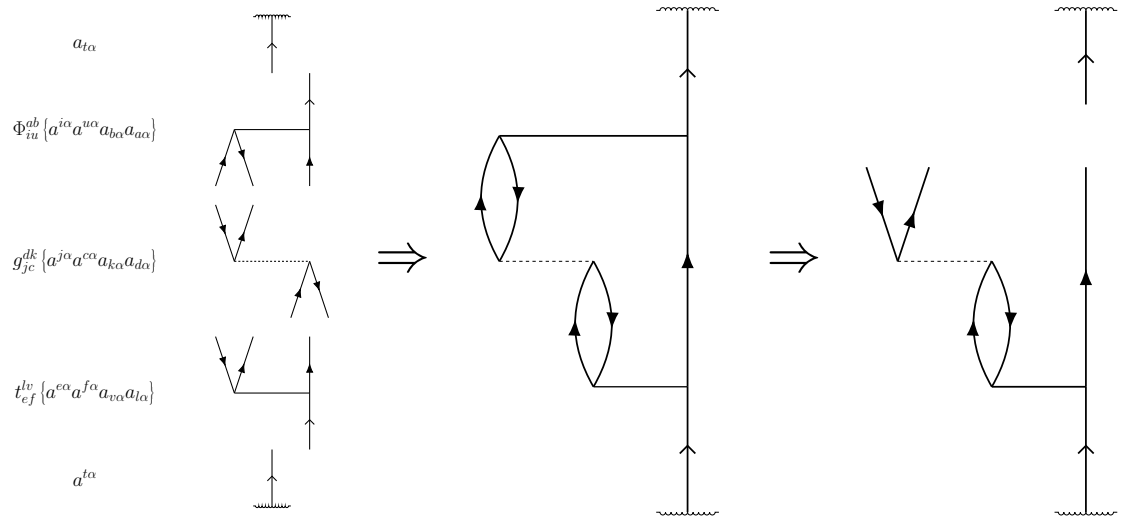

Figure 4.3: Goldstone diagram construction representing the automated generation of the residual term $r^{iu}_{ab} = g^{dk}_{jc}\, t^{lv}_{ef}\, \delta^u_t \delta^i_k \delta^f_b \delta^c_a \delta^j_l \delta^e_d \delta^t_v$

linear contribution of amplitude t^{iu}_{ab} with g^{bj}_{ia}:

$$r^{iu}_{ab} = \frac{\partial}{\partial \phi^{ab}_{iu}} \left\langle a_{t\alpha} \middle| \phi^{ab}_{iu} \left\{\hat{E}^{iu}_{ba}\right\} g^{dk}_{jc} \left\{\hat{E}^{jc}_{kd}\right\} t^{lv}_{ef} \left\{\hat{E}^{ef}_{vl}\right\} \middle| a^{t\alpha} \right\rangle \tag{4.2.0.2}$$

Showing one of the spin cases,

$$\begin{aligned} r^{iu}_{ab} =& \frac{\partial}{\partial \phi^{ab}_{iu}} \left\langle a_{t\alpha} \middle| \phi^{ab}_{iu} \left\{a^{i\alpha}a^{u\alpha}a_{b\alpha}a_{a\alpha}\right\} g^{dk}_{jc} \left\{a^{j\alpha}a^{c\alpha}a_{k\alpha}a_{d\alpha}\right\} t^{lv}_{ef} \left\{a^{e\alpha}a^{f\alpha}a_{v\alpha}a_{l\alpha}\right\} \middle| a^{t\alpha} \right\rangle \\ & [+\text{other spin variants}] \end{aligned} \tag{4.2.0.3}$$

a possible full contraction is

$$\begin{aligned} & \left\langle a_{t\alpha} \middle| \phi^{ab}_{iu} \left\{a^{i\alpha}a^{u\alpha}a_{b\alpha}a_{a\alpha}\right\} g^{dk}_{jc} \left\{a^{j\alpha}a^{c\alpha}a_{k\alpha}a_{d\alpha}\right\} t^{lv}_{ef} \left\{a^{e\alpha}a^{f\alpha}a_{v\alpha}a_{l\alpha}\right\} \middle| a^{t\alpha} \right\rangle \\ & \quad = \phi^{ab}_{iu}\, g^{dk}_{jc}\, t^{lv}_{ef}\, \delta^u_t \delta^i_k \delta^f_b \delta^c_a \delta^j_l \delta^e_d \delta^t_v\, [+\text{other full contractions}] \end{aligned} \tag{4.2.0.4}$$

for a residual contribution of

$$r^{iu}_{ab} = g^{dk}_{jc}\, t^{lv}_{ef}\, \delta^u_t \delta^i_k \delta^f_b \delta^c_a \delta^j_l \delta^e_d \delta^t_v\, [+\text{other full contractions} + \text{other spin variants}] \tag{4.2.0.5}$$

The automated procedure to generate this expression is equivalent to the Goldstone diagram construction in figure 4.3. This and other possible spin components are accounted for automatically, together with the factor of 4 associated with this diagram. In our pilot implementation, we do not identify equivalent terms in the

equations by the topologies of their diagrammatic construction. Furthermore, the equations are not factorised in this naive implementation, giving a suboptimal scaling of computational cost that remains to be addressed in future versions of the code. It is expected that the efficiency will be improved by a substantial factor when these steps are introduced through future code developments.

4.2.1 Classes defined

The module `occsfrd.wick` contains the classes used to evaluate the contractions in second quantization.

4.2.1.1 Indices

We designate three orbital subspaces: core, active, and virtual. We can also denote the core space as hole orbitals, and the active and virtuals as particle orbitals, with respect to the Fermi vacuum induced by doubly occupying the core. An `Index` object can be designated to refer to any of these subspaces, or generally to the entire Hilbert space. The purpose of an `Index` object is to keep track of the orbital indices over which *numpy.einsum* will run when performing the linear algebra operations.

The `Index` class has three attributes:

- `name: str` the name of the index, used to identify each index; can be a human-readable format
- `occupiedInVacuum: bool` whether or not the index refers to orbitals that are occupied in the Fermi vacuum; identifies the range of hole orbitals from particle orbitals
- `active: bool` whether or not the index refers to singly occupied orbitals. Usually these are only in the particle space (`occupiedInVacuum=False`), but this is not necessary

The subclass `SpecificOrbitalIndex` additionally allows an index to refer to a specific (usually active) orbital rather than a range of orbitals. It provides

Class (parameter: type)	Represents, *e.g.*:
`Index(name: String, occupiedInVacuum: Bool, active: Bool)`	i, a, t, u
`BasicOperator(index: Index, creationAnnihilation: Bool, spin: Bool)`	$a^{t\alpha}$
`OperatorProduct(operatorList: [BasicOperator, BasicOperator,...], prefactor: Float)`	$2a^{t\alpha}a_{i\beta}a^{j\beta}a_{u\alpha}$
`OperatorSum(summandList: [OperatorProduct, OperatorProduct,...])`	$2a^{t\alpha}a_{i\alpha}a^{j\alpha}a_{u\alpha}$ $+ 2a^{t\alpha}a_{i\beta}a^{j\beta}a_{u\alpha}$ $+ 2a^{t\beta}a_{i\alpha}a^{j\alpha}a_{u\beta}$ $+ 2a^{t\beta}a_{i\beta}a^{j\beta}a_{u\beta}$
`Tensor(name: String, lowerIndexTypes: [char,...], upperIndexTypes: [char,...], spinFree: Bool)`	t_2
`Vertex(tensor: Tensor, lowerIndices: [Index,...], upperIndices: [Index,...])`	$t_{2\,ab}^{\;\;ij}$
`TensorProduct(tensorList: [Tensor,...], prefactor: Float)`	$g_{ij}^{ab}t_{2\,cd}^{\;\;kl}$
`TensorSum(summandList: [TensorProduct,...])`	$2g_{ij}^{ab}t_{2\,cd}^{\;\;kl}\delta_k^i\delta_l^j\delta_c^a\delta_d^b$ $- g_{ij}^{ab}t_{2\,cd}^{\;\;kl}\delta_l^i\delta_k^j\delta_c^a\delta_d^b$

Table 4.1: Classes defined to allow automated equation generation, with examples of expressions they may represent

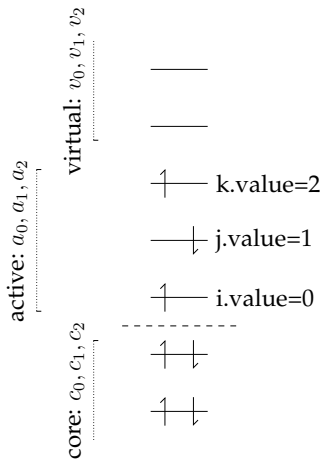

Figure 4.4: Core, active, and virtual orbital indices are specified. In the active space, specific orbital indices can be specified with a value instead of running over the whole range.

the attribute `value: int` which is the specific (0-indexed) index value of an orbital within a range. For example, a `SpecificOrbitalIndex` instantiated as an `Index` representing the active particle orbitals, with `value=0`, would refer to the first open-shell orbital. Having `Index` objects that can refer to individual open shell orbitals allows for slicing of the coefficient arrays properly when treating multideterminantal open shell states.

4.2.1.2 Operator Classes: `BasicOperator`, `OperatorProduct` `OperatorSum`

The fermionic operator algebra in second quantization is constructed from the elementary operators, represented by the `BasicOperator` class. Instances of the `BasicOperator` class have the attributes

- `index: Index` the `Index` object specifying the orbitals in which the operator creates or destroys an electron
- `spin: bool` whether the operator refers to an electron of spin up, designated `spin=True`, or down, designated `spin=False`
- `creation_annihilation: bool` `True` for creation operators, `False` for annihilation.

Additionally, the attribute `quasi_cre_ann` is a boolean that is `True` for quasiparticle creation operators and `False` for quasiparticle annihilation.

`OperatorProduct` objects represent a product of elementary operators as a list of its constituent `BasicOperator` objects, along with a list of contractions, if any have been made. Each contraction is represented as a 2-tuple, with the corresponding contravariant (superscript) `Index` followed by the corresponding covariant (subscript) one. An `OperatorProduct` also specifies a scalar prefactor (default =1). Where an operator product contains subsequences that are known to be in normal order, a list is provided of all the positions in the operatorList that correspond to the starts of the normal-ordered blocks. This facilitates faster contraction schemes by avoiding the checking of contractions within the same block, which will be zero by construction.

`OperatorSum` objects represent sums of operator products as a list of the summed `OperatorProduct` objects. This is the general class to represent any operator acting in the Fock space spanned by the elementary creation and annihilation operators.

Each of these operator types is equipped with methods for addition and multiplication with other operators, as well as Hermitian conjugation. Any expression in the second quantised operator algebra can now be expressed in terms of these operator classes.

4.2.1.3 Tensor Classes: `Tensor`, `SubDiagram`, `TensorProduct`, `TensorSum`

`Tensor` objects contain arrays such as the coefficients of some second-quantised operator, or some set of molecular integrals. The `Tensor` objects specify the orbital ranges of each index they may run over, which sets the dimensions of the array. The orbital type is specified by a single character:

- 'g': general
- 'c': core
- 'a': active

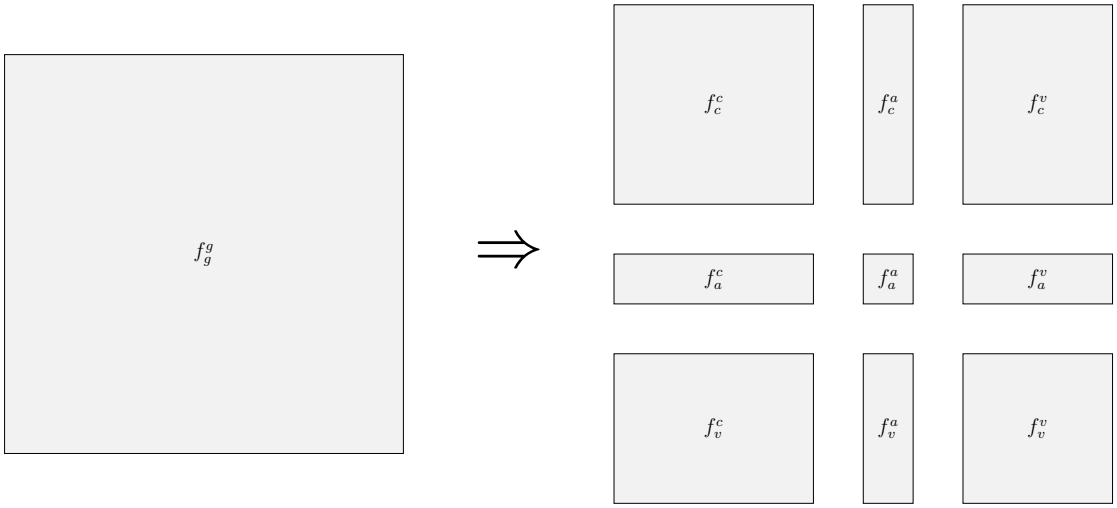

Figure 4.5: Elements in a Tensor.array viewed by SubDiagram objects

- 'v': virtual
- 'h': hole
- 'p': particle

`SubDiagram` is a subclass of `Tensor` that additionally contains a view of the array for its parent tensor, sliced by some subset of the tensor's orbital index ranges. Where a tensor is indexed over a range that includes more than one type (core, active, or virtual) of orbital, then each possible choice for the ranges of each index defines a `SubDiagram` object, representing the appropriate slice of its parent Tensor. This is equivalent to separating out each possible diagram fragment that may be represented by a tensor when lines for core, active, and virtual orbital spaces are distinguished. One important feature of the `SubDiagram` objects is that the array attribute refers to a slice of the array of the parent Tensor *in situ*, both when reading and updating. This avoids unnecessary duplication of the array elements when initialising a `Subdiagram(Tensor)` object.

`Vertex` objects represent tensors with actual indices assigned, rather than the abstract orbital ranges in `Tensor` objects. This is the link between the tensor the second-quantised operator algebra and the tensor algebra of coefficients. A `Vertex` contains a reference to its parent `Tensor` or `SubDiagram`, and the lists

Attribute	Type	Description
`tensorList`	`list`	List of the tensors being multiplied
`prefactor`	`float`	Prefactor
`vertexList`	`list`	List of the vertex objects with indices applied
`contractionsList`	`list`	List of the contractions applied in a tensor product
`normalOrderedSlices`	`list`	List of the positions in `tensorList` at which any normal ordered blocks begin
`lowerIndices`	`list`	List of the lower indices appearing on tensors in the tensor product
`upperIndices`	`list`	List of the upper indices appearing on tensors in the tensor product
`freeLowerIndices`	`list`	List of the lower indices that remain uncontracted in the tensor product. The order or the list identifies which particle each index refers to in the overall tensor product.
`freeUpperIndices`	`list`	List of the upper indices that remain uncontracted in the tensor product. The order or the list identifies which particle each index refers to in the overall tensor product.

Table 4.2: Attributes of a `TensorProduct` object, used to represent a single term in a CC equation

of `lowerIndices` and `upperIndices` representing the indices corresponding respectively to its covariant or contravariant components. The `lowerIndices` and `upperIndices` correspond to subscript and superscript indices, which accordingly contract with indices of creation and annihilation operators to represent a basis-invariant operator.

A `TensorProduct` object represents a composite tensor as a list of the constituent `Tensor` or `SubDiagram` objects, with some prefactor. It also stores a list of any contractions applied, each represented by a 2-tuple of the corresponding `Index` objects. At this stage the assignment of indices is made concrete by storing the list of tensors as a list of `Vertex` objects. The `__mul__()` methods of the `Tensor` objects are defined such that multiplying two of them returns the outer product of the corresponding tensors as a `TensorProduct` object. The extra indices required are constructed automatically, and the assignment of new

indices to the tensors is done by `Vertex` objects.

Storing a composite in terms of its constituent tensors is key to preventing the memory costs from increasing exponentially, which would prohibit the use of all but the very smallest basis sets. For example, each doubles amplitude appearing in a product would introduce an $\mathcal{O}(N^4)$ scaling memory cost. Specifying a list of contractions that have been made allows for tensors that result from the contractions of smaller tensors to be stored without having to store the result in full, so the increased memory cost for a tensor product is additive, rather than multiplicative.

A `TensorSum` represents a sum of `TensorProduct` objects as a list of its summands. This is the general form for any expression in the tensor algebra, and is the form in which our equations are stored. The terms in the sum are stored by reference in the list, so the memory footprint of creating a `TensorProduct` is negligible.

4.2.2 Routines to apply Wick's theorem

`getOperator(spinFree=True)` generates the second-quantised operator expression for a given `Vertex` or `TensorProduct` object. In the spin-free formalism (`spinFree=True`) this is an `OperatorSum` with 2^n terms, where n is the number of electrons on which the operator acts. For a product of N tensors, the i-th of which represents a n_i-body operator, then the spin-free operator product has $\prod_{i=1}^{N} 2^{n_i} = 2^{\sum_{i=1}^{N} n_i}$ terms. Naïvely, we choose to construct all of these terms for robustness, acknowledging that this is a bottleneck to be addressed.

The number of complete contraction patterns to test scales exponentially with the number of second quantised operators in the operator string. Firstly, it may be seen that a complete contraction may only arise from an even number of elementary second-quantised operators. This will always be the case when calculating quantities that conserve particle number. These can be represented generally by a string of $2n$ operators, of which n will be creation and n will be annihilation, in some order.

For a string of $2n = 2$ operators, there is 1 possible contraction pattern. For $2n = 4$, there are 3 ways to contract the first operator, each of which leaves 1 way to contract the remaining 2, for $1 \times 3 = 3$ possible contractions. Extending a string from $2n$ to $2n + 2$ operators introduces a factor of $2n + 1$ to the number of complete contractions. The total number of complete pairings of $2n$ operators to check is $1 \times 3 \times \cdots \times (2n + 1) = \frac{(2n)!}{2^n n!}$.

However, the vast majority of these will be zero. By checking all the possible pairs, a list of only the non-zero single contractions can be generated. This step takes $\mathcal{O}(n^2)$ time, returning a matrix whose elements M_{ij} are equal to 1 when the i-th operator in the string can contract (from the left) with the j-th operator, and 0 otherwise. This will be an upper-triangular matrix: an entry below the main diagonal would refer to a pair of operators that is already in normal order and so would not represent a possible contraction.

For the operator product $\hat{a}^{c_2}\hat{a}^{c_3}\hat{a}_{v_2}\hat{a}_{v_3}\hat{a}^{v_0}\hat{a}^{v_1}\hat{a}_{c_0}\hat{a}_{c_1}$, the possible contractions matrix will look like

$$\begin{array}{c} \\ \hat{a}^{c_2} \\ \hat{a}^{c_3} \\ \hat{a}_{v_2} \\ \hat{a}_{v_3} \\ \hat{a}^{v_0} \\ \hat{a}^{v_1} \\ \hat{a}_{c_0} \\ \hat{a}_{c_1} \end{array} \begin{array}{c} \begin{array}{cccccccc} \hat{a}^{c_2} & \hat{a}^{c_3} & \hat{a}_{v_2} & \hat{a}_{v_3} & \hat{a}^{v_0} & \hat{a}^{v_1} & \hat{a}_{c_0} & \hat{a}_{c_1} \end{array} \\ \begin{pmatrix} 0 & 0 & 0 & 0 & 0 & 0 & 1 & 1 \\ 0 & 0 & 0 & 0 & 0 & 0 & 1 & 1 \\ 0 & 0 & 0 & 0 & 1 & 1 & 0 & 0 \\ 0 & 0 & 0 & 0 & 1 & 1 & 0 & 0 \\ 0 & 0 & 0 & 0 & 0 & 0 & 0 & 0 \\ 0 & 0 & 0 & 0 & 0 & 0 & 0 & 0 \\ 0 & 0 & 0 & 0 & 0 & 0 & 0 & 0 \\ 0 & 0 & 0 & 0 & 0 & 0 & 0 & 0 \end{pmatrix} \end{array}$$

An operator product with more possible contractions might be $\hat{a}_{a_0}\hat{a}_{a_1}\hat{a}_{a_2}\hat{a}^{a_3}\hat{a}^{a_4}\hat{a}^{a_5}$, for which the possible contractions matrix is

$$\begin{array}{c} \\ \hat{a}_{a_0} \\ \hat{a}_{a_1} \\ \hat{a}_{a_2} \\ \hat{a}^{a_3} \\ \hat{a}^{a_4} \\ \hat{a}^{a_5} \end{array} \begin{array}{c} \begin{array}{cccccc} \hat{a}_{a_0} & \hat{a}_{a_1} & \hat{a}_{a_2} & \hat{a}^{a_3} & \hat{a}^{a_4} & \hat{a}^{a_5} \end{array} \\ \begin{pmatrix} 0 & 0 & 0 & 1 & 1 & 1 \\ 0 & 0 & 0 & 1 & 1 & 1 \\ 0 & 0 & 0 & 1 & 1 & 1 \\ 0 & 0 & 0 & 0 & 0 & 0 \\ 0 & 0 & 0 & 0 & 0 & 0 \\ 0 & 0 & 0 & 0 & 0 & 0 \end{pmatrix} \end{array}$$

This is done using a Fortran subroutine that carries out a recursive algorithm to generate all possible sets of contractions. A pseudocode for this Fortran subroutine can be found in the appendices, in section B.1.

The procedure to find complete contractions amounts to finding a complete set of n contracted pairs of operators where every operator has been included exactly once, while keeping track of the sign changes introduced by each successive contraction. The largest possible number of these will occur when any of the first n operators can contract with any of the second n, giving $n!$ possible full contractions. Although this is a significant reduction, it is still an exponential number of possible combinations.

Each of the first n operators being able to contract with any of the last n operators is a worst-case scenario. If instead there are subsequences that are known to be in normal order, only a smaller number will need to be checked. This will certainly be the case when contracting CC amplitudes and Hamiltonian matrix elements together that are each normal-ordered in order to generate CC equations. For this reason, the `OperatorProduct` objects contain a list of starting points for each block that is known to be in normal order, so that contractions within a block can be ignored.

The requirement to multiply and divide by a projection tensor presents a significant inefficiency, as the number of possible contractions scales factorially with the length of a string of operators. Projecting onto doubly excited states introduces four additional elementary operators into a second-quantised string, which would not be present in a many-body approach. At the present stage we tolerate this inefficiency as the equation generation only needs to be carried out once, and the length of the operator string is only related to the complexity of the ansatz and not the size of the (closed-shell part of the) system. However, this does present a barrier to treating higher excitations and higher powers in the exponential, and should be addressed in future versions of the code.

When deriving coupled cluster equations, and especially in a spin-summed formalism, operator sums appear with very many terms, which can be evaluated

independently. This presents an opportunity for parallelisation, which has not been done in the naïve implementation, being intended for later work.

`getEinsumInformation()` converts the contractions in a `TensorProduct` into a string for input to the einsum module allows the fast optimised routines provided by numpy to be employed to carry out the numerically intensive linear algebra operations. This involves keeping track of which `Index` objects represent an uncontracted index in the final tensor, and following which indices refer to the same particle as it propagates between the application of a series of operators. In a diagrammatic sense, this corresponds to tracing the lines through a diagram, from the initial inward line, to the final outward line. For multiple terms in a `TensorSum`, the uncontracted indices must be specified such that they correspond to the same ordering, such that the arrays are added together without any inadvertent transposition.

Given a product of tensors (and their associated arrays), with the einsum string specifying how the contractions are to be carried out, the routine `getContractedArray()` is the one that actually carries out the contraction. For specific orbital indices, a slice of the resulting array is taken.

4.2.3 Building an ansatz

4.2.3.1 Constructing a reference wavefunction

In the framework for which OCCSFrD is designed, a single reference wavefunction is used, consisting of potentially several Slater determinants. These determinants are generated by creation operators acting on the Fermi vacuum, acting in specific orbitals, rather than over a range. This is done by defining a `SpecificOrbitalIndex` subclass of `Index` objects, that are defined with a specific value of an index in its range. Usually the `SpecificOrbitalIndex` will be defined in the active range, and `value = 0` refers to the first open shell orbital, `value = 1` to the second, and so on.

The reference wavefunction, whether a single Gelfand–Tsetlin CSF or not, can be written as a linear combination of products of creation operators, with

coefficients determined by the spin coupling or other symmetries. OCCSFrD also contains a routine to carry out the genealogical spin coupling to build single G–T states of arbitrary total and projected spin. This is in the `UGA.py` submodule in the `reference` module.

4.2.3.2 The wave operator

The cluster operator is first constructed as the sum of the amplitude tensors for the excitations being included in the ansatz. The wave operator is then the exponential of the cluster operator, expressed as its Taylor series truncated to some finite order (presently only linear and quadratic have been considered, as higher order terms are computationally infeasible in the current implementation). If the `normalOrdered` toggle is set to be true, then no contractions will be considered within the string of second quantised operators generated by the wave operator. This means contractions between the amplitudes are neglected, and the resulting operator will correspond to the normal ordered exponential. The starting points of normal ordered blocks are also stored, so that the contraction routines later on will not waste time checking contractions that are not possible by construction.

4.2.4 Generating equations

For the work presented in this thesis, the equations are generated by the routine `getAmplitudeEquation_UnlinkedFormalism`, which generates the linked and unlinked parts of the coupled cluster amplitude equations, as defined by a given Hamiltonian, wave operator, and amplitudes.

The procedure to generate each part of the equations is as follows:

1. Obtain projection manifold from Hermitian conjugate of second quantised operator corresponding to amplitude tensor
2. Use Wick's theorem to find vacuum expectation value of `referenceOperator.conjugate() * projection manifold * Hamiltonian * wave operator * referenceOperator`

3. Remove projection tensor to obtain `result[0]`
4. Use Wick's theorem to find vacuum expectation value of `referenceOperator.conjugate() * projection manifold * wave operator * referenceOperator`
5. Remove projection tensor to obtain `result[1]`

Removing the projection tensor, i.e. cutting all the lines joining it into a diagram, generates the contribution to the residual that would contract with the projection tensor to give a scalar. This will be a sum of tensor products that all have the same free indices, which will be the ones that appeared in the projection tensor when the projection was still applied. The permutation of indices in differing contraction topologies (such as Coulomb-like and exchange-like) is automatically taken care of. This is one of the major difficulties with the many-body approach which we have chosen to bypass, at the cost of an inefficient brute-force approach in this naïve implementation.

4.2.5 Form of the Equations

The generated spin-free equations have many more terms than the closed shell or spin-orbital based equations. Table 4.3 shows the large number of terms in each set of equations. Many of these terms are equivalent and should be collated, for instance by identifying terms represented by Goldstone diagrams that are isomorphic graphs. The number of terms duplicated simply by spin summation already introduces an approximate factor of 2 to the computational cost for every pair of creation and annihilation operators appearing in the second quantised operator expression. For the most expensive term in the closed shell CCD equations this is $2^6 = 64$. Even more than that, there are terms that are topologically identical, leading to further sets of terms that should be identified as equivalent. In fact, for closed shell CCD (for which the equations terminate at quadratic order), it is known that there are 31 topologically distinct terms in the spin-free equations. Compared to our brute-force generated equations,

N, S	l-CCD	q-NOCCD	q-CCD	l-CCSD	q-NOCCSD	q-CCSD
0,0	196	2500	2500	224	4592	4592
1,0.5	924	19932	29604	1032	30948	23964
2,1	3772	150652	241084	4184	220016	324156
2,0	3772	150652	241084	4184	220016	324156

Table 4.3: Largest number of terms in each set of spin-free open shell coupled cluster equations for a spin-S CSF reference with N open-shell electrons

which have 2500 terms, this is a simplification by a factor of more than 80. While not every term will require the same scaling computation time, it gives a rough estimate of how much more efficient these quadratic-truncated NOECC schemes can be made. For higher-truncated ansätze, greater computational savings should be possible.

4.2.6 Workflow for generating equations

Choosing the configuration that constitutes the best reference wavefunction is a problem of chemical intuition. Considerations such as Hund's rules, local spin coupling, and spatial symmetry can be incorporated into the choice of CSF. A linear combination of CSFs may also be chosen, but this is still a single reference method since the coefficients are predetermined. Constructing such a single reference open-shell wavefunction can be done directly in the input file, by specifying the indices and the creation operators producing the CSF.

The level of theory specifies which excitations are to be included in the cluster operator. This is done in the input python file, and the amplitude tensors are generated automatically. The form of the wave operator can also be specified in terms of the order to which the exponential will be truncated and whether it will be overall normal ordered This allows complete generalisation of the same framework to different classes of excitations and different forms of the exponential wave operator.

The equations can then be saved, to be loaded in to a calculation as required. For a given ansatz and a given configuration, the equations only need to be generated once, saving the cost of repeating this expensive step.

4.2.6.1 Structure of an input file

The high-level steps to generate equations using OCCSFrD are approximately as follows, after importing the `occsfrd.ansatz`, `occsfrd.wick`, and `occsfrd.interface` modules:

1. Construct the reference CSF: `SpecificOrbitalIndex` objects are instantiated for the active orbitals, and the `Operator` object (`OperatorProduct`, or more generally `OperatorSum`) representing the creation of the open-shell reference from the closed-shell vacuum is also constructed.

2. Build the *ansatz*: `Tensor` objects are instantiated for the one- and two-body integrals and the cluster amplitudes, without arrays actually being assigned (an important feature is that numerical values, and even the array dimensions, do not appear until the equations are used in a calculation). The `TensorSum` object representing the wave operator is built, *e.g.* by `ansatz.utils.operatorExponential()`, to which can be passed a truncation level and a toggle for the normal-ordering of the exponential.

3. Choose desired equations and run contraction engine: the energy equations or a paticular set of amplitude equations are generated by the functions in `occsfrd.ansatz.normalorderedcc`. Closed diagrams such as energy equations or a check for intermediate normalisation can be generated by `getEnergyEquation()`, while our unlinked amplitude equations are generated by `getAmplitudeEquation_UnlinkedFormalism()`.

4. Save equations and/or run calculation: the equations may be used immediately for a calculation, or they may be saved using the `interface.storeequations` module.

As an example, a Python file to generate the quadratic-truncated {CCSD} equations for a one-electron doublet can be found in section B.2 in appendix B

4.2.6.2 Serialisation

Equations are saved as a dictionary that is serialised, using the pickle Python library, as a pickle (.pkl) file. The key:value pairs in the dictonary are:

- "equations": list of the TensorProduct objects corresponding to each type of residual equation
- "tensors": list of the Tensor objects appearing in the equations. It is important to pickle these objects so that the reference structure can be preserved when the equations are loaded up.
- "specificOrbitalIndices": list of the Index objects referring to specific (active) orbitals, in order that the references to them in other objects may be preserved.

For equations in an unlinked formalism, the equations are each saved in a 2-tuple. The first element is the expression for the residual with unlinked terms still included. The second element is the expression for the component of the unlinked terms that is not contracted to the Hamiltonian. The unlinked terms will be those components multiplied by the {CC} energy, truncated at the overall level defined by maxOrder.

Using a dictionary to store the equations allows the relationships between indices, tensors, and equations to be preserved throughout the pickling and unpickling process. Storing the equations as `TensorSum` objects was the first choice made as it was conceptually the simplest, but with the equations that have not been simplified, the large number of terms leads to large files, on the order of hundreds of megabytes, that are slow to read, and also take up space in memory when loaded in to a calculation. The storage and memory footprints might be reduced by storing just the einsum strings and tensors being viewed by each tensor product, although really the large number of terms still presents the most important inefficiency to be addressed.

4.3 Coupled cluster program

The stored equations are loaded into a purpose-built iterative coupled cluster solver, implemented in the `occsfrd.solve` module of the OCCSFrD package. The orbitals and the one- and two-electron integrals are calculated using the Hartree–Fock routines in PySCF or an alternative electronic structure code.[180] It will most often be the case for open-shell systems that the orbitals will be obtained from a ROHF calculation on the high spin state in the same configuration, but in principle any other choice of orbitals may be used. The amplitude tensors are initialised to zero, and the residuals calculated by applying the tensor contractions specified by the CC equations.

4.3.1 Tensor contractions

The tensor contractions specified in the equations are converted into the string format required by numpy.einsum. This requires identifying which indices are left uncontracted in the product, and tracking the indices that are contracted together, effectively tracing continuous paths through the diagram represented by the tensor product. Where indices specify a subrange or a specific value, the slice objects select the appropriate part of the arrays on which einsum will operate.

Contributions to a residual tensor may be specified with their indices in a different order. Such contributions must be compared, and the indices identified such that the correct contraction pattern can be specified. This is done by defining lists of the target upper and lower indices in order, before inspecting the contraction pattern.

For instance, the two contributions to the tensor

$$r^{c_0 c_1}_{a_0 v_0} = g^{c_2 c_1}_{a_0 v_1} t^{c_0 v_1}_{v_0 c_2} + g^{c_1 c_2}_{a_0 v_1} t^{c_0 v_1}_{v_0 c_2} \tag{4.3.1.1}$$

are converted to the strings 'abdf,cdgb->acgf' and 'abfd,cdgb->acgf' for application by einsum. The two resulting arrays are the appropriate transposes of each other, so be added together to give the correct sum of direct and exchange interactions.

The einsum.path is chosen as 'optimal', but the effect of this on the scaling of computational time has not yet been investigated. It is possible that an optimal einsum.path calculates the appropriate intermediate tensors without requiring the equations explicitly to be factorised.

The routine `getContractedArray` takes a tensor product and the einsum string encoding its contraction pattern, and carries out the generalised matrix multiplication using einsum. This is a prime opportunity for parallelisation: our spin adapted coupled cluster equations contain very many terms, which could each be evaluated independently.

4.3.2 Quasi-Newton solution scheme

The solution of coupled cluster equations is most commonly done by iteration of a perturbative quasi-Newton method to update the amplitudes. To solve the non-linear set of coupled cluster equations, Newton's method would require solving a linear set of equations at each step, by inverting the coupled cluster Jacobean. The full inverse of the coupled cluster Jacobean matrix is too expensive to calculate, so only the diagonal elements are computed. These are the same as the energy denominators obtained in perturbation theory from elements of the Fock matrix.

For an open shell system, the Fock matrix does not have a unique definition in a spatial orbital basis. Nevertheless, the Fock matrix can be modified to provide a suitable preconditioner for the iterative solution of coupled cluster equations. In the schemes used presently, this was done by only using the doubly occupied (core) orbitals.

The core-orbital Fock matrix does not in general guarantee convergence to a solution of the coupled cluster equations. However, a solution can be found by the Direct Inversion in the Iterative Subspace (DIIS). Using a small selection of amplitudes from previous iterations, a better estimate for the next iteration can be obtained by directly inverting the coupled cluster Jacobean. This speeds up convergence, and in some cases is necessary to achieve convergence at all. In calculations where excitations are allowed between singly occupied orbitals,

the redundant solutions lead to a failure to converge unless DIIS is used. Unless otherwise indicated, OCCSFrD uses a default subspace size of 12 iterations in all coupled cluster calculations.

4.3.3 Parameters

When there are intruder states or otherwise Fock matrix elements that are close together, it may be necessary to introduce a level shift to avoid energy denominators that are close to or equal to zero. While this does slow down the calculation, it can make convergence more stable, particularly for multi-determinantal states that would otherwise suffer from a multiple parentage problem. In cases where redundancies are present, the precise solution obtained will depend slightly on the level shift chosen. To guarantee repeatability, a well-defined procedure for choosing this level shift must be specified. Evangelista used the closed shell Fock matrix elements corresponding to the lowest virtual and highest core orbital: The level shift is applied with a multiplier for the order of excitation corresponding to the residual being calculated: it corresponds to an energy shift *per electron* for the particle and hole orbitals.

The DIIS subspace size may be specified as a parameter, if DIIS is being applied. By default it is set to 12 iterations.

The convergence criteria are applied to both the residual equations and the energy. The iterations continue until the L^2-norm of the residual vector is less than $10^{-\mathrm{Rthresh}}$ and the difference between energies at successive iterations is less than $10^{-\mathrm{Ethresh}}$. If the calculation hits $\mathrm{maxIter}$ iterations (set at 1000 by default) then it stops and reports a convergence failure.

The parameter `maxOrder` is defined so that when the energy expression is multiplied by the unlinked part of the CC equations, the terms exceeding the maximum order in the amplitudes can be ignored. If this is different from the highest order in the amplitude equations, there will be spurious disconnected terms introduced, which must be avoided in practical applications, to minimise

the size-extensivity error. Since the equations are saved elsewhere, this parameter is useful for being able to reuse the energy equations in the unlinked equations.

4.3.4 Running a calculation

Once a particular set of working equations is available, the calculation is run using routines in the `occsfrd.solve` module. Each iteration applies the perturbative update to the amplitudes and prints out the energy. The final amplitudes can be stored and reused for future calculations.

Just as for the equation generator, the input may take the form of a python file, for example, an input file for a quadratic {CCSD} calculation of the energy of a lithium atom in a cc-pCVTZ basis set can be found the appendices, in section B.3.

4.4 Outlook

The new OCCSFrD package has been developed for generating and solving general spin adapted coupled cluster equations for arbitrary reference states. The principal novel capabilities of the package are summarised here, as well as the limitations that should be addressed in a mature version of the code. The remaining chapters of this thesis will present results that serve to demonstrate the OCCSFrD package as a useful tool for spin-adapted coupled cluster calculations. These will also show the efficacy of NOECCSD in particular as an ansatz that can account for dynamical correlation at a level comparable to CCSD while also respecting the static correlation due to spin-coupling in open-shell systems.

4.4.1 Capabilities of the OCCSFrD Package

The first goal of the OCCSFrD package that has been achieved is to generate fully spin-adapted coupled cluster equations for a variety of spin-adapted reference states. The ability in principle exists to use any CC ansatz, at any truncation in either excitation level or power in the exponential, and any single CSF wavefunction, whether it consists of one or multiple determinants. However, to realise this in practice for systems of more than 2 open-shell electrons, higher than quadratic

powers in the amplitudes, or triple excitations in the cluster operator, significant improvements in efficiency will need to be made.

The solution of this range of CC equations is possible even in cases with redundancies caused by spectator excitations, using DIIS and level shifts if necessary. The non-uniqueness of the CC solutions is a theoretical deficiency that should be remedied by the proper treatment of redundancies. If this is addressed and a well-defined set of equations is implemented in OCCSFrD, it remains to be seen whether the present routines for solving CCSD equations will still be effective. It is likely that appropriate level shifts and use of DIIS will still be able to force convergence, but there will be some modifications to the Fock matrix preconditioner to make each iteration more efficient.

4.4.2 Features desirable in future versions

A more efficient contraction scheme would allow more complicated ansätze to be tackled, perhaps even to approach the theoretical limit of 8th-order terms. Brute force is reliable, but large number of terms presently limits practical applications to quadratic equations and 2 or 3 open shell orbitals. The scheme used by Evangelista et al in the Wick&D code[58] generates only terms with a unique contraction topology, rather than brute force generating every term in the sum separately.

Obtaining factorised equations, which may be possible using Wick&D, will allow for improved scaling methods. The many-body approach to constructing CC equations lends itself better to the formation and storage of appropriate intermediates in a factorised CC scheme.

For both of these major efficiency improvements, it will be important to verify numerically that the equations are indeed equivalent after simplification and factorisation to the complicated form currently generated by OCCSFrD.

When extending the OCCSFrD machinery to true multi-reference methods, it will become even more important to handle a proper treatment of the redundan-

cies. The CC implementation in OCCSFrD is not currently equipped to handle a genuine multireference theory.

5

A spin-adapted Coupled Cluster for high-spin states

The results in this chapter are published in the Faraday Discussions paper:

Gunasekera, A. D. *et al.* Multi-reference coupled cluster theory using the normal ordered exponential ansatz. *Faraday Discuss.* **254,** 170–190. doi:10.1039/D4FD00044G (6th Nov. 2024)

High-spin states are those with the maximum total spin, that is, total spin eigenfunctions with eigenvalue $S = N/2$ for N open-shell electrons. Of the $2S + 1$ degenerate (under zero external field) components of the resulting multiplet, the ones with open-shell electrons aligned all 'spin up' or all 'spin down' ($M_S = \pm S$) will have spin functions with only one term.[109] In the case that there is also not significant static correlation in the spatial wavefunction, these cases will be well represented by a single SD.

This chapter shows results from our spin-adapted NOECC approach applied to some such single-reference cases, using the OCCSFrD software package to achieve CCSD-quality energies while rigorously avoiding spin contamination. The claim is also examined that including terms only up to quadratic order in the amplitudes is still accurate enough to be comparable to traditional CCSD

methods. The resulting error is of similar significance to that which arises from neglecting the triple and higher excitations in the cluster operator.

5.1 Recreating the closed-shell results

For closed-shell systems, the NOECC results can be compared with traditional CC, as the excitations in the cluster operator will all commute and will be spin adapted in both theories, leading to identical *ansätze*. The only difference will be due to the truncation of the exponential: our spin-free quadratic CCSD equations have neglected the cubic and quartic terms that appear in the traditional CCSD equations.

5.1.1 Noble gases

A selection of single noble gas atoms were studied in several basis sets, to compare the performance of the quadratic-truncated CC implemented in OCCSFrD with traditional CC. Table 5.1 shows the RHF energies and CCSD correlation energies for single Helium, Neon, and Argon atoms calculated by PySCF,[180] alongside the lCCSD and q-NOECCSD correlation energies calculated by OCCSFrD. The correlated calculations were carried out for all electrons, with convergence in the energies to less than $10^{-10}\mathrm{E_H}$ and in the total squared amplitudes below 10^{-16}.

Atom	Basis: CC-pVT(X)Z	RHF	CCSD	lCCSD	qNOECCSD
He	D	-2.855160	-0.032434	-0.032673	-0.032434
	T	-2.861153	-0.039079	-0.039391	-0.039079
	Q	-2.861514	-0.040897	-0.041232	-0.040897
	5	-2.861625	-0.041527	-0.041868	-0.041527
Ne	D	-128.488776	-0.190861	-0.191689	-0.190862
	T	-128.531862	-0.278952	-0.281396	-0.278951
	Q	-128.543470	-0.327586	-0.330862	-0.327584
	5	-128.546770	-0.345800	-0.349400	-0.345798
Ar	D	-526.799865	-0.156362	-0.158924	-0.156361
	T	-526.813134	-0.253226	-0.259537	-0.253226
	Q	-526.816780	-0.308576	-0.316459	-0.308575
	5	-526.817341	-0.420334	-0.429047	-0.420332

Table 5.1: Energies in $\mathrm{E_H}$ of some noble gas atoms in a range of bases.

The quadratic-truncated normal-ordered exponential CCSD differs from the standard CCSD by only one or two $\mu\mathrm{E_H}$.

5.1.2 Equivalence with CC

The closed shell CCD equations terminate at quadratic order, and so the closed shell CCD equations generated by OCCSFrD should be identical to the established equations of closed shell CCD theory, up to the gathering of equivalent terms. We can confirm that this is the case by inspecting the residuals at each iteration in a calculation.

The normal ordering of the exponential has no effect in these closed shell cases, as the standard exponential is already in normal order.

5.1.2.1 Truncation errors

The closed shell CCSD equations have terms up to fourth order in the amplitudes. Neglecting the cubic and quartic terms in the CCSD equations for closed shell systems does introduce a truncation error, which for these atoms has been no more than one or two $\mu\mathrm{E_H}$. In cases without significant static correlation, the single-reference CCSD may be expected to differ from FCI on the order of $1 - 10\mathrm{mE_H}$, while the full inclusion of triples was seen in an early study of some small molecules in double-zeta basis sets to reduce this error to $0.05 - 0.5\mathrm{mE_H}$.[181] The neglect of terms of cubic and higher order has been of much less significance than the absence of triple and higher excitations in the cluster operator, which could be expected to contribute on the order of 10^{-3} or 10^{-4} $\mathrm{E_H}$ to the correlation energy.

5.1.2.2 Size consistency

To test for the size consistency of the method in closed shell cases we used a system of two neon atoms, comparing the energy at a large separation with twice then energy of an isolated atom. In a 6-31G basis set, the RHF energy of one neon atom was calculated and compared to that of two neon atoms separated by 10^9Å, and the correlation energy calculated using standard unrestricted CCSD[180] and

the linear and truncated NOECCSD framework for these closed-shell references. These data are shown in table 5.2.

Molecule	ROHF / $\mathrm{E_H}$	uCCSD / $\mathrm{mE_H}$	l-NOECCSD / $\mathrm{mE_H}$	q-NOECCSD / $\mathrm{mE_H}$
Ne	-128.473877	-115.118	-114.709	-115.119
$\mathrm{Ne_2}\left(r = 10^9 \text{Å}\right)$	-256.947754	-230.235	-229.418	-230.238

Table 5.2: ROHF energy in $\mathrm{E_H}$ and uCCSD, lNOECCSD, and qNOECCSD correlation energies in $\mathrm{mE_H}$ for a neon atom and for two neon atoms at 10^9Å separation in 6-31G basis.

The RHF energy for the neon dimer at $r = 10^9$Å was exactly (to machine precision) double that of the isolated neon atom, while the standard CCSD correlation energy was size consistent to within the convergence threshold, differing by $7.2 \times 10^{-14}\mathrm{E_H}$ between the dissociated dimer and twice the isolated atom. The size inconsistency in the linear NOECCSD was $2.0 \times 10^{-13}\mathrm{E_H}$, which was within the convergence threshold, while for the quadratic NOECCSD it was $1.8 \times 10^{-9}\mathrm{E_H}$. This small size inconsistency persisted over several different large separations of the neon dimer, and has likely arisen from the neglect of cubic and quartic terms in the CCSD equations. When the naïve truncation of the exponential at quadratic order was tested on the same system, the size inconsistency was 6 orders of magnitude larger, at $5.6 \times 10^{-3}\mathrm{E_H}$, confirming the importance of truncating the equations overall to avoid spurious disconnected terms that break both size extensivity and size consistency.

5.2 Doublets

To investigate the avoidance of spin contamination in our method, we next look at some open shell systems. We start with doublet electronic states because the single determinant ROHF reference can be correlated using standard unrestricted and spin-restricted spin-orbital coupled cluster implementations, which enables us to compare directly to our spin-free approach.

5.2.1 Lithium atom

The simplest non-trivial doublet case is the Lithium atom. With 3 electrons, this system allows a comparison with FCI and CCSD, in small and large basis sets.

ROHF / $\mathrm{E_H}$	uCCD / $\mathrm{mE_H}$	l-NOECCD / $\mathrm{mE_H}$	q-NOECCD / $\mathrm{mE_H}$	FCI / $\mathrm{mE_H}$
-7.432679265	-41.505947	-41.680942	-41.532939	-41.572154

(a) Coupled cluster and NOECC correlation energies calculated with only double excitations

ROHF / $\mathrm{E_H}$	uCCSD / $\mathrm{mE_H}$	l-NOECCSD / $\mathrm{mE_H}$	q-NOECCSD / $\mathrm{mE_H}$	FCI / $\mathrm{mE_H}$
-7.432679265	-41.546366	-41.694641	-41.545784	-41.572154

(b) Coupled cluster and NOECC correlation energies calculated with single and double excitations included

Table 5.3: ROHF energy in $\mathrm{E_H}$ and correlation energies in $\mathrm{mE_H}$ for the lithium atom in cc-PCVTZ basis, calculated using linear- and quadratic-truncated NOECC approaches, and the unrestricted CC[180] and FCI[180] correlation energies for comparison

5.2.1.1 Spectators

The redundancy introduced by spectator excitations affects the results already, even with only one active orbital. When single and double excitations are both included in the cluster operator, the same projected state is obtained by a core-to-virtual single excitation as by the two-body-operator representing the same excitation with the active orbital as a direct or exchange spectator. The fact that no unique solution is possible without further conditions leads to a failure of convergence unless DIIS is applied. In the linear ansatz, the redundant solutions all represent the same wavefunction, but in the quadratic ansatz this is no longer the case.

A different solution will be obtained for each combination of level shift and DIIS subspace size. These different solutions will now correspond to slightly different wavefunctions with slightly different energies.

The linear and quadratic NOECCSD results for the Lithium atom in the cc-PCVTZ basis set were obtained with a DIIS subspace of 12 iterations for a range of level shifts from 0 to 2 Hartree. The lNOECCSD energies differ by no more than 10^{-12} Hartree, which is within the convergence threshold, and show no visible dependence on the level shift. The qNOECCSD energies differ on the order of

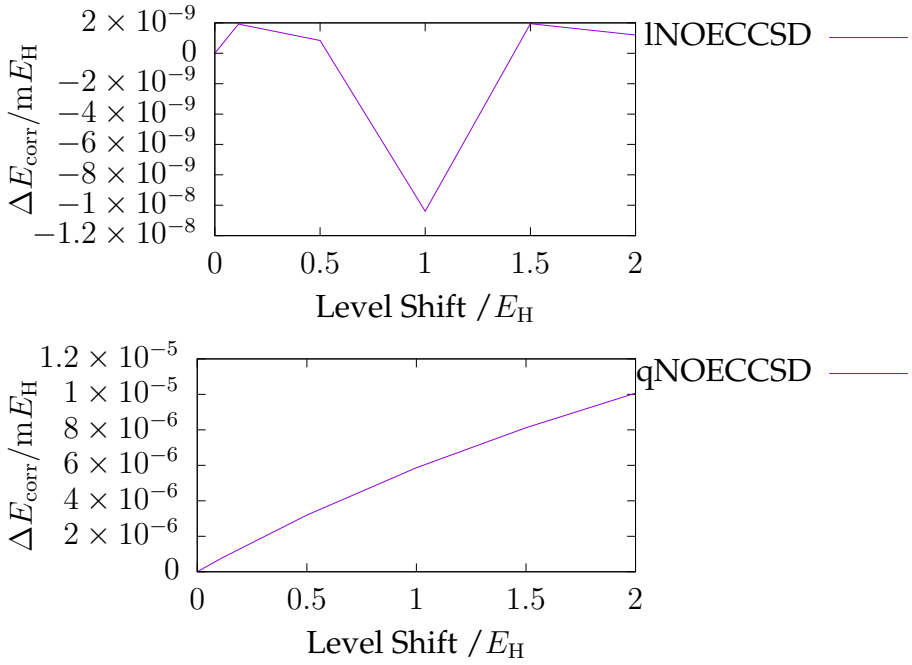

Figure 5.1: lNOECCSD and qNOECCSD correlation energies of Li in a cc-pCVTZ basis as a function of level shift (plotted as the difference, ΔE_{corr}, from the respective correlation energies at zero level shift).

10^{-8} Hartree, with a discrepancy from FCI that, to a first approximation, increases linearly ($R^2 = 0.992$) with the level shift. These differing trends and orders of magnitude are shown in figure 5.1 Although the energy tails off at higher values of the level shift, the gap between core and virtual orbitals in this system is less than $0.4\mathrm{E_H}$, so the level shift can be chosen small enough to fall well into this regime. Figure 5.2 shows that the effect of level shift on the calculated correlation energy is much less than the difference between the methods used.

5.2.2 First-row radicals

In Table 5.4 we present results for unrestricted CCSD (uCCSD),[180] Szalay and Gauss's spin-restricted CCSD (rCCSD)[60] and our normal-ordered exponential NOECCSD, truncated to linear and quadratic order. Szalay and Gauss's spin-restricted approach constrains the cluster amplitudes by imposing the exact S^2 expectation value, rather than fully spin-adapting the amplitudes. We also present results for the quadratic spin-free CCSD without normal-ordering. The

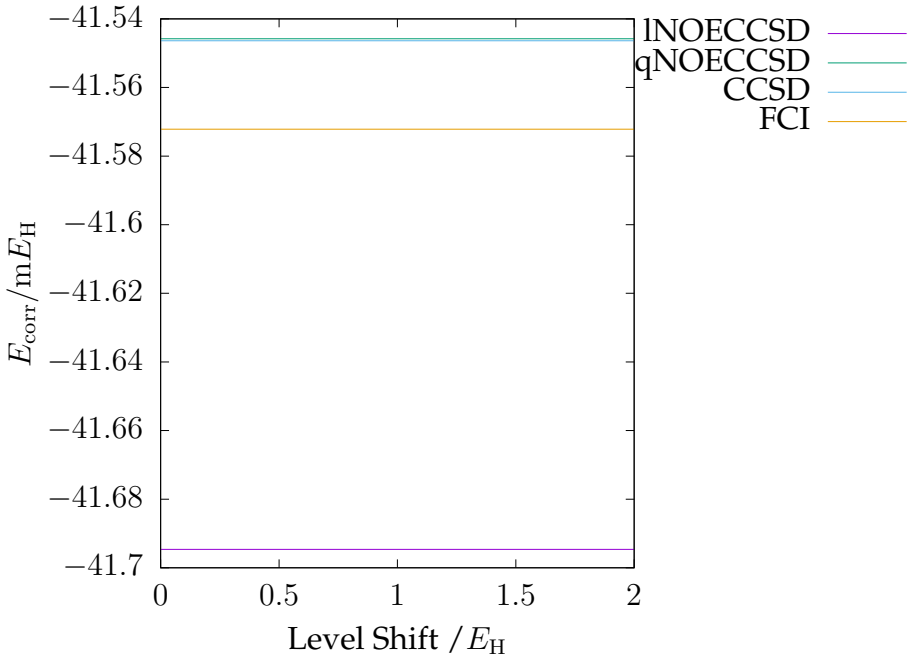

Figure 5.2: NOECCSD correlation energies of Li in a cc-pCVTZ basis as a function of level shift.

Molecule	uCCSD	rCCSD[60]	l-NOECCSD	q-NOECCSD	q-CCSD
^{2}CH	−141.105	−140.973	−137.013	−140.851	−141.049
^{2}OH	−230.302	−230.156	−223.133	−230.306	−230.331
^{2}CN	−354.724	−353.995	−325.369	−353.749	−354.454
^{2}NO	−433.834	−433.354	−402.668	−433.327	−434.265
$^2CH_3$	−199.002	−198.832	−191.233	−198.833	−198.974
$^2NH_2$	−220.008	−219.831	−211.911	−219.806	−219.991

Table 5.4: l-NOECCSD and q-NOECCSD correlation energies in $\mathrm{mE_H}$ for ROHF doublets states in a cc-pVTZ basis compared to unrestricted spin-orbital based CCSD (uCCSD), Szalay and Gauss's restricted CCSD (rCCSD) and spin-free quadratic CCSD (q-CCSD).

geometries were obtained from Szalay and Gauss[60] and we use the same cc-pVTZ basis as that work. In all cases, the ROHF state is used as the reference determinant. Energies were converged to 10^{-10} $\mathrm{E_H}$.

The rCCSD correlation energies are smaller than uCCSD due to the spin-restriction imposed on the amplitudes. The spin-free NOECCSD energies are in close agreement with rCCSD, differing by only 0.3 $\mathrm{mE_H}$. Exact agreement between spin-restricted and spin-adapted theories is not expected, even if we had not truncated the NOECCSD equations to quadratic order. The difference

between the two approaches is small in comparison to the expected magnitude of the contribution from the three-body excitations that are absent in both methods. The non normal-ordered spin-free CCSD correlation energies are universally lower than for NOECCSD, in some cases by as much as 0.8 $\mathrm{mE_H}$. This is because, without normal-ordering, quadratic terms involving active orbitals result in spurious additional energy contributions. For example $t^u_a t^i_u E^a_u E^u_i$ gives rise to an additional core to virtual excitation $t^u_a t^i_u E^a_i$ that (quasi-variationally) lowers the energy. Normal-ordering has no impact on the linear terms, but linearised NOECCSD only recovers about 90% of the correlation energy.

6

A Single-reference treatment for some multireference problems

In systems with two or more active orbitals, there are states for which a good zero-order approximation will require multiple determinants. The results of this chapter demonstrate our effectively single-reference CSF-based NOECC approach to some multideterminantal problems, such as the energy splitting between an open-shell singlet and triplet, and some cases of static correlation due to spatial degeneracy or near-degeneracy.

6.1 Seniority 2: Open-shell Singlets and Triplets

The results in this section for the beryllium atom, lithium dimer, and oxygen molecule are published in the Faraday Discussions paper:

Gunasekera, A. D. *et al.* Multi-reference coupled cluster theory using the normal ordered exponential ansatz. *Faraday Discuss.* **254,** 170–190. doi:10.1039/D4FD00044G (6th Nov. 2024)

With two open-shell orbitals, there are two CSFs possible with the same orbital occupation: the triplet and the open-shell singlet. An accurate treatment of the

singlet requires a two-determinant CSF as reference state (equation 2.3.2.2), to be compared to the single-determinant triplet state. The splitting between these two states presents a simple multireference problem, for which there is often spectroscopic data available for comparison.

6.1.1 Beryllium Atom

The ${}^3P$ and ${}^1P$ 2s2p excited states of the beryllium atom exemplify these electronic configurations, in a system simple enough to allow comparison to FCI.

Table 6.1 lists energies computed for the CSF references, and all-electron FCI and NOECCSD energies of the singlet ${}^1P$ and triplet ${}^3P$ states. uCCSD energies are also included for the triplet state, which has a single reference determinant. We use the cc-pCVTZ basis and the orbitals for both CSF references were generated from an ROHF calculation for the $M = 1$ triplet state. Energies are converged to 10^{-10} $\mathrm{E_H}$.

$2S+1$	CSF	uCCSD	l-NOECCSD	q-NOECCSD	FCI
3	-14.513129	-14.561352	-14.561504	-14.561358	-14.561412
1	-14.356425	$-$	-14.473941	-14.462727	-14.463057
Δ	0.156703	$-$	0.087563	0.098630	0.098355

Table 6.1: l-NOECCSD and q-NOECCSD $2s2p$ excited state energies and singlet-triplet gap Δ of the beryllium atom in $\mathrm{E_H}$ in a cc-pCVTZ basis, compared to the energies of the CSF references, the full CI energies, and the unrestricted CCSD energy for the triplet state.

The uCCSD, q-NOECCSD and FCI energies for the single-reference triplet state are all in excellent agreement, within 60 $\mu\mathrm{E_H}$. The agreement between CCSD and FCI is a consequence of the higher-order excitations all involving core-valence correlation, which is small for Be. We can also conclude that spin-contamination in the uCCSD wavefunction for this state is very small, and that the neglected cubic and higher NOECCSD contributions must also either be small in magnitude, or cancel.

The singlet CSF reference is almost $0.1\mathrm{E_H}$ above FCI, whereas the triplet reference was $0.05\mathrm{E_H}$ above the corresponding FCI energy. This is in part a

consequence of using the ROHF orbitals optimised for the triplet, but also because the correlation among singlet spin-coupled electrons is larger than triplet spin-coupled due to the Fermi heap in their joint probability distribution.[182] The effect of both orbital relaxation and correlation are well captured in the spin-free NOECCSD approach. At linear order, l-NOECCSD is within 10 $\mathrm{mE_H}$ of FCI, which reduces to 0.3 $\mathrm{mE_H}$ for q-NOECCSD. The singlet-triplet gap is also accurate to 0.3 $\mathrm{mE_H}$ compared to FCI.

A fully spin-adapted theory should recover the same energy for each of the $(2S+1)$ spin-projections of a state with total spin S. Our approach enables us to correlate arbitrary CSFs, and as a test of our method, we computed all-electron l-NOECCD energies of the $M = 1$ and $M = 0$ components of the triplet state. The $M = 1$ CSF is a single ROHF determinant, whereas the $M = 0$ CSF is a linear combination of two determinants (Eq. 2.3.2.3). The two calculations converged with energies that were identical at every iteration, confirming that our method is fully spin-adapted.

6.1.2 Lithium dimer

At dissociation, the ${}^1\Sigma_g^+$ and ${}^3\Sigma_u^+$ states of lithium dimer should have the same energy, and this should be equal to twice that of an isolated lithium atom in the ${}^2S$ state. The results of all-electron spin-free NOECCD and NOECCSD calculations assessing the extent to which this is true are presented in Tables 6.2 and 6.3, respectively. The orbitals of the ${}^3\Sigma_u^+$ state of Li_2 and the ${}^2S$ state of the Li atom were obtained from ROHF calculations. The ${}^1\Sigma_g^+$ state was constructed using the localised $1s$ and $2s$ orbitals of the ${}^3\Sigma_u^+$ state, ensuring that the energy expectation value of the open-shell singlet CSF exactly matches the ROHF energy of the triplet, and that both are exactly twice that of the doublet. The cc-pCVTZ basis was used and an interatomic distance of 10^9Å was chosen to represent the system of the two dissociated, but still spin-coupled, lithium atoms. All energies are converged to 10^{-10} $\mathrm{E_H}$. uCCD and uCCSD energies are also provided for comparison.

	uCCD	l-NOECCD	q-NOECCD
$\mathrm{Li}\,(^2S)$	-41.505947	-41.680942	-41.532939
$\mathrm{Li}_2\,(^3\Sigma_g^-), r = 10^9\text{Å}$	-83.011893	-83.389282	-83.091473
$\mathrm{Li}_2\,(^1\Sigma_g^+), r = 10^9\text{Å}$	$-$	-83.389289	-83.091788
$2E\,(^2S) - E\left(^3\Sigma_g^-\right)$	0.000000	0.027398	0.025595
$2E\,(^2S) - E\left(^1\Sigma_g^+\right)$	$-$	0.027404	0.025910

Table 6.2: l-NOECCD and q-NOECCD correlation energies in $\mathrm{mE_H}$ for Li and $\mathrm{Li_2}$ at a separation of 10^9Å in cc-pCVTZ basis, compared to unrestricted CCD.

	uCCSD	l-NOECCSD	q-NOECCSD
$\mathrm{Li}\,(^2S)$	-41.546366	-41.694641	-41.545784
$\mathrm{Li}_2\,(^3\Sigma_g^-), r = 10^9\text{Å}$	-83.092731	-83.389282	-83.091498
$\mathrm{Li}_2\,(^1\Sigma_g^+), r = 10^9\text{Å}$	$-$	-83.389289	-83.091947
$2E\,(^2S) - E\left(^3\Sigma_g^-\right)$	0.000000	0.000001	-0.000070
$2E\,(^2S) - E\left(^1\Sigma_g^+\right)$	$-$	0.000007	0.000379

Table 6.3: l-NOECCSD and 1-NOECCSD correlation energies in $\mathrm{mE_H}$ for Li and $\mathrm{Li_2}$ at a separation of 10^9Å in cc-pCVTZ basis, compared to unrestricted CCSD.

Both l-NOECCD and q-NOECCD show significant size-inconsistency errors of $0.03\ \mathrm{mE_H}$. Size consistency is violated because the cluster operator includes terms that excite fragment A with spectator orbitals on fragment B, and vice versa

$$\hat{E}^{qu}_{pu} \rightarrow \hat{E}^{q_A u_A}_{p_A u_A} + \hat{E}^{q_A u_B}_{p_A u_B} + \hat{E}^{q_B u_A}_{p_B u_A} + \hat{E}^{q_B u_B}_{p_B u_B} \tag{6.1.2.1}$$

The terms $\hat{E}^{q_A u_B}_{p_A u_B} + \hat{E}^{q_B u_A}_{p_B u_A}$ are non-vanishing in the molecule, but are absent in the cluster operators of fragments. The cluster operator is therefore not additively separable in the dissociative limit, which for CCD would require

$$\hat{E}^{qu}_{pu} \rightarrow \hat{E}^{q_A u_A}_{p_A u_A} + \hat{E}^{q_B u_B}_{p_B u_B} \tag{6.1.2.2}$$

The doubles spectator excitations correspond to single excitations when acting on the reference, the effect of which can be seen in the agreement of the NOECCD energy with the CCSD and NOECCSD energies, which is very good for the dimer, and very poor for the isolated atom. Since the l-NOECCSD and q-NOECCSD methods explicitly include the single excitations $\hat{E}^{q_A}_{p_A}$, $\hat{E}^{q_B}_{p_B}$ that were absent in NOECCD, size consistency can be restored numerically through the combined

action of the singles and doubles. The size-inconsistency errors are reduced to 7 $\mathrm{nE_H}$ for l-NOECCSD and 4 $\mu\mathrm{E_H}$ for q-NOECCSD. While the NOECCSD method is not rigorously size consistent, it is numerically very close to being size consistent in practice. Similar observations have been made by Hanauer and Köhn[57] for the ic-MRCC method, where they found that the magnitude of size-inconsistency errors depended critically on the way they removed the redundancies from their working equations. These small size-inconsistency errors may be due in part to the size-extensivity errors introduced by truncating our theory. The fact that q-NOECCSD has a larger error than l-NOECCSD would align with the presence of disconnected terms in the q-NOECCSD equations that do not appear in l-NOECCSD. This suggests that taking the full NOECCSD equations (5-NOECCSD for the Li atom and 6-NOECCSD for the dimer) could remove the errors, although this would be prohibitively expensive in our current version of the code.

6.1.3 Oxygen Molecule

Another archetypical singlet-triplet system is provided by the oxygen molecule. The lowest energy singlet state $^1\Delta_g$ lies 0.0359 $\mathrm{E_H}$ above the triplet $^3\Sigma_g^-$ ground state. Both states correspond to the open-shell configuration $\pi^1_{g,x}\pi^1_{g,y}$. The $O_2^{1,1}$ reference CSF for the $^3\Sigma_g^-$ is a single ROHF determinant, whereas the $O_2^{0,0}$ reference CSF for the $^1\Delta_g$ state is a linear combination of two determinants. Table 6.4 reports all-electron NOECCSD energies for the singlet and triplet states of $\mathrm{O_2}$ at a bond length of 1.2075Å using a cc-pCVTZ basis. For both CSFs, the orbitals were obtained from a ROHF calculation on the triplet state. We also report energies for the $^3\Sigma_g^-$ ground state computed by ROHF-uCCSD for comparison. All energies are converged to 10^{-10} $\mathrm{E_H}$.

As before, the q-NOECCSD energy is within 1 $\mathrm{mE_H}$ of the uCCSD energy, where they can be compared. The computed singlet-triplet gap of 0.0393 $\mathrm{E_H}$ is in good agreement with the experimental value of 0.0359 $\mathrm{E_H}$, considering that the experimental value is the adiabatic 0-0 energy, whereas we have computed the vertical electronic energy, and that triple excitations are not fully accounted

$^{2S+1}\Lambda$	Reference Energy	uCCSD	l-NOECCSD	q-NOECCSD
$^3\Sigma_g^-$	-149.653208	-150.223429	-150.238029	-150.222443
$^1\Delta_g$	-149.605647	–	-150.204043	-150.183136
$^1\Sigma_g^+$	-149.558086	–	-150.187127	-150.156285
$^1\Delta_g - {}^3\Sigma_g^-$	0.047561	–	0.033986	0.039307
$^1\Sigma_g^+ - {}^3\Sigma_g^-$	0.095122	–	0.0509029	0.066158

Table 6.4: l-NOECCSD and q-NOECCSD energies in $\mathrm{E_H}$ of the triplet ground state and lowest-lying open and closed shell singlet excited states of O_2 in a cc-pCVTZ basis set, compared to the CSF reference eneriges and the unrestricted CCSD energy of the triplet state.

for in our method. The $^1\Sigma_g^+$ state, which lies 0.0598 $\mathrm{E_H}$ above the triplet ground state, is a $\pi_{g,x}^2 + \pi_{g,y}^2$ configuration that is a symmetry-adapted linear combination of two closed-shell CSFs. Our single-reference open-shell formalism extends straightforwardly to this multi-determinant state and we obtain a singlet-triplet gap with q-NOECCSD of 0.0662 $\mathrm{E_H}$.

6.1.4 Carbene

The carbene (or methylene) diradical $^{\bullet\bullet}CH_2$ offers a chemically meaningful singlet-triplet system. The different singlet and triplet configurations have different equilibrium bond lengths and angles in the free molecule, with a closed-shell singlet lone pair favouring a more bent geometry with slightly longer bonds than the open-shell singlet or triplet. The electronic configuration also influences the behaviour of carbene and its related compounds in coordination chemistry.

When acting as a ligand, a $^{\bullet\bullet}CR_2$ compound can donate its two unpaired electrons to the metal centre in two different modes to form either a Fischer or a Schrock carbene. A Fischer carbene donates electron density from its singlet lone pair into a σ bond (with some π backbonding possible), while the Schrock carbenes have a formal double bond with the metal centre, corresponding to the two triplet-coupled unpaired electrons being contributed separately to a σ bond and a π bond.

The lowest energy state of the free methylene molecule is experimentally observed to be the $^3B_1$ triplet, which has an equilibrium bond angle of approxim-

ately $135°$. The lowest singlet state is the $^1A_1$ closed shell state with equilibrium bond angle of around $102°$. The $^1B_1$ open-shell singlet state is also accessible in our NOECCSD framework, using the triplet orbitals to construct an open shell singlet CSF reference. With the same orbital occupancy as the triplet, the open-shell singlet also favours a larger bond angle, with a minimum around $142°$

Energies of carbene in a cc-PVDZ basis were calculated for a range of H-C-H bond angles from $90°$ to $180°$, with the C-H bond lengths fixed at 1.10Å The qNOECCSD energies were calculated for the closed shell singlet and the triplet, as well as the open shell singlet starting from the triplet ROHF orbitals. They are plotted in figure 6.1, and the raw data are displayed in the appendices, in table A.2.

For the triplet state, the expected single reference behaviour is observed: CCSD reliably recovers 98.0% to 98.1% of the FCI correlation energy, with the spin-adapted qNOECCSD recovering 97.9% to 98.0%, confirming that the neglect of higher order terms in the exponential is less significant than triple excitations in the cluster operator. The closed shell singlet also shows good agreement between FCI and qNOECCSD in the weakly correlated region near the equilibrium bond angle, but the qNOECCSD energy becomes too high in the strongly correlated regime towards the linear geometry. In this strongly correlated region at large bond angles, it was observed that the singlet FCI sometimes collapsed down to the triplet energy, so the `fix_spin()` energy penalty method was applied to the FCI procedure in PySCF.If too large an energy penalty was used, sometimes the singlet would instead collapse up to the open shell singlet energy; the smooth FCI curves shown in figure 6.1 were obtained with energy penalty `ss=0.05`. The agreement between the open-shell singlet FCI solution and the open-shell singlet qNOECCSD energy was as good as that of the triplet CCSD with the corresponding FCI energy. The open-shell singlet using the triplet orbitals shows the correct qualitative behaviour only after applying the correlated qNOECCSD treatment: the reference has a linear equilibrium geometry, while the correct minimum at around $140°$ is seen in the qNOECCSD energy.

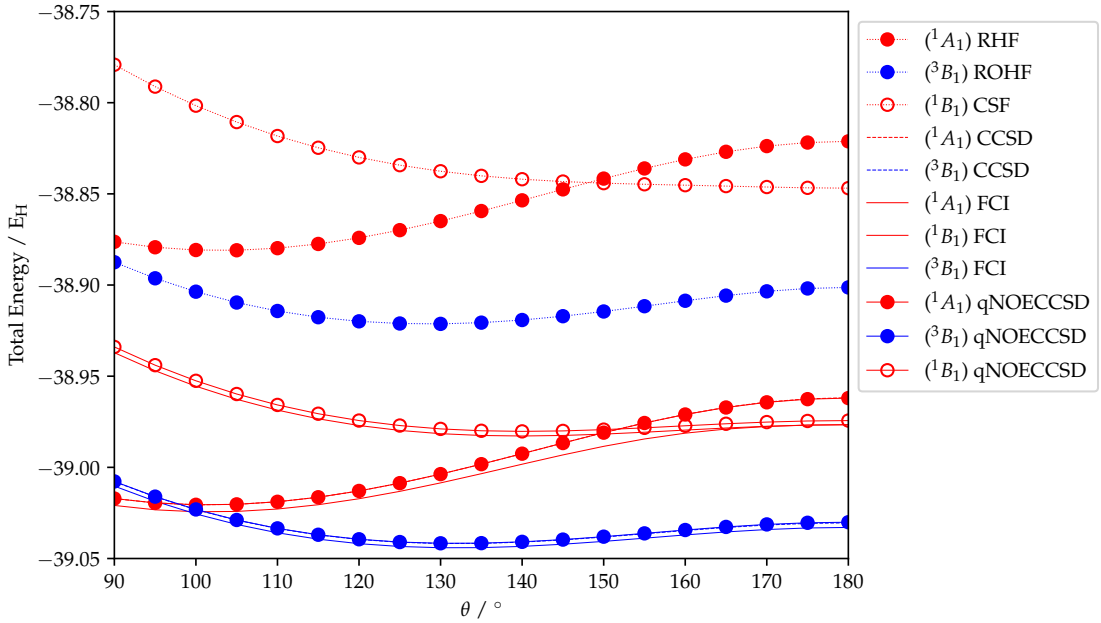

Figure 6.1: Total energies of CH_2 at $r = 1.10$Å for a range of bond angles from $90°$ to $180°$ in a cc-PVDZ basis. The qNOECCSD energies are shown along with those for the corresponding CSF reference states and the FCI solutions they approximate, as well as the standard CCSD energies for the high-spin cases.

The singlet-triplet gap and the bending mode frequencies of the two carbenes can be approximated by taking 3 different bond angles with the same bond lengths close to the minimum and fitting a quadratic for each potential energy surface. For a more accurate estimate of the potential energy minima for each of the three states, further calculations were performed in the larger cc-PVTZ basis, at angles close to the respective minima. Although it is possible to incorporate the zero-point vibrational energy contribution, this will not give an accurate estimate for the experimentally observable transitions, as the symmetric and asymmetric stretching modes have been neglected, and are likely to have a more significant zero-point contribution.

For the closed-shell singlet, triplet, and open-shell singlet, the respective equilibrium bond angles were calculated as $102.3°$, $132.8°$, and $141.8°$. The respective minimum energies were $-39.069558\mathrm{E_H}$, $-39.087153\mathrm{E_H}$, and $-39.032490\mathrm{E_H}$, giving the two excitation energies (neglecting zero-point energy) of $3862\mathrm{cm}^{-1}$ and $11997\mathrm{cm}^{-1}$. These energies have been calculated at the fixed C-H bond length

of 1.10Å, which is close to the equilibrium bond length of the $^1A_1$ state, but is longer than equilibrium bond length of around 1.06Å for the $^1B_1$ and $^3B_1$, so are not representative of the true experimental values.

The bending frequencies were calculated to be $484\mathrm{cm}^{-1}$, $677\mathrm{cm}^{-1}$, and $435\mathrm{cm}^{-1}$ respectively for the triplet, closed shell singlet, and open shell singlet. Comparing to the experimental bending frequency of $963\mathrm{cm}^{-1}$ for the triplet ground state, the calculation has predicted a bending frequency that is too low by approximately a factor of 2. Since this discrepancy is largely replicated in the FCI energies, its origin is likely in the poor harmonic approximation to the well potential, and in the inflexibility of enforcing a fixed bond length (which, moreover, is not optimal for each of the states). It would be expected that the bonding electron density would move further away from the central carbon as the angle decreases from equilibrium and closer as it increases, the effect of which cannot be accounted for in this model.

At the linear geometry, the two singlet states should become degenerate, forming a Δ_g pair of states that show a Renner–Teller effect in their splitting away from $180°$. This is confirmed by the FCI energies, but our results do not show this, with the $^1A_1$ state crossing above the $^1B_1$ in both the reference and qNOECCSD energies. It would be expected that the $^1B_1$ should be too high in energy, being constructed from orbitals that are not variationally optimised for that CSF. It turns out in this case that the more significant effect is the failure of the single determinant closed shell singlet CSF to capture the strong static correlation as the linear geometry is approached, causing the degeneracy to be broken in the opposite direction. While the correlated qNOECCSD treatment is able to reduce this effect somewhat, it still represents a qualitative failure of the single determinant picture, which our single CSF reference NOECCSD successfully addresses.

A previous MRCI study[183] found that the two singlet states are separated by $8245\mathrm{cm}^{-1}$ at their respective equilibrium geometries, from which our figure of

$8135\mathrm{cm}^{-1}$ differs by $-110\mathrm{cm}^{-1}$. At $-0.31\mathrm{kcal/mol}$, this may be considered agreement within chemical accuracy for an electronic energy difference (vibrational spectra would of course require higher accuracy, with experimental precision on the order of $1\mathrm{cm}^{-1}$).

6.1.5 H_4 rectangle

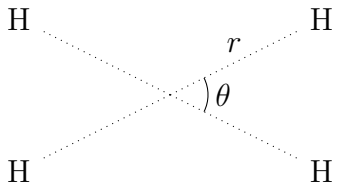

Figure 6.2: Diagram of the fixed radius rectangular H_4 model system

The H_4 rectangle provides an example of a near degeneracy becoming exact, showing the failure of single-determinant methods to obtain a smooth potential energy surface. A rectangle of fixed diameter can be defined by the (minor) angle between its two diagonals, as in the model described by van Voorhis *et al.*.[184] This may be considered as a modified form of the rectangular H_4 model of Piecuch *et al.*, but where the bond lengths in the two molecules are lengthened as they are brought closer together to keep the diagonals constant, as shown in figure 6.2. For a range of angles between $70°$ and $90°$, the energies of the H_4 rectangle at radii of 0.869Å and 1.738Å were calculated in a cc-pVTZ basis.

The lowest singlet and triplet FCI energies were also calculated at each angle. It was observed that the FCI solution for the singlet state collapsed onto the triplet close to the degeneracy, both at the shorter radius and the longer radius (even when the triplet was actually the higher in energy). In the PySCF FCI procedure the `fix_spin()` method was applied, which energetically penalises states of the wrong spin, which allowed the correct singlet FCI energies to be obtained.

The RHF energies show a cusp approaching $90°$ at both radii, and the CASSSCF energies are smooth, as expected. The open shell singlet CSF reference has been constructed from the triplet ROHF orbitals, with respect to which its

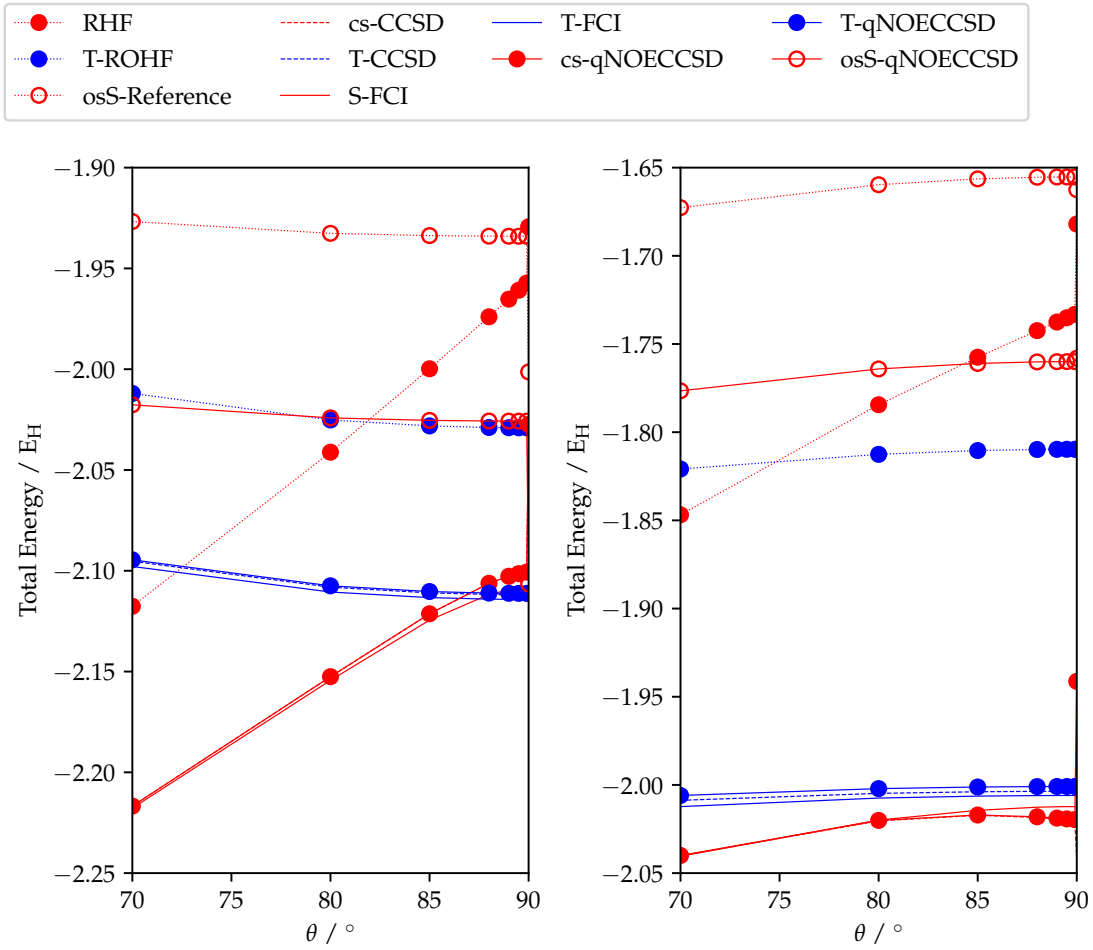

Figure 6.3: Energies of the H_4 rectangular model (figure 6.2) for $70° \leq \theta \leq 90°$ at $r = 0.869$Å and $r = 1.738$Å in a cc-PVTZ basis. The qNOECCSD energies are shown along with those for the corresponding CSF reference states and the FCI solutions they approximate, as well as the standard CCSD energies for the high-spin cases.

energy is not optimised, so is expected to be significantly too high in energy. Although this discrepancy will be carried over somewhat to the open shell singlet qNOECCSD energies, the inclusion of single excitations in the cluster operator and a quadratic *ansatz* should have accounted for some orbital relaxation. Other than at $90°$, this singlet qNOECCSD energy should well represent the open shell singlet excited state.

Even worse than the cusp (first-derivative discontinuity) approaching $90°$, the RHF energy itself is discontinuous at $90°$, showing an anomalously high energy where RHF was not able to accurately deal with the exact degeneracy, where the

D_{2h} symmetry of the rectangle is lifted to D_{4h} in the square. It would be expected that a symmetry-broken set of orbitals would be able to achieve a continuous energy, forming a degenerate pair with the solution approaching $90°$ from above.

Using a 2-electron open shell singlet reference has given a potential energy surface that approaches the degeneracy smoothly from both sides, but has not correctly captured the exact degeneracy at $90°$. The issue at the square geometry arises from the use of ROHF orbitals optimised for the triplet, which is invariant to rotations between the two degenerate orbitals. The open-shell triplet orbitals are therefore an arbitrary combination of the two degenerate orbitals, but the singlet CSF, without a further orbital optimisation, is not invariant to this choice of orbitals. The use of orbitals optimised for the appropriate single CSF reference wavefunction will be of paramount importance both to observing the correct behaviour at the degeneracy and for obtaining a quantitatively comparable open-shell singlet energy for the entire curve.

The closed-shell singlet CCSD and qNOECCSD energies in the partially dissociated rectangle are lower than the singlet FCI energy, demonstrating the non-variational nature of coupled cluster methods in general. This over-correlation was previously observed in CCD by Van Voorhis and Head-Gordon in a comparison with a variational CCD method.[184] That variational CC method also showed a cusp at $90°$, but (being a variational method) was confirmed to be an upper bound to the FCI energy. The fact that the closed-shell CCSD and qNOECCSD energies actually begin to decrease towards $90°$ shows a strongly correlated regime that has led to the failure of these approaches due to an instability in the (non-variational) coupled cluster equations.

For the closed shell configuration, chemical intuition suggests that the minimum energy would be at an arrangement that represents two separate H_2 molecules at close to their equilibrium bond lengths, around 0.74Å. For the smaller rectangle of radius $r = 0.869$Å, this is an angle of about $\theta = 50°$, and for the larger rectangle of $r = 1.738$Å it is about $\theta = 25°$, so it is no surprise to see the energy decrease away from $90°$ for the closed shell singlet. For the diradical

singlet and triplet CSFs, the square geometry is a minimum at the shorter radius, and a maximum at the longer. For this system of 4 hydrogen atoms approaching complete dissociation, a tetra-radical singlet CSF reference might be expected to show a minimum at the square geometry, but checking this is presently not within the capabilities of the OCCSFrD code.

6.1.5.1 Dissociating the H_4 square

As well as looking at a range of angles approaching the degeneracy, investigating the range of H-H distances in the square geometry can provide a multireference system with which to test the behaviour of the NOECCSD approach.[185] In the same cc-pVTZ basis, the energies of the H_4 square were calculated at a radius (i.e. side length $/\sqrt{2}$) between 0.7Å and 2.0Å.

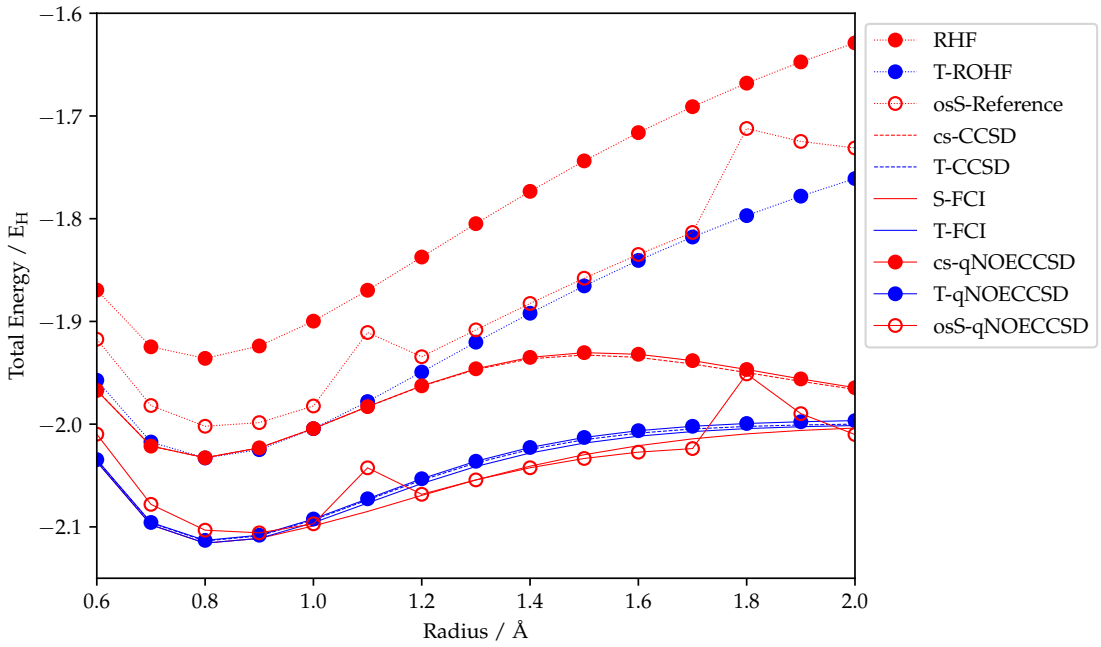

Figure 6.4: Energies of the H_4 square at radii from 0.7Å to 2.0Å in a cc-PVTZ basis. The qNOECCSD energies are shown along with those for the corresponding CSF reference states and the FCI solutions they approximate, as well as the standard CCSD energies for the high-spin cases.

The most obvious feature of the CSF and qNOECCSD energies for the hydrogen square is that they are not smooth for the open-shell singlet, appearing to be too high at 1.1Å and from 1.8Å onwards. As seen in the rectangular H_4

model when it reaches the square geometry, this arises because there is not a unique choice of orbitals to form the ROHF wavefunctions. A different choice of active orbitals that gives the same triplet ROHF energy can form a different state with a different energy when repopulated as a singlet - the single-CSF open shell singlet is not orbitally invariant in the active space.

For the regions where a smooth energy can be obtained for the open-shell singlet CSF, the correlated energy that results from applying qNOECCSD to this reference approaches the singlet FCI curve very closely in the intermediate regime, although after 1.4Å it begins to drop below the FCI energy, exhibiting the non-variationality that is a known property of projective CC methods. Even at shorter bond lengths and towards dissociation, the open-shell singlet qNOECCSD is much closer to FCI than the singlet CC energies obtained from the closed shell reference, whether or not the exponential was truncated at quadratic order. Under the spatial degeneracy of the D_{4h} square geometry, it is necessary to include 2 determinants in the reference for the ground state at all bond lengths.

At the shorter bond lengths, the singlet FCI ground state energy matches the triplet, and the open shell singlet qNOECCSD energy is too high, and so qNOECCSD predicts too large an equilibrium distance for the singlet. This can be attributed either to the need to include terms above quadratic order in the exponential or three-body correlations due to stronger dynamic correlation (since the electrons are on average closer together), or to the need to account for orbital relaxation, as evidenced by the large energy difference between the reference and the CASSCF.

The high-spin (single determinant) case of the triplet is quite well-behaved for the whole curve. The qNOECCSD and spin-orbital CCSD energies closely match FCI, but the agreement between coupled cluster treatments is better than with FCI at short distances, while towards dissociation the neglect of higher powers in qNOECCSD appears to have prevented it from approaching the exact energy at dissociation, as the standard spin-orbital-based uCCSD does.

At longer distances towards dissociation, the tetra-radical states may be expected to contribute, so the 2-electron open shell singlet may not be sufficient to account for the static correlation. In the 4-electron singlet space, there are two G-T states (see branching diagram, figure 2.3), both of which can contribute to the wavefunction for 4 fully dissociated hydrogen atoms in an overall singlet. The quintet would also be relevant towards dissociation, although this would probably be a dissociative state, rather than showing a binding curve as the lower multiplicity spin states do. If qNOECCSD equations were available for the tetraradical CSFs it could be expected that smooth binding curves would be attainable by diagonalising within either the singlet or triplet subspaces of qNOECCSD wavefunctions. Such a procedure is effectively a non-orthogonal configuration interaction, in which the dynamic correlation has already been incorporated into the reference functions. This would not be a proper MRCC, with the amplitudes in the cluster operator for each of the reference functions unable to react in the presence of differing static correlation as represented by the changing coefficients in the linear CI expansion. Since it makes more sense to treat dynamic correlation as a correction to a reference that includes static and non-dynamical correlation, the opposite approach may be more appropriate, which would correspond exactly to internally-contracted MRCC.

It was also observed for the closed shell singlet that the traditional CCSD did not converge above 1.7Å unless DIIS was applied, and for 1.7Å the CCSD energy was unexpectedly low without DIIS. This reflects the familiar breakdown of the single-reference description of singlet H_4 as it approaches dissociation.

6.2 Higher Seniority

Although the OCCSFrD code is presently not efficient enough to derive the spin-adapted NOECCSD equations at higher than quadratic order or for more than 2 open-shell electrons, it was possible to obtain the linear CCSD equations for the high-spin three-electron quartet and both doublets of 3 electrons. While the $\mathbf{d} = (121)$ doublet is a two-determinant CSF, effectively being a 1-electron

doublet in the third orbital (say, orbital k) coupled to an open-shell singlet in the first two orbitals (i and j):

$$\hat{O}_3^{\frac{1}{2},+\frac{1}{2}}\left((121)\right) = \frac{1}{\sqrt{2}}\Big(\hat{a}^{i\alpha}\hat{a}^{j\beta} - \hat{a}^{i\beta}\hat{a}^{j\alpha}\Big)\hat{a}^{k\alpha} \tag{6.2.0.1}$$

the other doublet, $\mathbf{d} = (112)$, requires 3 determinants:

$$\hat{O}_3^{\frac{1}{2},+\frac{1}{2}}\left((112)\right) = \frac{1}{\sqrt{3}}\Big(\hat{a}^{i\alpha}\hat{a}^{j\alpha}\hat{a}^{k\beta} - \frac{1}{2}\hat{a}^{i\beta}\hat{a}^{j\alpha}\hat{a}^{k\alpha} - \frac{1}{2}\hat{a}^{i\alpha}\hat{a}^{j\beta}\hat{a}^{k\alpha}\Big) \tag{6.2.0.2}$$

The fact that this is not the same as the two-determinant CSF produced by coupling a 1-electron doublet in orbital i with a 2-electron open-shell singlet in orbitals j and k is a manifestation of the fact that the ordering of orbitals matters in a genealogical coupling scheme.

6.2.1 Nitrogen Atom

As a test of the lCCSD equations for seniority 3 states, energies were calculated for the quartet and doublets for the $2s^2 2p^3$ configuration of the nitrogen atom.

$\lvert N, S, M_S, \mathbf{d}\rangle$	Reference Energy	uCCSD	l-NOECCSD	FCI
$\lvert 1, \frac{1}{2}, +\frac{1}{2}, (1)\rangle$	-54.259609	-54.411862	-54.402932	-54.432857
$\lvert 3, \frac{3}{2}, +\frac{3}{2}, (111)\rangle$	-54.397358	-54.520323	-54.525747	-54.525236
$\lvert 3, \frac{1}{2}, +\frac{1}{2}, (112)\rangle$	-54.290852	$-$	-54.434113	(-54.432857)
$\lvert 3, \frac{1}{2}, +\frac{1}{2}, (121)\rangle$	-54.290852	$-$	-54.434087	(-54.432857)

Table 6.5: Energies in E_H of the quartet ground state and low-lying doublet excited states of the nitrogen atom in a cc-pVTZ basis set, compared to the CSF reference eneriges and the unrestricted CCSD energies.

The fact that both of the seniority-3 (triradical) doublets, which are lower than the seniority-1 doublet, are accessible in our NOECCSD framework is a demonstration of its general applicability to arbitrary CSFs. Other single-reference CSF approaches have normally only been demonstrated for two-determinant CSFs such as the 2-electron open-shell singlet.

For the high-spin quartet it was seen as before that the linear CC energies were lower than full CI, with the quadratic terms expected to restore the quasi-variational upper bound as seen in the spin-orbital based CCSD energies. It

remains to be seen whether additional complications arise when targetting these states with quadratic terms included.

It is also interesting to note that, while the two tri-radical doublet CSFs constructed out of the quartet ROHF orbitals are degenerate, l-NOECCSD has broken the degeneracy by about $0.025\,\mathrm{mE_H}$. The degeneracy of the two references might be an artefact due to being constructed out of the high-spin orbitals. It is unclear whether this may also be broken, even in the references but also in the correlated energies, if the orbitals are independently optimised for each CSF.

7 Conclusions

7.1 Achievements of the present work

We have developed a novel formulation of the single-reference normal-ordered exponential coupled-cluster method to correlate multi-determinant states, NOECC. The *ansatz* is rigorously spin-adapted and recovers the dynamic correlation and orbital relaxation of an arbitrary configuration state function, without spin contamination. Both high- and low-spin states of an atom or molecule can be correlated.

Our working equations are derived from a reformulation of the unlinked coupled-cluster equations, which we prove are equivalent to solving fully connected equations. The method formally terminates at an order in the cluster amplitudes given by $4+\min(n, 2N_r)$, where n is the number of open-shell orbitals and N_r is the highest rank of excitations included in the cluster operator. If the equations are not truncated at a lower order than $4 + \min(n, 2N_r)$, the theory is fully size extensive. In this way, we circumvent the requirement for the inverse of the normal ordered exponential, for which the closed form is not known. We have developed code to automatically generate spin-adapted equations in a truncated form, while keeping the size extensivity errors as small as possible.

The NOECCSD method truncated at second-order has been examined numerically using a set of small atoms and molecules, with encouraging results.

Our energies for doublet systems are comparable to those found by Szalay and Gauss using a spin-restricted formalism and the singlet-triplet energy splitting are shown to be in excellent agreement with FCI for the $[\mathrm{He}]\,2s2p$ configuration of beryllium and within 10 kJ/mol of experiment for the oxygen molecule. Numerical tests of size consistency reveal that, while the method is not rigorously size consistent, size-inconsistency errors are on the order of $\mu\mathrm{E_H}$ for the cases tested. In common with many MRCC methods, the NOECC wavefunction contains spectator excitations that lead to a set of redundant amplitudes in the residual equations. Although this leads to an infinite family of solutions, we find that different amplitude solutions yield energies which are exactly the same in the linear case, and which in the quadratic case differ by much less than the contribution due to triple excitations, by two or more orders of magnitude.

NOECC is a single-reference method in the sense that coefficients of the multi-determinant reference state are not relaxed. However, since our formulation does not rely on the absence of active-to-active excitations in the cluster operator, it is not limited to single CSF reference wavefunctions, but can in principle be used to correlate MCSCF states such as CASSCF, RASSCF[148] or GASSCF[149] references to recover the dynamic correlation of highly multi-reference states, without spin contamination. While such a fully multi-reference approach would be appropriate for cases such as bond dissociation or near-degeneracies, the generalised single-reference NOECC framework remains highly suited for strongly correlated single configurational wavefunctions, such as specific spin states in organic radicals or high- and low-spin transition metal clusters.

The work presented in this thesis demonstrates a new implementation of an automated equation generator for coupled cluster methods, applicable to general single reference wavefunctions, whether single or multiple determinants. A set of spin-adapted coupled cluster equations, truncated to linear and quadratic orders in the amplitudes, has been automatically derived for CSFs of 0,1, and 2 open-shell electrons, and linear CCSD equations for the CSFs of 3 open-shell electrons. Additionally, the Oxygen molecule was used to demonstrate a case of a

linear combination of closed shell CSFs where the coefficients are predetermined by spatial symmetry.

A simple unlinked formalism for the single-reference spin-adapted normal-ordered exponential coupled cluster has been derived, and its formal termination properties detailed. Because this is a generalised single-reference framework, the active-active excitations can be included in the ansatz without breaking intermediate normalisation. The size-extensivity violation due to truncation of the exponential is kept to a minimum by truncating the energy-dependent amplitude equations overall to the specified order in the amplitudes, avoiding the spurious inclusion of higher-order disconnected terms.

Up to quadratic terms in the amplitudes, the spin-adapted NOECCSD energies and splittings have been shown for a range of high and low spin CSFs in small molecules, showing that the qualitative behaviour of multireference wavefunctions can be observed in some cases with a single CSF reference, even when constructed from the 'wrong' orbitals. In some cases, the qualitative behaviour is only recovered after the application of the correlated qNOECCSD treatment, showing that both static correlation in the reference and dynamic correlation on top of it are important to reproduce the correct behaviour in multireference cases.

7.1.1 MRCC

The NOECC method satisfies some of the criteria set out by Köhn and coworkers for a MRCC theory, but is not a genuine multireference theory. It is applicable to multideterminantal cases of spin-coupling and spatial degeneracy, but does not treat multiple CSFs in an un-biased way and so cannot in general obtain smooth potential energy surfaces.

7.1.1.1 Spin-purity

Our formulation of a NOECC theory is trivially spin-pure, being constructed in terms of spin-preserving operators applied to a spin-adapted reference state, with

no spin-contamination appearing at any stage. In section 6.1.1, we confirmed that the $M_S = 0$ triplet CSF was degenerate with the $M_S = 1$ component at every iteration of a calculation, indicating numerically that our equations are spin-adapted.

7.1.1.2 Compatibility with SRCC

The state-specific NOECC method we have proposed is a single-reference method in the sense that we correlate a single reference CSF representative of the electronic eigenstate under consideration. In general, the CSF is a specific linear combination of many determinants. In the case that the CSF is a single closed-shell determinant, NOECC reduces identically to conventional spin-free coupled-cluster theory. Moreover, in high-spin open-shell cases the reference is a single determinant, making it seamlessly compatible with SRCC methods.

Many of the problems associated with combining results from MRCC methods with SRCC methods stem from the use of a CASSCF reference, where it is often challenging to keep the reference space consistent across different regions of the potential energy surface. In the context of state-specific NOECC, this problem becomes one of choosing an appropriate CSF reference. Some regions of the potential energy surface will not be well represented by a single CSF[8] and there the state-specific approach is expected to be less accurate.

7.1.1.3 Projected Schrödinger equation

A proper residual equation[5, 6, 35] is defined as one that is equivalent to solving a projected Schrödinger equation. In general, the amplitude equations for methods using the JM *ansätze*, where each reference determinant has its own wave operator, do not correspond to a projected Schrödinger equation (a notable exception being Hanrath's MRexpT[163, 167] method). The NOECC approach projects onto a complete first-order interacting space and therefore does satisfy the condition of having a proper residual equation.

It is important to note that, for multideterminant cases, this is not a first-order interacting space from any one of the determinants in the reference. Neither is it the spin-completion of such a projection manifold in the sense of Herrmann and Hanrath's inclusion of higher-body excitations with spectators to generate all determinants of the desired excited configuration. This 'interacting space' approximation to the singles and doubles projection manifold was already noted by Paldus and Li,[11] who suggested (as later confirmed by Herrmann and Hanrath[73]) that the spin incompleteness introduced only a very small additional error.

The linear dependencies appearing in the projection manifold due to spectating excitations lead to non-unique solutions. While the convergence issues that this would present were possible to address with DIIS, the fact that they do differ in energy means that this method cannot be considered mature until a choice is made to find a unique solution, by sufficiency conditions or other means.

For closed shell spin-free CCSD calculations, a transformation can be carried out on the projection manifold so that the excited bra and ket states form a biorthogonal basis.[76] The appropriate biorthogonal basis for open shell spin-adapted calculations has not been derived, and it is not clear whether a unique choice for such a biorthogonalisation exists; for triply-excited states it does not even for a closed shell reference.

7.1.1.4 Size extensivity

The question of size extensivity is not as simple for open-shell spin adapted reference states as it is for the closed shell or spin-orbital based theories. As shown in section 3.5, solving for the amplitude equations is equivalent to solving for a corresponding set of equations comprising only connected terms. For a given open-shell configuration, the energy of a CSF reference is size-extensive, in the limit of large number of core electrons. Our NOECC method is therefore size extensive with respect to the core orbitals, when all terms are included up to the finite order at which the equations terminate. Truncating our equations at a

lower order introduces a size-extensivity error, although this has been minimised by avoiding the introduction of spurious unlinked terms.

Extensivity with respect to the active orbital subspace is not guaranteed by inspecting the connected form of one set of equations, as CSFs with more open-shell orbitals will be treated with different single-reference equations. The extensivity of the total energy relies on an extensive energy for the reference CSFs, which only makes sense if a particular family of reference CSFs is chosen with a systematically increasing number of active orbitals. For the high spin CSF this can be done, being a single-determinant ROHF calculation.

For low spin CSFs, when a particular spin-coupling is chosen, it is not yet clear if an extensive reference energy is obtained when the orbitals are taken from a high spin ROHF calculation, or even if the energy of an orbitally-optimised CSF resulting from a multi-determinantal ROHF calculation is size-extensive. Considering the correlation energy as the number of active orbitals is taken to infinity, the complexity of the equations as formulated by OCCSFrD will scale exponentially. Although the size-extensivity of the correlation energy will be inherited from FCI, so too will the exponential cost. Since NOECC is only useful when there are a handful of open-shell orbitals, the relevant extensivity consideration is really only with respect to the occupied subspace, and is guaranteed by the connected form of our equations as before, when taken to their full terminating order.

7.1.1.5 Size consistency

More pertinent for open shell systems with small numbers of open-shell orbitals is the numerical study of size consistency. Size consistency requires that the energy of a molecule composed of two infinitely separated spin-coupled fragments is equal to the sum of the energies of the isolated fragments. For size consistency to be satisfied, the reference CSF must dissociate into the corresponding CSFs for the constituent fragments, and non-vanishing higher-order excitations present

in the NOECC wave operator for the molecule must be representable through products of lower-order excitations of the fragments.

Our test case of two Neon atoms at large separation showed that the size inconsistency due to our quadratic-truncated unlinked equations could be almost completely removed in closed shell systems when the correct truncation procedure was taken. We then used the homolytic bond fission of Li_2 as the simplest non-trivial test case for open-shell systems. Using the CSFs formed from the singlet- and triplet-coupling of the separate lithium atoms each in their doublet ground state, the qNOECCSD correlation energy was shown to be nearly size consistent. The large size-inconsistencies in NOECCD were attributed to the presence of spectating excitations that effectively allowed single excitations to be counted in the dimer, where only doubles were counted in the monomer.

The appropriate CSF for spin-coupled, but non-interacting fragments is the one constructed from Clebsch–Gordon coupling of the spins of the fragments. For example, a two-electron open-shell triplet and singlet are formed by high-spin or low-spin coupling two one-electron doublet states, respectively.

7.1.1.6 Orbital invariance

The NOECC method proposed is invariant to core-core and virtual-virtual rotations in the same way as standard coupled-cluster theory. The reference CSF is not in general invariant to active-active rotations. This is in contrast to a CASSCF reference function, used in ic-MRCC methods, which is invariant to active-active rotations[186]. The precise subset of active-active orbital rotations under which a single Gel'fand-Tsetlin CSF reference is invariant is revealed by its GUGA representation. For a single CSF, the orbital invariance subgroup only contains rotations among sets of consecutive orbitals forming a single maximally open-shell configuration, and is not sufficient to reproduce the smooth potential energy surfaces achievable with a complete active space.

For any given excitation order, the NOE cluster operator $\hat{T}$ consists of all possible excitations from the set of core and active orbitals to the set of active

and virtual orbitals. The NOE wave operator $\{e^{\hat{T}}\}$ is therefore invariant to orbital rotations within each of these sets. If a certain subset of these excitations were excluded, the wave operator ceases to be orbital invariant. Our proposed NOECC method includes all excitations of a given type and therefore retains all orbital invariance properties of the reference CSF.

7.1.1.7 Multireference treatment

Formally our NOECC method treats a single CSF as the reference, and so cannot be considered a genuine multireference method. It does address the need for multiple determinants in low-spin reference states, and so can solve some problems that have historically required a multireference treatment. However, it is only applicable to cases in which the static correlation is determined by spin or other symmetry constraints, and does not use an unbiased treatment of a multidimensional model space. This fundamentally prevents it from being able to obtain smooth potential energy surfaces, leaving a major part of the motivation for MRCC unsolved.

Hypothetically, a single-reference approach in which new equations are derived for e.g. a CASSCF reference wavefunction could be considered a genuine multireference method, with CASSCF treating the active space equally before an internally-contracted-style NOECC approach to the dynamic correlation. The derivation of new equations for each reference would however present a computational bottleneck that is not feasible in the current version of OCCSFrD. However, there is great scope in the future to optimise this step, or perhaps to store equations for MCSCF references with a range of coefficients to look up when running a calculation, which could make such an approach possible.

7.1.1.8 Computational cost

The computational scaling of our NOECC method is not optimised, being equivalent to un-factorised traditional coupled cluster. However, the correct factorisation scheme should be possible in the future, and would lead to methods that scale

similarly to the single-reference equivalents. Ultimately, the reduced-scaling methods being developed for CC in general would be required to bring the cost down in order to be practicable for large molecules.

The prefactor in the computational cost is currently prohibitively large for all but very small calculations. The python implementation in OCCSFrD is very slow and should be replaced with a compiled language for performance, both in the derivation of open-shell equations and in the coupled-cluster solver. There is great scope for parallelisation to make use of high-performance computing for larger calculations, but implementation of this is also left for future work.

The only formal aspect of the NOECC method making it any more expensive than SRCC is the complexity of the open-shell CSF, with which it scales exponentially. This is not unexpected: even at the mean-field level, a genuinely multireference treatment of static correlation, as in CASSCF, shares this limitation.

7.1.1.9 Theoretical simplicity

Conceptually NOECC does not involve anything more complicated than the choice of a CSF reference that well captures the static correlation. This is a matter of chemical intuition and appropriate consideration of symmetry arguments, akin to the problems of active space selection in CAS calculations.

The equations generated by OCCSFrD are presently too complicated for human interpretation. Factorising and simplifying them would not only reduce the overhead cost of computational storage and memory, but would greatly improve interpretability of the equations, in terms of identifying which correlation processes are important or not. Preliminary attempts were made to use graph-theoretic techniques from the Networkx python package in OCCSFrD, but were never completed. Packages such as Wick&D and SeQuant, designed for similar problems, might instead be able to provide the necessary capabilities.

7.1.1.10 Numerical stability

Without DIIS, the spectating excitations lead to a failure to converge to a defined set of amplitudes in open shell systems. The specific choice of DIIS subspace size and level-shift parameter determine which one out of the family of solutions is reached. This is numerically stable, but not uniquely defined.

Additional constraints on the amplitudes, such as enforcing exact size consistency of the open-shell energy, might lead to a unique choice of converged amplitudes, but this requires further investigation. Also, the need for level shifts that significantly increase the required number of iterations might be obviated by a more appropriate effective Fock-matrix preconditioner.

7.1.2 Towards a model chemistry

Since Köhn's MRCC wishlist is largely motivated by the same considerations as the original model chemistry mission, the evaluation of NOECC as a model chemistry will largely result in the same conclusions. As for all methods, efficiency and cost-effectiveness is key, and it has already been shown that the additional cost of NOECC over SRCC is comparable to that required for any MR treatment, beyond the inefficiencies of our implementation. Size extensivity has already been examined, and the argument for correct dissociation into open-shell fragments is exactly the same as for size consistency.

7.1.2.1 General applicability

Although NOECC can correctly describe the start- and end-points of dissociation, it cannot continuously describe the intermediate region. A 'genuine' multireference method, as previously described, would be required to smoothly traverse this region.

It is a general approach to open-shell systems, and while it cannot target general excited states, it can treat excited states that are the lowest in their

respective spin sector. Our NOECC method extends the domain of single-determinant coupled cluster to general single-reference wavefunctions, including high- and low-spin open-shell systems

7.1.2.2 Invariance to rotations among degenerate orbitals

The invariance of the energy to rotations among the occupied and virtual spaces has already been seen. An additional criterion stated for a model chemistry was the invariance to rotations among sets of degenerate orbitals. Where degenerate orbitals are open-shell, the effect of rotations among them is influenced by the spin-coupling. A high-spin CSF is invariant to the open-shell orbital rotations, and NOECC will not change this. The matter is more complicated for low-spin CSFs of more than 2 orbitals.

In general, a single Gel'fand–Tsetlin CSF is only invariant to rotations among orbitals that are consecutively coupled to a high-spin configuration. Since the actual state of the many-electron system is determined by the genealogy of the spin coupling, the order of coupling steps that increase or decrease the total spin has physical consequences that cannot be ignored. For the case of an isolated nitrogen atom, the two triradical doublet CSFs constructed from the quartet ROHF orbitals are degenerate, but differ slightly when linear NOECCSD is applied. Since these two CSFs can be related by a unitary transformation among the three open-shell orbitals, it must be concluded that the linear NOECCSD is not orbitally invariant for low-spin CSFs. Whether this is a symmetry-breaking artefact of the truncation to linear order or a genuine effect in low spin CSFs is not clear.

7.2 Perspectives

This thesis has displayed some of our perspectives on correlation and on the choices that should be made in developing a coupled cluster theory for strongly correlated systems.

7.2.1 Strong correlation

Our view on strong correlation is that it should be used to refer to systems that require a genuine multireference method, being not well represented by a single reference function, whether of one or multiple determinants. If a single CSF is the appropriate reference for a given system, then the choice of orbitals is a mean-field problem with spin-coupling incorporated (in much the same way that Hartree–Fock is a mean-field problem with exchange incorporated). Our current procedure for constructing low-spin CSFs out of high-spin ROHF orbitals does not accurately reflect this, but should be replaced by a CSF-ROHF procedure, such as that implemented in ORCA.[138, 140] When quadratic terms are included in the NOECCSD equations, the effect of this incorrect choice of orbitals is reduced, reflecting the relative insensitivity of coupled cluster to the choice of orbitals in the reference.

7.2.2 Choice of cluster operator vs. projection manifold

We have taken the view that coupled cluster methods should be governed by the excitations in the cluster operator, and not by the states generated (as is the case for CI methods). This has led to the choice not to include higher body operators with spectators in the projection manifold, ignoring any desire for spin-completeness of the projection manifold. Although a lower energy may be achieved if a larger projection space is taken, the spin incompleteness error is only small if spectators are included up to the excitation level in the cluster operator.

The physical motivation for coupled cluster as modelling dynamical correlation as a product of independent excitation processes is what leads to the normal-ordered exponential ansatz. The appropriate combination of a normal-ordered exponential ansatz for dynamical correlation with a linear ansatz for static correlation has still not been found for cases of ‘genuine’ strong correlation, but the distinction is now clear between the general single-reference problem and the true multireference problem that remains.

7.3 Future work

7.3.1 Next steps

Having shown that NOECC can provide a viable treatment of dynamic correlation on top of a statically correlated reference state, there remain a few improvements to both the theory and the implementation to be made. Accomplishing these would result in a fully general single-reference method applicable to transition metal complexes and other open-shell systems with accuracy comparable to single-determinant coupled cluster.

7.3.1.1 Implementation

The efficiency savings that should be made to the OCCFrD code have already been laid out, and must be completed before it is of any use for more than proof-of-concept calculations. The collection of equivalent terms, ideally deriving each distinct term only once (rather than wasting computational effort on each repeated derivation) would lead to huge savings in the prefactor. Generating factorised equations would allow the correct scaling to be achieved. Allowing equations to be built using a "many-body" approach, rather than a projective approach, could save time in the derivation of spin-free equations, and possibly facilitate the identification of factorised intermediates and unique contraction topologies. An implementation of the above in C++ or Fortran would offer a significant speedup over the current Python code.

7.3.1.2 Theory

Using low-spin CSF references with optimised orbitals is a key feature that should be implemented as soon as possible. Codes to do this are already available,[139, 140] so it is a matter of interfacing with OCCSFrD to input the correct orbitals. While it is more involved to use orbitals from e.g. ORCA than from PySCF, this should still be achievable without too much difficulty.

The more difficult theoretical question is how to uniquely determine the redundant amplitudes, other than picking the essentially arbitrary choice that

results from a given level shift and DIIS subspace size. In the first instance, a solution is offered by the icMRCC approaches: the number of amplitudes is reduced to only those that generate linearly independent excitations in the projection manifold using a Schmidt decomposition. However, it should be noted that spectating excitations represent distinct correlation processes that have different effects in a product of excitations, even if they generate the same state when linearly applied to the reference. Treating these independently, while usually only a small correction, should offer the freedom to restore exact size consistency for open-shell subsystems. The required additional constraints should be determined by analysing the open shell cluster amplitudes, and it is not clear whether a projective approach to obtain these is possible or if they require a many-body construction.

7.3.2 Longer term

In the longer term, the goals of genuine multireference CC remain. While the requirement has been addressed that a model chemistry should be spin-adapted for closed and open shells, the continuous and smooth general applicability across molecular geometries is not yet accomplished. Genuine MRCC is still an area of active research, even with implementations of icMRCC and Mk-MRCC becoming more widely used, and perhaps some formulation is possible based on a normal-ordered exponential and multiple CSF references. Even at the MCSCF level, the question of active space selection is still debated in multireference quantum chemistry. A state-specific method like NOECC could offer a route to methods using state-selection rather than space-selection, although this would still require careful consideration of each chemical system of interest.

The general single-reference NOECC framework already developed might also be extended to derive analytic gradients, allowing more direct comparisons with simulations and spectroscopic experiments. Hyperfine coupling constants, for example, are an example of a property for which fully spin-adapted analytic gradients would be particularly useful.

An equation-of-motion method for excitation, ionisation, and attachment energies would complete the picture of general applicability of a theoretical model chemistry. For a normal-ordered exponential form of the wave operator, the correct form of the similarity-transformed Hamiltonian has to be carefully considered. The series expansion for the inverse of the wave operator can be truncated at successive orders to obtain improved approximations to the ground state, giving good accuracy even at only one or two terms.[187] For excited states the error due to truncation may prove much more severe.

Appendices

A
Data

Angle / °	Reference				FCI		
	RHF	T-ROHF	osS-REF	CASSCF(2,2)	S1	S2	T
90	-38.876301	-38.887493	-38.779181	-38.897971	-39.020890	-38.937111	-39.010302
95	-38.879288	-38.896308	-38.791178	-38.900829	-39.023281	-38.947017	-39.018580
100	-38.880800	-38.903651	-38.801622	-38.902198	-39.024350	-38.955510	-39.025560
105	-38.880931	-38.909603	-38.810620	-38.902165	-39.024179	-38.962679	-39.031309
110	-38.879784	-38.914244	-38.818280	-38.900828	-39.022859	-38.968605	-39.035895
115	-38.877475	-38.917652	-38.824705	-38.917652	-39.020498	-38.973370	-39.039388
120	-38.874133	-38.919910	-38.829997	-38.919910	-39.017219	-38.977056	-39.041862
125	-38.869900	-38.921099	-38.834259	-38.921099	-39.013170	-38.979748	-39.043400
130	-38.864935	-38.921308	-38.837597	-38.921308	-39.008524	-38.981536	-39.044093
135	-38.859417	-38.920635	-38.840125	-38.920635	-39.003482	-38.982518	-39.044039
140	-38.853544	-38.919189	-38.841965	-38.919189	-38.998280	-38.982802	-39.043353
145	-38.847534	-38.917098	-38.843249	-38.917098	-38.993183	-38.982508	-39.042161
150	-38.841623	-38.914513	-38.844123	-38.914513	-38.988477	-38.981769	-39.040608
155	-38.836056	-38.911617	-38.844739	-38.911617	-38.984435	-38.980734	-39.038852
160	-38.831080	-38.908628	-38.845239	-38.908628	-38.981255	-38.979562	-39.037065
165	-38.826926	-38.905809	-38.845734	-38.905809	-38.979000	-38.978418	-39.035427
170	-38.823798	-38.903457	-38.846249	-38.903457	-38.977583	-38.977461	-39.034107
175	-38.821853	-38.901877	-38.846688	-38.901877	-38.976834	-38.976826	-39.033249
180	-38.821194	-38.901318	-38.846867	-38.901318	-38.976604	-38.976604	-39.032952

Table A.1: Mean-field and FCI energies of carbene in cc-pVDZ basis at a bond length of $r = 1.10$Å

Angle / °	CCSD		qNOECCSD			
	S	T	cs	T	osS	Δ
90	-39.017117	-39.007818	-39.017116	-39.007728	-38.933960	0.421339
95	-39.019499	-39.016148	-39.019498	-39.016062	-38.943959	0.414666
100	-39.020533	-39.023169	-39.020532	-39.023083	-38.952534	0.407737
105	-39.020299	-39.028949	-39.020299	-39.028862	-38.959775	0.400515
110	-39.018887	-39.033557	-39.018886	-39.033467	-38.965766	0.392963
115	-39.016397	-39.037063	-39.016396	-39.036969	-38.970590	0.385046
120	-39.012944	-39.039545	-39.012944	-39.039444	-38.974330	0.376744
125	-39.008664	-39.041084	-39.008664	-39.040975	-38.977072	0.368058
130	-39.003710	-39.041771	-39.003710	-39.041651	-38.978908	0.359020
135	-38.998256	-39.041707	-38.998257	-39.041574	-38.979936	0.349694
140	-38.992499	-39.041006	-38.992502	-39.040856	-38.980265	0.340189
145	-38.986656	-39.039795	-38.986663	-39.039624	-38.980015	0.330664
150	-38.980959	-39.038219	-38.980974	-39.038024	-38.979320	0.321336
155	-38.975646	-39.036437	-38.975678	-39.036214	-38.978328	0.312477
160	-38.970950	-39.034624	-38.971008	-39.034370	-38.977199	0.304421
165	-38.967077	-39.032959	-38.967173	-39.032673	-38.976096	0.297544
170	-38.964194	-39.031616	-38.964333	-39.031301	-38.975174	0.292243
175	-38.962420	-39.030743	-38.962595	-39.030406	-38.974565	0.288885
180	-38.961821	-39.030441	-38.962010	-39.030095	-38.974352	0.287733

Table A.2: CCSD and qNOECCSD energies of carbene in cc-pVDZ basis at a bond length of $r = 1.10$Å. For completeness, the level shift Δ used for the open-shell NOECCSD calculations is also given.

Angle / °	Reference				FCI	
	RHF	T-ROHF	osS-REF	CASSCF(2,2)	S	T
70.0	-2.117628	-2.012003	-1.926730	-2.125672	-2.217773	-2.097875
80.0	-2.041179	-2.025182	-1.932599	-2.054650	-2.154352	-2.110543
85.0	-1.999791	-2.028120	-1.933707	-2.021394	-2.124503	-2.113317
88.0	-1.974006	-2.028919	-1.933994	-2.028919	-2.111746	-2.114068
89.0	-1.965246	-2.029032	-1.934034	-2.029032	-2.109536	-2.114174
89.5	-1.960834	-2.029060	-1.934044	-2.029060	-2.108961	-2.114200
89.9	-1.957289	-2.029069	-1.934047	-2.029069	-2.108775	-2.114209
90.0	-1.929345	-2.029070	-2.001346	-2.029070	-2.108767	-2.114209

(a) Mean-field and FCI energies of the H_4 rectangle at $r = 0.869$Å

Angle / °	CCSD		qNOECCSD			
	S	T	cs	T	osS	Δ
70.0	-2.216756	-2.095277	-2.216753	-2.094572	-2.017669	0.470940
80.0	-2.152558	-2.108137	-2.152549	-2.107470	-2.024153	0.412605
85.0	-2.121364	-2.110965	-2.121343	-2.110309	-2.025387	0.387248
88.0	-2.106252	-2.111731	-2.106219	-2.111078	-2.025707	0.373139
89.0	-2.102758	-2.111839	-2.102727	-2.111187	-2.025752	0.368610
89.5	-2.101465	-2.111866	-2.101435	-2.111214	-2.025763	0.366378
89.9	-2.100686	-2.111875	-2.100657	-2.111223	-2.025766	0.364608
90.0	-2.027431	-2.111875	-2.027427	-2.111223	-2.106606	0.364167

(b) CCSD and qNOECCSD energies of the H_4 rectangle at $r = 0.869$Å. For completeness, the level shift Δ used for the open-shell NOECCSD calculations is also given.

Angle / °	Reference				FCI	
	RHF	T-ROHF	osS-REF	CASSCF(2,2)	S	T
70.0	-1.846844	-1.820872	-1.672701	-1.870754	-2.040429	-2.012292
80.0	-1.784437	-1.812567	-1.659677	-1.824068	-2.019957	-2.007452
85.0	-1.757507	-1.810415	-1.656374	-1.810415	-2.014395	-2.006340
88.0	-1.742420	-1.809807	-1.655447	-1.809807	-2.012635	-2.006037
89.0	-1.737543	-1.809720	-1.655314	-1.809720	-2.012370	-2.005994
89.5	-1.735131	-1.809698	-1.655281	-1.809698	-2.005984	-2.005984
89.9	-1.733214	-1.809691	-1.655271	-1.809691	-2.005980	-2.005980
90.0	-1.681984	-1.809691	-1.662517	-1.809691	-2.012280	-2.005980

(a) Mean-field and FCI energies of the H_4 rectangle at $r = 1.738$Å

Angle / °	CCSD		qNOECCSD			
	S	T	cs	T	osS	Δ
70.0	-2.040177	-2.008732	-2.040007	-2.008732	-1.776554	0.225479
80.0	-2.020398	-2.004787	-2.020113	-2.004787	-1.764136	0.187346
85.0	-2.017222	-2.003883	-2.017059	-2.003883	-1.761017	0.172283
88.0	-2.018432	-2.003637	-2.018069	-2.003637	-1.760143	0.164296
89.0	-2.019363	-2.003602	-2.018823	-2.003602	-1.760018	0.161793
89.5	-2.019913	-2.003594	-2.019266	-2.003594	-1.759986	0.160570
89.9	-2.020387	-2.003591	-2.019651	-2.003591	-1.759976	0.159605
90.0	-2.042783	-2.003591	-1.941278	-2.003591	-1.758091	0.159366

(b) CCSD and qNOECCSD energies of the H_4 rectangle at $r = 1.738$Å. For completeness, the level shift Δ used for the open-shell NOECCSD calculations is also given.

Radius / Å	Reference				FCI	
	RHF	T-ROHF	osS-REF	CASSCF(2,2)	S	T
0.7	-1.924713	-2.017399	-1.981869	-2.017399	-2.098036	-2.098036
0.8	-1.935963	-2.032934	-2.002046	-2.032934	-2.115818	-2.115818
0.9	-1.923914	-2.024840	-1.998502	-2.024840	-2.111220	-2.111220
1.0	-1.899716	-2.004418	-1.982327	-2.004418	-2.099088	-2.095945
1.1	-1.869649	-1.978016	-1.910787	-1.978016	-2.085009	-2.076797
1.2	-1.837316	-1.949249	-1.934371	-1.949249	-2.069376	-2.057807
1.3	-1.804821	-1.920195	-1.908222	-1.920195	-2.054296	-2.041246
1.4	-1.773395	-1.892037	-1.882518	-1.892037	-2.040920	-2.028103
1.5	-1.743732	-1.865415	-1.857937	-1.865415	-2.029774	-2.018428
1.6	-1.716201	-1.840643	-1.834836	-1.840643	-2.020960	-2.011709
1.7	-1.690964	-1.817838	-1.813379	-1.817838	-2.014307	-2.007235
1.8	-1.668048	-1.797003	-1.712188	-1.797003	-2.009485	-2.004338
1.9	-1.647390	-1.778068	-1.724783	-1.778068	-2.006104	-2.002494
2.0	-1.628871	-1.760925	-1.731162	-1.760925	-2.003792	-2.001329

(a) Mean-field and FCI energies of the H_4 square at radii from 0.7Å to 2.0Å

Radius / Å	CCSD		qNOECCSD			
	S	T	cs	T	osS	Δ
0.7	-2.021316	-2.096124	-2.021363	-2.096124	-2.078075	0.384032
0.8	-2.032695	-2.113665	-2.032697	-2.113665	-2.103208	0.377382
0.9	-2.023049	-2.108801	-2.023045	-2.108801	-2.105792	0.357132
1.0	-2.004334	-2.093236	-2.004311	-2.093236	-2.097016	0.331105
1.1	-1.983050	-2.073790	-1.982945	-2.073790	-2.042519	0.302485
1.2	-1.962985	-2.054531	-1.962687	-2.054531	-2.068289	0.273951
1.3	-1.946791	-2.037792	-1.946091	-2.037792	-2.054275	0.247127
1.4	-1.936391	-2.024629	-1.934999	-2.024629	-2.042457	0.222756
1.5	-1.932674	-2.015125	-1.930389	-2.015125	-2.033414	0.201044
1.6	-1.935004	-2.008735	-1.931977	-2.008735	-2.027257	0.181914
1.7	-1.947672	-2.004679	-1.938173	-2.004679	-2.023764	0.165162
1.8	-1.949783	-2.002217	-1.946792	-2.002217	-1.951106	0.150529
1.9	-1.958337	-2.000778	-1.955955	-2.000778	-1.989764	0.137750
2.0	-1.966184	-1.999965	-1.964503	-1.999965	-2.010116	0.126575

(b) CCSD and qNOECCSD energies of the H_4 square at radii from 0.7Å to 2.0Å. For completeness, the level shift Δ used for the open-shell NOECCSD calculations is also given.

B Code

B.1 Recursive contraction engine pseudocode

```
recursive subroutine cdrive(idx,list,nlist,n,nc,clist,ncmax,seq
   ,iseq,sgnflps,fermsgn,sgnflp)
 implicit none
 integer :: idx, n, iseq
 integer :: nlist(n), list(n,n), nc, ncmax, clist(n,ncmax), seq
    (2,n)
 integer :: i, j, jdx, jseq, k
 logical :: lnew, sgnflp(n), sgnflps(ncmax), fermsgn(n)

 if index > n: #reached end of string
  return

 if (2*iseq == n): #found full contraction
  numContractions++
  if numContractions > maxContractions: #maximum possible
     number of contractions allocated
    stop
  end if

  for i in range(1, iseq):
   contractionsList[seq(1,i),numContractions] = seq[2,i]
   sgnflps(nc) = (sgnflps[nc] != sgnflp[i])
  return
 end if

 ! currently have iseq contractions involving elements up to
    idx-1
```

```
 # make sure index not in sequence
 lnew = True
 for j in range(1, iseq):
  if (index == seq[2,j]) then
   lnew = False
   exit
  end if

 if (lnew):
 # search over contractions for element index
 for i in range(1, nlist[index]):
  lnew = True
  for j in range(1, iseq)
   if (list[i,index] == seq[2,j]):
    lnew = False #already in sequence
    exit
   end if

  jseq = iseq+1
  seq[1,jseq] = index
  seq[2,jseq] = list[i,index]
  for k in range(seq[1,jseq]+1,seq[2,jseq]-1):
   fermsgn[k] = not fermsgn[k] #alternate sign for operators
      between contracting pair

  sgnflp[jseq] = (fermsgn[seq[1,jseq]] == fermsgn[seq[2,jseq]])

  call cdrive(index+1,list,nlist,n,nc,clist,ncmax,seq,jseq,
     sgnflps,fermsgn,sgnflp)

  # finished searching, remove sequence
  for k in range(seq[1,jseq]+1,seq[2,jseq]-1)
   fermsgn[k] = not fermsgn[k]
  seq[:,jseq] = 0
  sgnflp[jseq] = False

 else:
  call cdrive(index+1,list,nlist,n,nc,clist,ncmax,seq,iseq,
     sgnflps,fermsgn,sgnflp)

end subroutine
```

B.2 Equation generator input file

```
from occsfrd import ansatz, wick, interface
```

```
openShellIndex = wick.index.SpecificOrbitalIndex("i")
openShellIndex.value = 0
doubletOperator = wick.operator.BasicOperator(openShellIndex,
   True, True)

hTensor = wick.tensor.Tensor("h", ['g'], ['g'])
hTensor.getAllDiagramsActive()
gTensor = wick.tensor.Tensor("g", ['g', 'g'], ['g', 'g'])
gTensor.getAllDiagramsActive()
Hamiltonian = sum(hTensor.diagrams) + 0.5 * sum(gTensor.diagrams
   )

t1Tensor = wick.tensor.Tensor("{t_{1}}", ['p'], ['h'])
t1eTensor = wick.tensor.Tensor("{t_{1}}", ['v'], ['a'])
t2Tensor = wick.tensor.Tensor("{t_{2}}", ['p', 'p'], ['h', 'h'])
t2eTensor = wick.tensor.Tensor("{t_{2e}}", ['p', 'p'], ['h','a
   '])

t1Tensor.getAllDiagramsActive()
t1eTensor.getAllDiagramsActive()
t2Tensor.getAllDiagramsActive()
t2eTensor.getAllDiagramsActive()

amplitudeTensors = [t1Tensor, t1eTensor, t2Tensor, t2eTensor]
amplitudeDiagrams = t1Tensor.diagrams + t1eTensor.diagrams +
   t2Tensor.diagrams + t2eTensor.diagrams# + t2xTensor.diagrams

T = sum(t1Tensor.diagrams) + sum(t1eTensor.diagrams) + 0.5 * sum
   (t2Tensor.diagrams) + 0.5 * sum(t2eTensor.diagrams)# + 0.5 *
   sum(t2xTensor.diagrams)

expT = ansatz.utils.operatorExponential(T, trunc=2,
   normalOrdered=True)
normalisationCheck = ansatz.normalorderedcc.getEnergyEquation(
   expT, referenceOperator=doubletOperator)
energyEquation = ansatz.normalorderedcc.getEnergyEquation(
   Hamiltonian * expT, referenceOperator=doubletOperator)
amplitudeEquations = [ansatz.normalorderedcc.
   getAmplitudeEquation_UnlinkedFormalism(Hamiltonian, expT,
   tDiagram, referenceOperator=doubletOperator) for tDiagram in
   amplitudeDiagrams]

equations = [(energyEquation, normalisationCheck)] +
   amplitudeEquations

interface.storeequations.save("N1S0.5equations", equations, [
   hTensor, gTensor] + amplitudeTensors, [openShellIndex])
interface.texify.texify(equations, "N1S0.5equations")
```

B.3 OCCSFrD input file

```
import numpy as np
from pyscf import gto, ao2mo, scf, fci, mp, cc
from occsfrd import wick, ansatz, solve, interface

bohr = 0.529177249

H2sep = 1.605 * bohr

mol = gto.Mole()
mol.verbose = 1
mol.atom = 'Li 0 0 0'
mol.spin = 1
mol.basis = 'cc-pcvtz'
mol.build()

Enuc = mol.energy_nuc()

mf = scf.ROHF(mol)
mf.conv_tol = 1e-14
mf.kernel()

print("Nuclear repulsion energy:", Enuc, "ROHF electronic
   energy:", mf.energy_elec(), "Total ROHF energy:", mf.e_tot
   )

equationsDict = interface.storeequations.load("/home/dpt02/
   dpt/iclb0552/code/OpenShellCC/equations/
   UnlinkedNormalOrdered/CCSD/quadraticNO/N1S0.5equations")

quadraticCCSD = solve.cc.runUnlinkedCC(mf, equationsDict,
   levelShift=2, verbosity=0, Rtol=16, Etol=12, maxIter=1000,
    nDIIS=12, maxOrder=2)
print("Total CCD energy:", mf.e_tot + quadraticCCSD["
   correlation energy"])
```

References

1. Gunasekera, A. D., Lee, N. & Tew, D. P. Multi-reference coupled cluster theory using the normal ordered exponential ansatz. *Faraday Discuss.* **254,** 170–190. doi:10.1039/D4FD00044G (6th Nov. 2024).
2. Pople, J. A. Nobel Lecture: Quantum chemical models. en. *Rev. Mod. Phys.* **71,** 1267–1274. ISSN: 0034-6861, 1539-0756. doi:10.1103/RevModPhys.71.1267 (Oct. 1999).
3. Bartlett, R. J. Many-Body Perturbation Theory and Coupled Cluster Theory for Electron Correlation in Molecules. en. *Ann. Rev. Phys. Chem.* **32.** Publisher: Annual Reviews, 359–401. ISSN: 0066-426X, 1545-1593. doi:10.1146/annurev.pc.32.100181.002043 (Oct. 1981).
4. Bartlett, R. J. & Musial, M. Coupled-cluster theory in quantum chemistry. *Rev. Mod. Phys.* **79,** 291. doi:10.1103/RevModPhys.79.291 (Feb. 2007).
5. Köhn, A., Hanauer, M., Mück, L. A., Jagau, T.-C. & Gauss, J. State-specific multireference coupled-cluster theory. *WIREs Comput. Mol. Sci.* **3,** 176–197. doi:https://doi.org/10.1002/wcms.1120 (Oct. 2012).
6. Lyakh, D. I., Musial, M., Lotrich, V. F. & Bartlett, R. J. Multireference Nature of Chemistry: The Coupled-Cluster View. *Chem. Rev.* **112,** 182–243. doi:10.1021/cr2001417 (Dec. 2011).
7. Evangelista, F. A. Perspective: Multireference coupled cluster theories of dynamical electron correlation. *J. Chem. Phys.* **149,** 030901 (July 2018).
8. Marti-Dafcik, D., Lee, N., Burton, H. G. A. & Tew, D. P. Spin-coupled molecular orbitals: chemical intuition meets quantum chemistry. arXiv: 2402.08858 [physics.chem-ph] (2024).
9. Lindgren, I. A coupled-cluster approach to the many-body perturbation theory for open-shell systems. *Int. J. Quantum Chem.* **14,** 33–58. doi:10.1002/qua.560140804 (Mar. 1978).
10. Li, X. & Paldus, J. Multiconfigurational spin-adapted single-reference coupled cluster formalism. *Int. J. Mol. Sci.* **48,** 269–285 (Mar. 1993).
11. Li, X. & Paldus, J. Automation of the implementation of spin-adapted open-shell coupled-cluster theories relying on the unitary group formalism. *J. Chem. Phys.* **101,** 8812–8826. doi:10.1063/1.468074 (Nov. 1994).
12. Li, X. & Paldus, J. in *Recent Advances in Coupled-Cluster Methods* 183–219 (World Scientific, May 1997).
13. Li, X. & Paldus, J. Unitary-group-based open-shell coupled-cluster method with corrections for connected triexcited clusters. I. Theory. *Int. J. Quantum Chem.* **70,** 65–75 (Oct. 1998).

14. Li, X. & Paldus, J. Unitary group based open-shell coupled cluster method with corrections for connected triexcited clusters. II. Applications. *Mol. Phys.* **94,** 41–54 (1998).

15. Coester, F. Bound states of a many-particle system. *Nucl. Phys.* **7,** 421–424. ISSN: 0029-5582. doi:https://doi.org/10.1016/0029-5582(58)90280-3 (1958).

16. Coester, F. & Kümmel, H. Short-range correlations in nuclear wave functions. *Nucl. Phys.* **17,** 477–485. ISSN: 0029-5582. doi:https://doi.org/10.1016/0029-5582(60)90140-1 (1960).

17. Sinanoğlu, O. Many-Electron Theory of Atoms and Molecules. I. Shells, Electron Pairs vs Many-Electron Correlations. *J. Chem. Phys.* **36,** 706–717. ISSN: 0021-9606. doi:10.1063/1.1732596 (Feb. 1962).

18. Čížek, J. On the Correlation Problem in Atomic and Molecular Systems. Calculation of Wavefunction Components in Ursell-Type Expansion Using Quantum-Field Theoretical Methods. *J. Chem. Phys.* **45,** 4256–4266. ISSN: 0021-9606. doi:10.1063/1.1727484 (Dec. 1966).

19. Čížek, J. & Paldus, J. Correlation problems in atomic and molecular systems III. Rederivation of the coupled-pair many-electron theory using the traditional quantum chemical methodst. *Int. J. Quantum Chem.* **5.** Publisher: John Wiley & Sons, Ltd, 359–379. ISSN: 1097-461X. doi:10.1002/qua.560050402 (July 1971).

20. Pople, J. A., Krishnan, R., Schlegel, H. B. & Binkley, J. S. Electron correlation theories and their application to the study of simple reaction potential surfaces. en. *Int. J. Quantum Chem.* **14,** 545–560. ISSN: 1097-461X. doi:10.1002/qua.560140503 (1978).

21. Bartlett, R. J. & Purvis, G. D. Many-body perturbation theory, coupled-pair many-electron theory, and the importance of quadruple excitations for the correlation problem. en. *Int. J. Quantum Chem.* **14,** 561–581. ISSN: 1097-461X. doi:10.1002/qua.560140504 (1978).

22. Taylor, P. R., Bacskay, G. B., Hush, N. S. & Hurley, A. C. Unlinked cluster effects in molecular electronic structure. I. The HCN and HNC molecules. en. *J. Chem. Phys.* **69,** 1971–1979. ISSN: 0021-9606, 1089-7690. doi:10.1063/1.436848 (Sept. 1978).

23. Purvis III, G. D. & Bartlett, R. J. A full coupled-cluster singles and doubles model: The inclusion of disconnected triples. *J. Chem. Phys.* **76,** 1910–1918. ISSN: 0021-9606. doi:10.1063/1.443164 (Feb. 1982).

24. Noga, J. & Bartlett, R. J. The full CCSDT model for molecular electronic structure. en. *J. Chem. Phys.* **86,** 7041–7050. ISSN: 0021-9606, 1089-7690. doi:10.1063/1.452353 (June 1987).

25. Scuseria, G. E. & Schaefer, H. F. A new implementation of the full CCSDT model for molecular electronic structure. *Chem. Phys. Lett.* **152,** 382–386. ISSN: 0009-2614. doi:10.1016/0009-2614(88)80110-6 (Nov. 1988).

26. Raghavachari, K., Trucks, G. W., Pople, J. A. & Head-Gordon, M. A fifth-order perturbation comparison of electron correlation theories. *Chem. Phys. Lett.* **157,** 479–483. ISSN: 0009-2614. doi:10.1016/S0009-2614(89)87395-6 (May 1989).

27. Bartlett, R. J., Watts, J. D., Kucharski, S. A. & Noga, J. Non-iterative fifth-order triple and quadruple excitation energy corrections in correlated methods. *Chem. Phys. Lett.* **165,** 513–522. ISSN: 0009-2614. doi:10.1016/0009-2614(90)87031-L (Feb. 1990).

28. Olsen, J., Roos, B. O., Jo/rgensen, P. & Jensen, H. J. A. Determinant based configuration interaction algorithms for complete and restricted configuration interaction spaces. *J. Chem. Phys.* **89,** 2185–2192. ISSN: 0021-9606. doi:10.1063/1.455063 (Aug. 1988).

29. Roos, B. O., Taylor, P. R. & Sigbahn, P. E. M. A complete active space SCF method (CASSCF) using a density matrix formulated super-CI approach. *Chem. Phys.* **48,** 157–173. ISSN: 0301-0104. doi:10.1016/0301-0104(80)80045-0 (May 1980).

30. Siegbahn, P. E. M., Almlöf, J., Heiberg, A. & Roos, B. O. The complete active space SCF (CASSCF) method in a Newton–Raphson formulation with application to the HNO molecule. en. *J. Chem. Phys.* **74,** 2384–2396. ISSN: 0021-9606, 1089-7690. doi:10.1063/1.441359 (Feb. 1981).

31. Andersson, K., Malmqvist, P. A., Roos, B. O., Sadlej, A. J. & Wolinski, K. Second-order perturbation theory with a CASSCF reference function. *J. Phys. Chem.* **94.** Publisher: American Chemical Society, 5483–5488. ISSN: 0022-3654. doi:10.1021/j100377a012 (July 1990).

32. Angeli, C., Cimiraglia, R., Evangelisti, S., Leininger, T. & Malrieu, J.-P. Introduction of n-electron valence states for multireference perturbation theory. *J. Chem. Phys.* **114,** 10252–10264. ISSN: 0021-9606. doi:10.1063/1.1361246 (June 2001).

33. Mukherjee, D., Moitra, R. K. & Mukhopadhyay, A. Correlation problem in open-shell atoms and molecules. *Mol. Phys.* **30,** 1861–1888 (Feb. 1975).

34. Jeziorski, B. & Monkhorst, H. J. Coupled-cluster method for multideterminantal reference states. *Phys. Rev. A* **24,** 1668 (Oct. 1981).

35. Kong, L. Connection between a few Jeziorski-Monkhorst ansatz-based methods. *Int. J. Quantum Chem.* **109,** 441–447 (Sept. 2008).

36. Kutzelnigg, W. Quantum chemistry in Fock space. I. The universal wave and energy operators. *J. Chem. Phys.* **77,** 3081–3097. ISSN: 0021-9606. doi:10.1063/1.444231 (Sept. 1982).

37. Haque, M. A. & Mukherjee, D. Application of cluster expansion techniques to open shells: Calculation of difference energies. *J. Chem. Phys.* **80,** 5058–5069 (May 1984).

38. Stolarczyk, L. Z. & Monkhorst, H. J. Coupled-cluster method in Fock space. I. General formalism. *Phys. Rev. A* **32,** 725 (Jan. 1985).

39. Kaldor, U. The Fock space coupled cluster method: theory and application. *Theor. Chim. Acta* **80,** 427–439 (Nov. 1991).

40. Musial, M. & Bartlett, R. J. Intermediate Hamiltonian Fock-space multireference coupled-cluster method with full triples for calculation of excitation energies. *J. Chem. Phys.* **129,** 044101. ISSN: 0021-9606. doi:10.1063/1.2952521 (July 2008).

41. Musiał, M. & Bartlett, R. J. Multi-reference Fock space coupled-cluster method in the intermediate Hamiltonian formulation for potential energy surfaces. *J. Chem. Phys.* **135,** 044121. ISSN: 0021-9606. doi:10.1063/1.3615500 (July 2011).

42. Nooijen, M. & Bartlett, R. J. General spin adaptation of open-shell coupled cluster theory. *J. Chem. Phys.* **104,** 2652–2688. doi:10.1063/1.471010 (Feb. 1996).

43. Nooijen, M. Many-body similarity transformations generated by normal ordered exponential excitation operators. *J. Chem. Phys.* **104,** 2638–2651 (Feb. 1996).

44. Nooijen, M. & Bartlett, R. J. Similarity transformed equation-of-motion coupled-cluster study of ionized, electron attached, and excited states of free base porphin. *J. Chem. Phys.* **106,** 6449–6455 (Apr. 1997).

45. Nooijen, M. & Bartlett, R. J. Similarity transformed equation-of-motion coupled-cluster theory: Details, examples, and comparisons. *J. Chem. Phys.* **107,** 6812–6830 (Nov. 1997).

46. Mukherjee, D. Normal ordering and a Wick-like reduction theorem for fermions with respect to a multi-determinantal reference state. *Chem. Phys. Lett.* **274,** 561–566. ISSN: 0009-2614. doi:10.1016/S0009-2614(97)00714-8 (15th Aug. 1997).

47. Kutzelnigg, W. & Mukherjee, D. Normal order and extended Wick theorem for a multiconfiguration reference wave function. *J. Chem. Phys.* **107,** 432–449. doi:10.1063/1.474405 (July 1997).

48. Piecuch, P., Kucharski, S. A. & Bartlett, R. J. Coupled-cluster methods with internal and semi-internal triply and quadruply excited clusters: CCSDt and CCSDtq approaches. en. *J. Chem. Phys.* **110,** 6103–6122. ISSN: 0021-9606, 1089-7690. doi:10.1063/1.478517 (Apr. 1999).

49. Shavitt, I. Graph theoretical concepts for the unitary group approach to the many-electron correlation problem. *Int. J. Quantum Chem.* **12,** 131–148. ISSN: 1097-461X. doi:10.1002/qua.560120819 (S11 1977).

50. Matsen, F. A. in *Advances in Quantum Chemistry* (ed Löwdin, P.-O.) 223–250 (Academic Press, 1st Jan. 1978). doi:10.1016/S0065-3276(08)60238-5.

51. Hinze, J. *The Unitary group for the evaluation of electronic energy matrix elements Lecture notes in chemistry* **22.** ISBN: 978-0-387-10287-0 (Springer-Verlag, 1981).

52. Robb, M. A. & Niazi, U. The unitary group approach in Configuration Interaction (CI) methods. *Comput. Phys. Rep.* **1,** 127–236. ISSN: 0167-7977. doi:10.1016/0167-7977(84)90007-8 (1st May 1984).

53. Li, X. & Paldus, J. Unitary group based open-shell coupled cluster approach and triplet and open-shell singlet stabilities of Hartree–Fock references. *J. Chem. Phys.* **103,** 6536–6547. ISSN: 0021-9606. doi:10.1063/1.470380 (15th Oct. 1995).

54. Li, X. & Paldus, J. Unitary group based state specific open-shell-singlet coupled-cluster method: Application to ozone and comparison with Hilbert and Fock space theories. *J. Chem. Phys.* **102,** 8059–8070. ISSN: 0021-9606, 1089-7690. doi:10.1063/1.469005 (22nd May 1995).

55. Janssen, C. L. & Schaefer, H. F. The automated solution of second quantization equations with applications to the coupled cluster approach. en. *Theor. Chim. Acta* **79,** 1–42. ISSN: 1432-2234. doi:10.1007/BF01113327 (Jan. 1991).

56. Kong, L. *Internally Contracted Multireference Coupled Cluster Method and Normal-Order-Based Automatic Code Generator* en. Publisher: University of Waterloo. PhD Thesis (Apr. 2009).

57. Hanauer, M. & Köhn, A. Pilot applications of internally contracted multireference coupled cluster theory, and how to choose the cluster operator properly. *J. Chem. Phys.* **134,** 204111 (May 2011).
58. Evangelista, F. A. Automatic derivation of many-body theories based on general Fermi vacua. *J. Chem. Phys.* **157,** 064111. ISSN: 0021-9606. doi:10.1063/5.0097858 (Aug. 2022).
59. Gaudel, B. *et al. SeQuant Framework for Symbolic and Numerical Tensor Algebra. I. Core Capabilities* Nov. 2025. doi:10.48550/arXiv.2511.09943.
60. Szalay, P. G. & Gauss, J. Spin-restricted open-shell coupled-cluster theory. *J. Chem. Phys.* **107,** 9028–9038. doi:10.1063/1.475220 (1st Dec. 1997).
61. Mahapatra, U. S., Datta, B., Bandyopadhyay, B. & Mukherjee, D. State-Specific Multi-Reference Coupled Cluster Formulations: Two Paradigms. *Adv. Quantum Chem.* **30,** 163–193. doi:10.1016/S0065-3276(08)60507-9 (1998).
62. Mahapatra, U. S., Datta, B. & Mukherjee, D. A size-consistent state-specific multireference coupled cluster theory: Formal developments and molecular applications. *J. Chem. Phys.* **110,** 6171–6188. ISSN: 0021-9606. doi:10.1063/1.478523 (Apr. 1999).
63. Datta, D. & Mukherjee, D. A compact spin-free combinatoric open-shell coupled cluster theory applied to single-reference doublets. *Int. J. Quantum Chem.* **108,** 2211–2222 (May 2008).
64. Datta, D. & Mukherjee, D. An explicitly spin-free compact open-shell coupled cluster theory using a multireference combinatoric exponential ansatz: Formal development and pilot applications. *J. Chem. Phys.* **131,** 044124. doi:10.1063/1.3185356 (July 2009).
65. Datta, D. & Gauss, J. A Non-antisymmetric Tensor Contraction Engine for the Automated Implementation of Spin-Adapted Coupled Cluster Approaches. *J. Chem. Theor. Comput.* **9,** 2639–2653. ISSN: 1549-9618. doi:10.1021/ct400216h (11th June 2013).
66. Adam, R. G., Waigum, A. & Köhn, A. Multireference Coupled-Cluster Theory: The Internally Contracted Route. en. *WIREs Comput. Mol. Sci.* **15.** _eprint: https://wires.onlinelibrary.wiley.com/doi/pdf/10.1002/wcms.70023, e70023. ISSN: 1759-0884. doi:10.1002/wcms.70023 (2025).
67. Banerjee, A. & Simons, J. The coupled-cluster method with a multiconfiguration reference state. *Int. J. Quantum Chem.* **19,** 207–216 (Feb. 1981).
68. Evangelista, F. A. & Gauss, J. An orbital-invariant internally contracted multireference coupled cluster approach. *J. Chem. Phys.* **134,** 114102. ISSN: 0021-9606. doi:10.1063/1.3559149 (Mar. 2011).
69. Evangelista, F. A., Hanauer, M., Köhn, A. & Gauss, J. A sequential transformation approach to the internally contracted multireference coupled cluster method. *J. Chem. Phys.* **136,** 204108 (May 2012).
70. Aoto, Y. A. & Köhn, A. Internally contracted multireference coupled-cluster theory in a multistate framework. *J. Chem. Phys.* **144,** 074103. ISSN: 0021-9606. doi:10.1063/1.4941604 (Feb. 2016).

71. Hanauer, M. & Köhn, A. Communication: Restoring full size extensivity in internally contracted multireference coupled cluster theory. *J. Chem. Phys.* **137,** 131103. ISSN: 0021-9606. doi:10.1063/1.4757728 (Oct. 2012).

72. Köhn, A., Black, J. A., Aoto, Y. A. & Hanauer, M. Improved and simplified orthogonalisation scheme and connected triples correction within the internally contracted multireference coupled-cluster method. *Mol. Phys.* **118.** _eprint: https://doi.org/10.1080/00268976.2020.1743889, e1743889. ISSN: 0026-8976. doi:10.1080/00268976.2020.1743889 (Nov. 2020).

73. Herrmann, N. & Hanrath, M. Generation of spin-adapted and spin-complete substitution operators for (high spin) open-shell coupled cluster of arbitrary order. *J. Chem. Phys.* **153,** 164114. doi:10.1063/5.0026762 (Oct. 2020).

74. Herrmann, N. & Hanrath, M. Analysis of different sets of spin-adapted substitution operators in open-shell coupled cluster theory. *Mol. Phys.* **120,** e2005836 (Nov. 2021).

75. Herrmann, N. & Hanrath, M. A correctly scaling rigorously spin-adapted and spin-complete open-shell CCSD implementation for arbitrary high-spin states. *J. Chem. Phys.* **156,** 054111 (Feb. 2022).

76. Helgaker, T., Olsen, J. & Jorgensen, P. *Modern Electronic Structure Theory* ISBN: 978-1-118-53147-1 (Wiley-Blackwell, 2013).

77. Adler, T. B., Werner, H.-J. & Manby, F. R. Local explicitly correlated second-order perturbation theory for the accurate treatment of large molecules. *J. Chem. Phys.* **130,** 054106. ISSN: 0021-9606. doi:10.1063/1.3040174 (7th Feb. 2009).

78. Tew, D. P., Helmich, B. & Hättig, C. Local explicitly correlated second-order Møller–Plesset perturbation theory with pair natural orbitals. *J. Chem. Phys.* **135,** 074107. ISSN: 0021-9606. doi:10.1063/1.3624370 (21st Aug. 2011).

79. Kato, T. On the eigenfunctions of many-particle systems in quantum mechanics. en. *Commun. Pure Appl. Math.* **10,** 151–177. ISSN: 1097-0312. doi:10.1002/cpa.3160100201 (1957).

80. Tew, D. P. & Klopper, W. New correlation factors for explicitly correlated electronic wave functions. *J. Chem. Phys.* **123,** 074101. ISSN: 0021-9606. doi:10.1063/1.1999632 (15th Aug. 2005).

81. Krause, C. & Werner, H.-J. Comparison of explicitly correlated local coupled-cluster methods with various choices of virtual orbitals. *Phys. Chem. Chem. Phys.* **14,** 7591–7604. ISSN: 1463-9084. doi:10.1039/C2CP40231A (14th May 2012).

82. Schmitz, G. & Hättig, C. Accuracy of Explicitly Correlated Local PNO-CCSD(T). *J. Chem. Theory Comput.* **13,** 2623–2633. ISSN: 1549-9618. doi:10.1021/acs.jctc.7b00180 (13th June 2017).

83. Ma, Q. & Werner, H.-J. Scalable Electron Correlation Methods. 8. Explicitly Correlated Open-Shell Coupled-Cluster with Pair Natural Orbitals PNO-RCCSD(T)-F12 and PNO-UCCSD(T)-F12. *J. Chem. Theory Comput.* **17,** 902–926. ISSN: 1549-9618. doi:10.1021/acs.jctc.0c01129 (9th Feb. 2021).

84. Szabo, A. & Ostlund, N. S. *Modern Quantum Chemistry: Introduction to Advanced Electronic Structure Theory* ISBN: 978-0-486-69186-2 (Courier Corporation, 2nd July 1996).

85. Shavitt, I. & Bartlett, R. J. *Many-Body Methods in Chemistry and Physics: MBPT and Coupled-Cluster Theory* ISBN: 978-0-521-81832-2 (Cambridge University Press, Aug. 2009).

86. Dreizler, R. M. & Gross, E. K. U. *Density Functional Theory* en. ISBN: 978-3-642-86107-9 978-3-642-86105-5. doi:10.1007/978-3-642-86105-5 (Springer, Berlin, Heidelberg, 1990).

87. Medvedev, M. G., Bushmarinov, I. S., Sun, J., Perdew, J. P. & Lyssenko, K. A. Density functional theory is straying from the path toward the exact functional. *Sci.* **355.** Publisher: American Association for the Advancement of Science, 49–52. doi:10.1126/science.aah5975 (Jan. 2017).

88. Born, M. & Oppenheimer, R. Zur Quantentheorie der Molekeln. en. *Ann. Phys.* **389,** 457–484. ISSN: 1521-3889. doi:10.1002/andp.19273892002 (1927).

89. Nelson, T. R. *et al.* Non-adiabatic Excited-State Molecular Dynamics: Theory and Applications for Modeling Photophysics in Extended Molecular Materials. *Chem. Rev.* **120.** Publisher: American Chemical Society, 2215–2287. ISSN: 0009-2665. doi:10.1021/acs.chemrev.9b00447 (Feb. 2020).

90. Born, M. & Huang, K. *Dynamical Theory Of Crystal Lattices* ISBN: 978-0-19-267008-3. doi:10.1093/oso/9780192670083.001.0001 (Oxford University Press, Aug. 1954).

91. Mok, D. K. W., Neumann, R. & Handy, N. C. Dynamical and Nondynamical Correlation. *J. Phys. Chem.* **100.** Publisher: American Chemical Society, 6225–6230. ISSN: 0022-3654. doi:10.1021/jp9528020 (Jan. 1996).

92. Ganoe, B. & Shee, J. On the notion of strong correlation in electronic structure theory. en. *Faraday Discuss.* **254.** Publisher: The Royal Society of Chemistry, 53–75. ISSN: 1364-5498. doi:10.1039/D4FD00066H (Nov. 2024).

93. Löwdin, P.-O. en. in *Advances in Chemical Physics* 207–322 (John Wiley & Sons, Ltd, 1958). ISBN: 978-0-470-14348-3. doi:10.1002/9780470143483.ch7.

94. Pople, J. & Binkley, J. Correlation energies for AH n molecules and cations. *Mol. Phys.* **29.** Publisher: Taylor & Francis, 599–611. ISSN: 0026-8976. doi:10.1080/00268977500100511 (Feb. 1975).

95. Hehre, W. J., Stewart, R. F. & Pople, J. A. Self-Consistent Molecular-Orbital Methods. I. Use of Gaussian Expansions of Slater-Type Atomic Orbitals. *J. Chem. Phys.* **51,** 2657–2664. ISSN: 0021-9606. doi:10.1063/1.1672392 (Sept. 1969).

96. Pritchard, B. P., Altarawy, D., Didier, B., Gibson, T. D. & Windus, T. L. New Basis Set Exchange: An Open, Up-to-Date Resource for the Molecular Sciences Community. *J. Chem. Inf. Mod.* **59.** Publisher: American Chemical Society, 4814–4820. ISSN: 1549-9596. doi:10.1021/acs.jcim.9b00725 (Nov. 2019).

97. Ditchfield, R., Hehre, W. J. & Pople, J. A. Self-Consistent Molecular-Orbital Methods. IX. An Extended Gaussian-Type Basis for Molecular-Orbital Studies of Organic Molecules. *J. Chem. Phys.* **54,** 724–728. ISSN: 0021-9606. doi:10.1063/1.1674902 (Jan. 1971).

98. Dunning Jr., T. H. Gaussian basis sets for use in correlated molecular calculations. I. The atoms boron through neon and hydrogen. *J. Chem. Phys.* **90,** 1007–1023. ISSN: 0021-9606. doi:10.1063/1.456153 (Jan. 1989).

99. Feller, D. Application of systematic sequences of wave functions to the water dimer. *J. Chem. Phys.* **96,** 6104–6114. ISSN: 0021-9606. doi:10.1063/1.462652 (Apr. 1992).

100. KLOPPER, W. Highly accurate coupled-cluster singlet and triplet pair energies from explicitly correlated calculations in comparison with extrapolation techniques. *Mol. Phys.* **99,** 481–507. ISSN: 0026-8976. doi:10.1080/00268970010017315 (Mar. 2001).

101. Feller, D., Peterson, K. A. & Grant Hill, J. On the effectiveness of CCSD(T) complete basis set extrapolations for atomization energies. *J. Chem. Phys.* **135,** 044102. ISSN: 0021-9606. doi:10.1063/1.3613639 (July 2011).

102. Clark, T., Chandrasekhar, J., Spitznagel, G. W. & Schleyer, P. V. R. Efficient diffuse function-augmented basis sets for anion calculations. III. The 3-21+G basis set for first-row elements, Li–F. en. *J. Comput. Chem.* **4,** 294–301. ISSN: 1096-987X. doi:10.1002/jcc.540040303 (1983).

103. Kendall, R. A., Dunning Jr., T. H. & Harrison, R. J. Electron affinities of the first-row atoms revisited. Systematic basis sets and wave functions. *J. Chem. Phys.* **96,** 6796–6806. ISSN: 0021-9606. doi:10.1063/1.462569 (May 1992).

104. Hariharan, P. C. & Pople, J. A. The influence of polarization functions on molecular orbital hydrogenation energies. en. *Theor. Chim. Acta* **28,** 213–222. ISSN: 1432-2234. doi:10.1007/BF00533485 (Sept. 1973).

105. Van Duijneveldt, F. B., van Duijneveldt-van de Rijdt, J. G. C. M. & van Lenthe, J. H. State of the Art in Counterpoise Theory. *Chem. Rev.* **94.** Publisher: American Chemical Society, 1873–1885. ISSN: 0009-2665. doi:10.1021/cr00031a007 (Nov. 1994).

106. Slater, J. C. The Theory of Complex Spectra. *Phys. Rev.* **34.** Publisher: American Physical Society, 1293–1322. doi:10.1103/PhysRev.34.1293 (Nov. 1929).

107. Fock, V. Konfigurationsraum und zweite Quantelung. de. *Z. Phys.* **75,** 622–647. ISSN: 0044-3328. doi:10.1007/BF01344458 (Sept. 1932).

108. Wick, G. C. The Evaluation of the Collision Matrix. en. *Phys. Rev.* **80,** 268–272. ISSN: 0031-899X. doi:10.1103/PhysRev.80.268 (Oct. 1950).

109. Pauncz, R. *Spin Eigenfunctions: Construction and Use* 374 pp. ISBN: 978-1-4684-8526-4 (Springer Science & Business Media, 6th Dec. 2012).

110. Stanton, J. F. On the extent of spin contamination in open-shell coupled-cluster wave functions. *J. Chem. Phys.* **101,** 371–374. ISSN: 0021-9606. doi:10.1063/1.468144 (1st July 1994).

111. Datta, D. & Mukherjee, D. The spin-free analogue of Mukherjee's state-specific multireference coupled cluster theory. *J. Chem. Phys.* **134,** 054122. ISSN: 0021-9606. doi:10.1063/1.3537740 (7th Feb. 2011).

112. Fano, U. & Racah, G. *Irreducible Tensorial Sets* 188 pp. (Academic Press, 1959).

113. Kaplan, I. G. Group-theoretical Methods in Quantum-chemical Calculations. *Russ. Chem. Rev.* **48,** 550. ISSN: 0036-021X. doi:10.1070/RC1979v048n06ABEH002344 (1979).

114. Paldus, J. & Sarma, C. R. Clifford algebra unitary group approach to many-electron correlation problem. en. *J. Chem. Phys.* **83.** Publisher: AIP Publishing, 5135–5152. ISSN: 0021-9606. doi:10.1063/1.449726 (Nov. 1985).

115. Gel'fand, I. M. *Izrail M. Gelfand: collected papers* ed. by Gindikin, S. G. ISBN: 978-0-387-13619-6 (Springer-Verlag, Berlin, 1987).

116. Shavitt, I. *Introduction to the Unitary Group Approach* en. Argonne National Laboratory, Aug. 2005.

117. Koch, R. d. M., Ives, N. & Stephanou, M. On subgroup adapted bases for representations of the symmetric group. *arXiv:1112.4316 [hep-th, physics:math-ph, physics:quant-ph].* doi:10.1088/1751-8113/45/13/135204 (19th Dec. 2011).

118. Molev, A. I. Gelfand-Tsetlin bases for classical Lie algebras. *arXiv:math/0211289.* arXiv: math/0211289 (4th Dec. 2002).

119. Hersh, P. & Lenart, C. Combinatorial Constructions of Weight Bases: The Gelfand-Tsetlin Basis. *Electron. J. Combin.* **17,** R33. ISSN: 1077-8926. doi:10.37236/305 (22nd Feb. 2010).

120. Jeziorski, B., Paldus, J. & Jankowski, P. Unitary group approach to spin-adapted open-shell coupled cluster theory. *Int. J. Quantum Chem.* **56,** 129–155. ISSN: 1097-461X. doi:10.1002/qua.560560302 (1995).

121. Paldus, J. & Boyle, M. J. Unitary Group Approach to the Many-Electron Correlation Problem via Graphical Methods of Spin Algebras. *Phys. Scr.* **21,** 295–311. ISSN: 0031-8949, 1402-4896. doi:10.1088/0031-8949/21/3-4/012 (1st Jan. 1980).

122. Kaplan, I. G. *Symmetry of many-electron systems* xii+370. ISBN: 978-0-12-397150-0 (Academic Press, New York, 1975).

123. Weyl, H. *The Classical Groups | Princeton University Press* en. ISBN: 9780691057569. Feb. 1997.

124. Fulton, W. & Harris, J. in *Representation Theory: A First Course* 75–88 (Springer New York, New York, NY, 2004). ISBN: 978-1-4612-0979-9. doi:10.1007/978-1-4612-0979-9_6.

125. Gulania, S. & Whitfield, J. D. Young frames for quantum chemistry. *arXiv:1904.10469 [physics, physics:quant-ph]* (23rd Apr. 2019).

126. Akin, K., Buchsbaum, D. A. & Weyman, J. Schur functors and Schur complexes. *Adv. Math.* **44,** 207–278. ISSN: 0001-8708. doi:10.1016/0001-8708(82)90039-1 (June 1982).

127. Paldus, J. Unitary-group approach to the many-electron correlation problem: Relation of Gelfand and Weyl tableau formulations. *Phys. Rev. A* **14,** 1620–1625. doi:10.1103/PhysRevA.14.1620 (1st Nov. 1976).

128. Kent, R. D., Schlesinger, M. & Shavitt, I. Graphical unitary group approach to spin–spin interaction. *Int. J. Quantum Chem.* **41,** 89–103. ISSN: 1097-461X. doi:10.1002/qua.560410110 (1992).

129. Burton, P. J. & Gould, M. D. A unitary group formulation of the complete active space configuration interaction method. II. An approach based on the subgroup chain $U(n = n_0 + n_1 + n_2) = U(n_0) \times U(n_1 + \mathrm{in}_2) = U(n_0) \times U(n_1) \times U(n_2)$. *J. Chem. Phys.* **96,** 5261–5271. ISSN: 0021-9606, 1089-7690. doi:10.1063/1.462711 (Apr. 1992).

130. Wu, W. & Zhang, Q. An efficient algorithm for evaluating the standard Young-Yamanouchi orthogonal representation with two-column Young tableaux for symmetric groups. *J. Phys. A: Math. Gen.* **25,** 3737–3747. ISSN: 0305-4470, 1361-6447. doi:10.1088/0305-4470/25/13/022 (7th July 1992).

131. Nagel, J. G. & Moshinsky, M. Operators that Lower or Raise the Irreducible Vector Spaces of U_{n-1} Contained in an Irreducible Vector Space of U_n. *J. Math. Phys.* **6,** 682–694. ISSN: 0022-2488. doi:10.1063/1.1704326 (1st May 1965).

132. Hartree, D. R. & Hartree, W. Self-consistent field, with exchange, for beryllium. *Proc. R. Soc. London A - Math. Phys. Sci.* **150.** Publisher: Royal Society, 9–33. doi:10.1098/rspa.1935.0085 (May 1935).

133. Hall, G. G. The molecular orbital theory of chemical valency VIII. A method of calculating ionization potentials. *Proc. R. Soc. London A - Math. Phys. Sci.* **205.** Publisher: Royal Society, 541–552. doi:10.1098/rspa.1951.0048 (Mar. 1951).

134. Roothaan, C. C. J. New Developments in Molecular Orbital Theory. *Rev. Mod. Phys.* **23.** Publisher: American Physical Society, 69–89. doi:10.1103/RevModPhys.23.69 (Apr. 1951).

135. Møller, C. & Plesset, M. S. Note on an Approximation Treatment for Many-Electron Systems. *Phys. Rev.* **46.** Publisher: American Physical Society, 618–622. doi:10.1103/PhysRev.46.618 (Oct. 1934).

136. Roothaan, C. C. J. Self-Consistent Field Theory for Open Shells of Electronic Systems. *Rev. Mod. Phys.* **32.** Publisher: American Physical Society, 179–185. doi:10.1103/RevModPhys.32.179 (Apr. 1960).

137. Edwards, W. D. & Zerner, M. C. A generalized restricted open-shell Fock operator. en. *Theor. Chim. Acta* **72,** 347–361. ISSN: 1432-2234. doi:10.1007/BF01192227 (Dec. 1987).

138. Leyser da Costa Gouveia, T., Maganas, D. & Neese, F. Restricted Open-Shell Hartree–Fock Method for a General Configuration State Function Featuring Arbitrarily Complex Spin-Couplings. *J. Phys. Chem. A* **128,** 5041–5053. ISSN: 1089-5639. doi:10.1021/acs.jpca.4c00688 (27th June 2024).

139. Burton, H. G. A. *Geometric direct minimization for low-spin restricted open-shell Hartree-Fock* arXiv:2507.23127 [physics]. Aug. 2025. doi:10.48550/arXiv.2507.23127.

140. Neese, F. Response of a General Restricted Open-Shell Hartree–Fock Wave Function. I: Formalism, Analytic Gradients, and Electric and Magnetic Response Properties. *J. Phys. Chem. A.* ISSN: 1089-5639. doi:10.1021/acs.jpca.5c05207 (Oct. 2025).

141. Langhoff, S. R. & Davidson, E. R. Configuration interaction calculations on the nitrogen molecule. en. *Int. J. Quantum Chem.* **8,** 61–72. ISSN: 1097-461X. doi:10.1002/qua.560080106 (1974).

142. Siegbahn, P. E. M. A new direct CI method for large CI expansions in a small orbital space. *Chem. Phys. Lett.* **109,** 417–423. ISSN: 0009-2614. doi:10.1016/0009-2614(84)80336-X (Aug. 1984).

143. Huron, B., Malrieu, J. P. & Rancurel, P. Iterative perturbation calculations of ground and excited state energies from multiconfigurational zeroth-order wavefunctions. en. *J. Chem. Phys.* **58,** 5745–5759. ISSN: 0021-9606, 1089-7690. doi:10.1063/1.1679199 (June 1973).

144. Buenker, R. J. & Peyerimhoff, S. D. Individualized configuration selection in CI calculations with subsequent energy extrapolation. en. *Theor. Chim. Acta* **35,** 33–58. ISSN: 1432-2234. doi:10.1007/BF02394557 (Aug. 1974).

145. Harrison, R. J. Approximating full configuration interaction with selected configuration interaction and perturbation theory. *J. Chem. Phys.* **94,** 5021–5031. ISSN: 0021-9606. doi:10.1063/1.460537 (Apr. 1991).

146. Tubman, N. M., Lee, J., Takeshita, T. Y., Head-Gordon, M. & Whaley, K. B. A deterministic alternative to the full configuration interaction quantum Monte Carlo method. *J. Chem. Phys.* **145,** 044112. ISSN: 0021-9606. doi:10.1063/1.4955109 (July 2016).

147. Holmes, A. A., Tubman, N. M. & Umrigar, C. J. Heat-Bath Configuration Interaction: An Efficient Selected Configuration Interaction Algorithm Inspired by Heat-Bath Sampling. *J. Chem. Theor. Comput.* **12.** Publisher: American Chemical Society, 3674–3680. ISSN: 1549-9618. doi:10.1021/acs.jctc.6b00407 (Aug. 2016).

148. Malmqvist, P. A., Rendell, A. & Roos, B. O. The restricted active space self-consistent-field method, implemented with a split graph unitary group approach. *J. Phys. Chem.* **94,** 5477–5482 (July 1990).

149. Ma, D., Li Manni, G. & Gagliardi, L. The generalized active space concept in multiconfigurational self-consistent field methods. *J. Chem. Phys.* **135,** 044128 (July 2011).

150. Schrödinger, E. Quantisierung als Eigenwertproblem. en. *Ann. Phys.* **385,** 437–490. ISSN: 1521-3889. doi:10.1002/andp.19263851302 (1926).

151. Bloch, C. Sur la théorie des perturbations des états liés. *Nucl. Phys.* **6,** 329–347. ISSN: 0029-5582. doi:10.1016/0029-5582(58)90116-0 (Mar. 1958).

152. Goldstone, J. Derivation of the Brueckner many-body theory. *Proc. R. Soc. London A - Math. Phys. Sci.* **239,** 267–279. doi:10.1098/rspa.1957.0037 (Feb. 1957).

153. Frantz, L. M. & Mills, R. L. Many-body basis for the optical model. *Nucl. Phys.* **15,** 16–32. ISSN: 0029-5582. doi:10.1016/0029-5582(60)90278-9 (Feb. 1960).

154. Levy, B. & Berthier, G. Generalized brillouin theorem for multiconfigurational SCF theories. en. *Int. J. Quantum Chem.* **2,** 307–319. ISSN: 1097-461X. doi:10.1002/qua.560020210 (1968).

155. Koch, S. & Kutzelnigg, W. Comparison of CEPA and CP-MET methods. en. *Theor. Chim. Acta* **59,** 387–411. ISSN: 1432-2234. doi:10.1007/BF00553396 (July 1980).

156. Purvis III, G. D. & Bartlett, R. J. The reduced linear equation method in coupled cluster theory. *J. Chem. Phys.* **75,** 1284–1292. ISSN: 0021-9606. doi:10.1063/1.442131 (Aug. 1981).

157. Taube, A. G. & Bartlett, R. J. Rethinking linearized coupled-cluster theory. *J. Chem. Phys.* **130,** 144112. ISSN: 0021-9606. doi:10.1063/1.3115467 (Apr. 2009).

158. Battaglia, S., Fransén, L., Fdez. Galván, I. & Lindh, R. Regularized CASPT2: an Intruder-State-Free Approach. *J. Chem. Theor. Comput.* **18.** Publisher: American Chemical Society, 4814–4825. ISSN: 1549-9618. doi:10.1021/acs.jctc.2c00368 (Aug. 2022).

159. Saunders, V. R. & Hillier, I. H. A "Level–Shifting" method for converging closed shell Hartree–Fock wave functions. en. *Int. J. Quantum Chem.* **7,** 699–705. ISSN: 1097-461X. doi:10.1002/qua.560070407 (1973).

160. Ghigo, G., Roos, B. O. & Malmqvist, P.-Å. A modified definition of the zeroth-order Hamiltonian in multiconfigurational perturbation theory (CASPT2). *Chem. Phys. Lett.* **396,** 142–149. ISSN: 0009-2614. doi:10.1016/j.cplett.2004.08.032 (Sept. 2004).

161. Pulay, P. Convergence acceleration of iterative sequences. the case of scf iteration. *Chem. Phys. Lett.* **73,** 393–398 (July 1980).

162. Scuseria, G. E., Lee, T. J. & Schaefer III, H. F. Accelerating the convergence of the coupled-cluster approach: The use of the DIIS method Author links open overlay panel. *Chem. Phys. Lett.* **130,** 236–239 (Oct. 1986).

163. Hanrath, M. An exponential multireference wave-function Ansatz. *J. Chem. Phys.* **123,** 084102 (Aug. 2005).

164. Hubač, I. & Neogrády, P. Size-consistent Brillouin-Wigner perturbation theory with an exponentially parametrized wave function: Brillouin-Wigner coupled-cluster theory. *Phys. Rev. A* **50.** Publisher: American Physical Society, 4558–4564. doi:10.1103/PhysRevA.50.4558 (Dec. 1994).

165. Mášik, J. & Hubač, I. en. in *Quantum Systems in Chemistry and Physics. Trends in Methods and Applications* (eds McWeeny, R., Maruani, J., Smeyers, Y. G. & Wilson, S.) 283–308 (Springer Netherlands, Dordrecht, 1997). ISBN: 978-94-011-4894-8. doi:10.1007/978-94-011-4894-8_16.

166. Kaldor, U. Intruder states and incomplete model spaces in multireference coupled-cluster theory: The 2${p}^{2}$ states of Be. *Phys. Rev. A* **38,** 6013–6016. doi:10.1103/PhysRevA.38.6013 (Dec. 1988).

167. Hanrath, M. Initial applications of an exponential multi-reference wavefunction ansatz. *Chem. Phys. Lett.* **420,** 426–431 (Mar. 2006).

168. Löwdin, P.-O. Quantum theory of cohesive properties of solids. *Adv. Phys.* **5,** 1–171. doi:10.1080/00018735600101155 (1956).

169. Lindgren, I. & Mukherjee, D. On the connectivity criteria in the open-shell coupled-cluster theory for general model spaces. *Phys. Rep.* **151,** 93–127 (July 1987).

170. Stolarczyk, L. Z. & Monkhorst, H. J. Coupled-cluster method in Fock space. II. Brueckner-Hartree-Fock method. *Phys. Rev. A* **32,** 743 (Jan. 1985).

171. Stolarczyk, L. Z. & Monkhorst, H. J. Coupled-cluster method in Fock space. III. On similarity transformation of operators in Fock space. *Phys. Rev. A* **37,** 1908 (Mar. 1988).

172. Stolarczyk, L. Z. & Monkhorst, H. J. Coupled-cluster method in Fock space. IV. Calculation of expectation values and transition moments. *Phys. Rev. A* **37,** 1926 (Mar. 1988).

173. Lindgren, I. Linked-Diagram and Coupled-Cluster Expansions for Multi-Configurational, Complete and Incomplete Model Spaces. *Phys. Scr.* **32,** 291–302. doi:10.1088/0031-8949/32/4/009 (Apr. 1985).

174. Sen, S., Shee, A. & Mukherjee, D. Inclusion of orbital relaxation and correlation through the unitary group adapted open shell coupled cluster theory using non-relativistic and scalar relativistic Hamiltonians to study the core ionization potential of molecules containing light to medium-heavy elements. *J. Chem. Phys.* **148,** 054107. doi:10.1063/1.5018086 (Feb. 2018).

175. Chakravarti, D., Sen, S. & Mukherjee, D. Reappraisal of the normal ordered Jeziorski-Monkhorst ansatz in the UGA-OSCC theory for a study of IP, EA and EE. *Mol. Phys.* **119.** doi:10.1080/00268976.2021.1979676 (Sept. 2021).

176. Pal, S., Prasad, M. D. & Mukherjee, D. Development of a size-consistent energy functional for open shell states. *Theor. Chim. Acta* **66,** 311–332 (Sept. 1984).

177. Bunge, A. Electronic Wavefunctions for Atoms. III. Partition of Degenerate Spaces and Ground State of C. *J. Chem. Phys.* **53,** 20–28. ISSN: 0021-9606. doi:10.1063/1.1673766 (July 1970).

178. Kállay, M. & Surján, P. R. Computing coupled-cluster wave functions with arbitrary excitations. *J. Chem. Phys.* **113,** 1359–1365. ISSN: 0021-9606. doi:10.1063/1.481925 (July 2000).

179. Kállay, M. & Surján, P. R. Higher excitations in coupled-cluster theory. *J. Chem. Phys.* **115,** 2945–2954. ISSN: 0021-9606. doi:10.1063/1.1383290 (Aug. 2001).

180. Sun, Q. *et al.* PySCF: the Python-based simulations of chemistry framework. *WIREs Comput. Mol. Sci.* **8,** e1340. ISSN: 1759-0884. doi:10.1002/wcms.1340 (2018).

181. Kucharski, S. A. & Bartlett, R. J. The coupled-cluster single, double, triple, and quadruple excitation method. *J. Chem. Phys.* **97,** 4282–4288. ISSN: 0021-9606. doi:10.1063/1.463930 (Sept. 1992).

182. Tew, D. P., Klopper, W. & Helgaker, T. Electron correlation: The many-body problem at the heart of chemistry. *J. Comput. Chem.* **28,** 1307–1320 (Jan. 2007).

183. Green Jr., W. H., Handy, N. C., Knowles, P. J. & Carter, S. Theoretical assignment of the visible spectrum of singlet methylene. English. *J. Chem. Phys.* **94,** 118–132. ISSN: 0021-9606. doi:10.1063/1.460385 (1991).

184. Van Voorhis, T. & Head-Gordon, M. Benchmark variational coupled cluster doubles results. en. *J. Chem. Phys.* **113,** 8873–8879. ISSN: 0021-9606, 1089-7690. doi:10.1063/1.1319643 (Nov. 2000).

185. Paldus, J., Piecuch, P., Pylypow, L. & Jeziorski, B. Application of Hilbert-space coupled-cluster theory to simple $(H_2)_2$ model systems: Planar models. *Phys. Rev. A* **47.** Publisher: American Physical Society, 2738–2782. doi:10.1103/PhysRevA.47.2738 (Apr. 1993).

186. Kong, L. Orbital Invariance Issue in Multireference Methods. *Int. J. Quantum Chem.* **110,** 2603–2613 (Oct. 2009).

187. Sen, S., Shee, A. & Mukherjee, D. Formulation and implementation of a unitary group adapted state universal multi-reference coupled cluster (UGA-SUMRCC) theory: Excited and ionized state energies. *J. Chem. Phys.* **137,** 074104. doi:10.1063/1.4742058 (Aug. 2012).